

# Chapter 3

## Lepton Magnetic Moments: Basics

### 3.1 Equation of Motion for a Lepton in an External Field

For the measurement of the anomalous magnetic moment of a lepton we have to investigate the motion of a relativistic point–particle of charge  $Q_\ell e$  ( $e$  the positron charge) and mass  $m_\ell$  in an external electromagnetic field  $A_\mu^{\text{ext}}(x)$ . The equation of motion of a charged Dirac particle in an external field is given by (see (2.91))

$$\begin{aligned} & (i\hbar\gamma^\mu\partial_\mu + Q_\ell\frac{e}{c}\gamma^\mu(A_\mu + A_\mu^{\text{ext}}(x)) - m_\ell c) \psi_\ell(x) = 0 \\ & (\square g^{\mu\nu} - (1 - \xi^{-1})\partial^\mu\partial^\nu) A_\nu(x) = -Q_\ell e\bar{\psi}_\ell(x)\gamma^\mu\psi_\ell(x). \end{aligned} \tag{3.1}$$

What we are looking for is the solution of the Dirac equation with an external field as a relativistic one–particle problem, neglecting the radiation field in a first step. We thus are interested in a solution of the first of the above equations, which we may write as

$$i\hbar\frac{\partial\psi_\ell}{\partial t} = \left(-c\boldsymbol{\alpha}\left(i\hbar\nabla - Q_\ell\frac{e}{c}\mathbf{A}\right) - Q_\ell e\Phi + \beta m_\ell c^2\right)\psi_\ell, \tag{3.2}$$

with  $\beta = \gamma^0$ ,  $\boldsymbol{\alpha} = \gamma^0\boldsymbol{\gamma}$  and  $A^\mu{}^{\text{ext}} = (\Phi, \mathbf{A})$ . For the interpretation of the solution the non–relativistic limit plays an important role, because many relativistic problems in QED may be most easily understood in terms of the non–relativistic problem as a starting point, which usually is easier to solve. We will consider a lepton  $e^-$ ,  $\mu^-$  or  $\tau^-$  with  $Q_\ell = -1$  in the following and drop the index  $\ell$ .

#### 1. Non–relativistic limit

For studying the non–relativistic limit of the motion of a Dirac particle in an external field it is helpful and more transparent to work in natural units.<sup>1</sup> In order to get from

---

<sup>1</sup>The general rules of translation read:  $p^\mu \rightarrow p^\mu$ ,  $d\mu(p) \rightarrow \hbar^{-3}d\mu(p)$ ,  $m \rightarrow mc$ ,  $e \rightarrow e/(\hbar c)$ ,  $e^{ipx} \rightarrow e^{i\frac{px}{\hbar}}$ , spinors:  $u, v \rightarrow u/\sqrt{c}, v/\sqrt{c}$ .

the Dirac spinor  $\psi$  the two component Pauli spinors in the non-relativistic limit, one has to perform an appropriate unitary transformation, called Foldy–Wouthuysen transformation. Looking at the Dirac equation (3.2)

$$i\hbar \frac{\partial \psi}{\partial t} = \mathbf{H} \psi, \quad \mathbf{H} = c \boldsymbol{\alpha} \left( \mathbf{p} - \frac{e}{c} \mathbf{A} \right) + \beta mc^2 + e \Phi$$

with

$$\beta = \gamma^0 = \begin{pmatrix} 1 & 0 \\ 0 & -1 \end{pmatrix}, \quad \boldsymbol{\alpha} = \gamma^0 \boldsymbol{\gamma} = \begin{pmatrix} 0 & \boldsymbol{\sigma} \\ \boldsymbol{\sigma} & 0 \end{pmatrix},$$

we note that  $\mathbf{H}$  has the form

$$\mathbf{H} = \beta mc^2 + c \mathcal{O} + e \Phi$$

where  $[\beta, \Phi] = 0$  is commuting and  $\{\beta, \mathcal{O}\} = 0$  anti-commuting. In the absence of an external field spin is a conserved quantity in the rest frame, i.e. the Dirac equation must be equivalent to the Pauli equation. This fixes the unitary transformation to be performed in the case  $A_\mu^{\text{ext}} = 0$ :

$$\psi' = \mathbf{U} \psi, \quad \mathbf{H}' = \mathbf{U} \left( \mathbf{H} - i\hbar \frac{\partial}{\partial t} \right) \mathbf{U}^{-1} = \mathbf{U} \mathbf{H} \mathbf{U}^{-1} \quad (3.3)$$

where the time-independence of  $\mathbf{U}$  has been used, and we obtain

$$i\hbar \frac{\partial \psi'}{\partial t} = \mathbf{H}' \psi'; \quad \psi' = \begin{pmatrix} \varphi' \\ 0 \end{pmatrix}, \quad (3.4)$$

where  $\varphi'$  is the Pauli spinor. In fact  $\mathbf{U}$  is a Lorentz boost matrix

$$\mathbf{U} = \mathbf{1} \cosh \theta + \mathbf{n} \boldsymbol{\gamma} \sinh \theta = e^{\theta \mathbf{n} \boldsymbol{\gamma}} \quad (3.5)$$

with

$$\mathbf{n} = \frac{\mathbf{p}}{|\mathbf{p}|}, \quad \theta = \frac{1}{2} \text{arccosh} \frac{p^0}{mc} = \text{arcsinh} \frac{|\mathbf{p}|}{mc}$$

and we obtain, with  $p^0 = \sqrt{\mathbf{p}^2 + m^2 c^2}$ ,

$$\mathbf{H}' = cp^0 \beta; \quad [\mathbf{H}', \boldsymbol{\Sigma}] = 0, \quad \boldsymbol{\Sigma} = \boldsymbol{\alpha} \gamma_5 = \begin{pmatrix} \boldsymbol{\sigma} & \mathbf{0} \\ \mathbf{0} & \boldsymbol{\sigma} \end{pmatrix} \quad (3.6)$$

where  $\Sigma$  is the spin operator. Actually, there exist two projection operators  $U$  one to the upper and one to the lower components:

$$U_+ \psi = \begin{pmatrix} \varphi' \\ 0 \end{pmatrix}, \quad U_- \psi = \begin{pmatrix} 0 \\ \chi \end{pmatrix},$$

given by

$$U_+ = \frac{(p^0 + mc) \mathbf{1} + \mathbf{p}\boldsymbol{\gamma}}{\sqrt{2p^0}\sqrt{p^0 + mc}}, \quad U_- = \frac{(p^0 + mc) \mathbf{1} - \mathbf{p}\boldsymbol{\gamma}}{\sqrt{2p^0}\sqrt{p^0 + mc}}.$$

For the spinors we have

$$U_+ u(p, r) = \sqrt{\frac{2p^0}{c}} \begin{pmatrix} U(r) \\ 0 \end{pmatrix}, \quad U_- v(p, r) = \sqrt{\frac{2p^0}{c}} \begin{pmatrix} 0 \\ V(r) \end{pmatrix}$$

with  $U(r)$  and  $V(r) = i\sigma_2 U(r)$  the two component spinors in the rest system.

We now look at the lepton propagator. The Feynman propagator reads

$$\begin{aligned} iS_{F\alpha\beta}(x-y) &\equiv \langle 0|T\{\psi_\alpha(x)\bar{\psi}_\beta(y)\}|0\rangle \\ &= \int \frac{d^4 p}{(2\pi)^4} \frac{\not{p} + mc}{p^2 - m^2 c^2 + i\varepsilon} e^{-ip(x-y)} \end{aligned}$$

where<sup>2</sup>

$$S_{F\alpha\beta}(z; m^2) = (i\hbar\gamma^\mu \partial_\mu + mc) \Delta_F(z; m^2) = \Theta(z^0) S^+(z) + \Theta(-z^0) S^-(z)$$

with retarded positive frequency part represented by

$$\Theta(z^0) S^+(z) = \int \frac{d^4 p}{(2\pi)^4} \frac{c}{2\omega_p} \frac{\sum_r u_\alpha(p, r) \bar{u}_\beta(p, r)}{p^0 - \omega_p + i0} e^{-ipz}$$

---

<sup>2</sup>The positive frequency part is given by

$$\begin{aligned} iS_{\alpha\beta}^+(x-y) &\equiv \langle 0|\psi_\alpha(x)\bar{\psi}_\beta(y)|0\rangle \\ &= c \sum_r \int d\mu(p) u_\alpha(p, r) \bar{u}_\beta(p, r) e^{-ip(x-y)} = \int d\mu(p) (\not{p} + mc) e^{-ip(x-y)} \end{aligned}$$

and the negative frequency part by

$$\begin{aligned} -iS_{\alpha\beta}^-(x-y) &\equiv \langle 0|\bar{\psi}_\beta(y)\psi_\alpha(x)|0\rangle \\ &= c \sum_r \int d\mu(p) v_\alpha(p, r) \bar{v}_\beta(p, r) e^{ip(x-y)} = \int d\mu(p) (\not{p} - mc) e^{ip(x-y)}. \end{aligned}$$

and the advanced negative frequency part by

$$\Theta(-z^0) S^-(z) = - \int \frac{d^4 p}{(2\pi)^4} \frac{c}{2\omega_p} \sum_r v_\alpha(p, r) \bar{v}_\beta(p, r) e^{ipz} .$$

Using

$$\begin{aligned} \sum_r u_\alpha(p, r) \bar{u}_\beta(p, r) &= \frac{2\omega_p}{c} \mathbf{U}(\mathbf{p}) \gamma_+ \mathbf{U}(\mathbf{p}) \\ \sum_r v_\alpha(p, r) \bar{v}_\beta(p, r) &= \frac{2\omega_p}{c} \mathbf{U}(\mathbf{p}) \gamma_- \mathbf{U}(\mathbf{p}) \end{aligned}$$

with

$$\gamma_\pm = \frac{1}{2} (\mathbf{1} \pm \gamma^0) ; \quad \gamma^0 \gamma_\pm = \pm \gamma_\pm , \quad \gamma_+ \gamma_- = \gamma_- \gamma_+ = 0$$

the projection matrices for the upper and lower components, respectively. We thus arrive at our final representation which allows one to perform a systematic expansion in  $1/c$ :

$$S_F(x-y) = \int \frac{d^4 p}{(2\pi)^4} e^{-ip(x-y)} \mathbf{U}(\mathbf{p}) \left( \frac{\gamma_+}{p^0 - \omega_p + i0} - \frac{\gamma_-}{p^0 + \omega_p - i0} \right) \mathbf{U}(\mathbf{p}) . \quad (3.7)$$

The  $1/c$ -expansion simply follows by expanding the matrix  $\mathbf{U}$ :

$$\mathbf{U}(\mathbf{p}) = \exp \theta \frac{\mathbf{p}}{|\mathbf{p}|} \gamma = \exp \theta \frac{\mathbf{p}\boldsymbol{\gamma}}{2mc} ; \quad \theta = \sum_{n=0}^{\infty} \frac{(-1)^n}{2n+1} \left( \frac{\mathbf{p}^2}{m^2 c^2} \right)^n .$$

The non-relativistic limit thus reads:

$$S_F(x-y)_{\text{NR}} = \int \frac{d^4 p}{(2\pi)^4} e^{-ip(x-y)} \left( \frac{\gamma_+}{p^0 - (mc^2 + \frac{\mathbf{p}^2}{2m}) + i0} - \frac{\gamma_-}{p^0 + (mc^2 + \frac{\mathbf{p}^2}{2m}) - i0} \right)$$

i.e.

$$S_F(x-y) = S_F(x-y)_{\text{NR}} + O(1/c) .$$

## 2. Non-relativistic lepton with $A_\mu^{\text{ext}} \neq 0$

Again we start from the Dirac equation (3.2). In order to get the non-relativistic representation for small velocities we have to split off the phase of the Dirac field, which is due to the rest energy of the lepton:

$$\psi = \hat{\psi} e^{-i\frac{mc^2}{\hbar}t} \quad \text{with} \quad \hat{\psi} = \begin{pmatrix} \hat{\varphi} \\ \hat{\chi} \end{pmatrix}.$$

Consequently, the Dirac equation takes the form

$$i\hbar \frac{\partial \hat{\psi}}{\partial t} = (\mathbf{H} - mc^2) \hat{\psi}$$

and describes the coupled system of equations

$$\begin{aligned} \left( i\hbar \frac{\partial}{\partial t} - e\Phi \right) \hat{\varphi} &= c\sigma \left( \mathbf{p} - \frac{e}{c}\mathbf{A} \right) \hat{\chi} \\ \left( i\hbar \frac{\partial}{\partial t} - e\Phi + 2mc^2 \right) \hat{\chi} &= c\sigma \left( \mathbf{p} - \frac{e}{c}\mathbf{A} \right) \hat{\varphi}. \end{aligned}$$

For  $c \rightarrow \infty$  we obtain

$$\hat{\chi} \simeq \frac{1}{2mc} \sigma \left( \mathbf{p} - \frac{e}{c}\mathbf{A} \right) \hat{\varphi} + O(1/c^2)$$

and hence

$$\left( i\hbar \frac{\partial}{\partial t} - e\Phi \right) \hat{\varphi} \simeq \frac{1}{2m} \left( \sigma \left( \mathbf{p} - \frac{e}{c}\mathbf{A} \right) \right)^2 \hat{\varphi}.$$

As  $\mathbf{p}$  does not commute with  $\mathbf{A}$ , we may use the relation

$$(\sigma\mathbf{a})(\sigma\mathbf{b}) = \mathbf{ab} + i\sigma(\mathbf{a} \times \mathbf{b})$$

to obtain

$$\left( \sigma \left( \mathbf{p} - \frac{e}{c}\mathbf{A} \right) \right)^2 = \left( \mathbf{p} - \frac{e}{c}\mathbf{A} \right)^2 - \frac{e\hbar}{c} \sigma \cdot \mathbf{B}; \quad \mathbf{B} = \text{rot}\mathbf{A}.$$

This leads us to the *Pauli equation* (W. Pauli 1927)

$$i\hbar \frac{\partial \hat{\varphi}}{\partial t} = \hat{\mathbf{H}} \hat{\varphi} = \left( \frac{1}{2m} \left( \mathbf{p} - \frac{e}{c}\mathbf{A} \right)^2 + e\Phi - \frac{e\hbar}{2mc} \sigma \cdot \mathbf{B} \right) \hat{\varphi} \quad (3.8)$$

which up to the spin term is nothing but the non-relativistic Schrödinger equation. The last term is the one this book is about: it has the form of a potential energy of a magnetic dipole in an external field. In leading order in  $1/c$  the lepton behaves as a particle which has besides a charge also a magnetic moment

$$\boldsymbol{\mu} = \frac{e\hbar}{2mc} \boldsymbol{\sigma} = \frac{e}{mc} \mathbf{S}; \quad \mathbf{S} = \hbar \mathbf{s} = \hbar \frac{\boldsymbol{\sigma}}{2} \quad (3.9)$$

with  $\mathbf{S}$  the angular momentum. For comparison: the orbital angular momentum reads

$$\boldsymbol{\mu}_{\text{orbital}} = \frac{Q}{2M} \mathbf{L} = g_l \frac{Q}{2M} \mathbf{L}; \quad \mathbf{L} = \mathbf{r} \times \mathbf{p} = -i\hbar \mathbf{r} \times \nabla = \hbar \mathbf{l}$$

and thus the total magnetic moment is

$$\boldsymbol{\mu}_{\text{total}} = \frac{Q}{2M} (g_l \mathbf{L} + g_s \mathbf{S}) = \frac{m_e}{M} \mu_B (g_l \mathbf{l} + g_s \mathbf{s}) \quad (3.10)$$

where

$$\mu_B = \frac{e\hbar}{2m_e c} \quad (3.11)$$

is Bohr's magneton. As a result for the electron:  $Q = -e$ ,  $M = m_e$ ,  $g_l = -1$  and  $g_s = -2$ . The last remarkable result is due to Dirac (1928) and tells us that the gyromagnetic ratio ( $\frac{e}{mc}$ ) is twice as large as the one from the orbital motion.

The Foldy–Wouthuysen transformation for arbitrary  $A_\mu$  cannot be performed in closed analytic form. However, the expansion in  $1/c$  can be done in a systematic way (see e.g. [1]) and yields the effective Hamiltonian

$$\begin{aligned} H' = & \beta \left( mc^2 + \frac{(\mathbf{p} - \frac{e}{c}\mathbf{A})^2}{2m} - \frac{\mathbf{p}^4}{8m^3c^2} \right) + e\Phi - \beta \frac{e\hbar}{2mc} \boldsymbol{\sigma} \cdot \mathbf{B} \\ & - \frac{e\hbar^2}{8m^2c^2} \text{div}\mathbf{E} - \frac{e\hbar}{4m^2c^2} \boldsymbol{\sigma} \cdot \left[ (\mathbf{E} \times \mathbf{p} + \frac{i}{2}\text{rot}\mathbf{E}) \right] \\ & + O(1/c^3). \end{aligned} \quad (3.12)$$

The additional terms are  $\frac{\mathbf{p}^4}{8m^3c^2}$  originating from the relativistic kinematics,  $\frac{e\hbar^2}{8m^2c^2} \text{div}\mathbf{E}$  is the Darwin term as a result of the fluctuations of the electrons position and  $\frac{e\hbar}{4m^2c^2} \boldsymbol{\sigma} \cdot \left[ (\mathbf{E} \times \mathbf{p} + \frac{i}{2}\text{rot}\mathbf{E}) \right]$  is the spin–orbit interaction energy. The latter plays an important role in setting up a muon storage ring in the  $g - 2$  experiment (magic energy tuning). As we will see, however, in such an experiment the muons are required to be highly relativistic such that relativistic kinematics is required. The appropriate modifications, the Bargmann–Michel–Telegdi equation [2], will be discussed in Chap. 6.

## 3.2 Magnetic Moments and Electromagnetic Form Factors

### 3.2.1 Main Features: An Overview

Our particular interest is the motion of a lepton in an external field under consideration of the full relativistic quantum behavior. It is controlled by the QED equations of motion (3.1) with an external field added (3.2), specifically a constant magnetic field.

For slowly varying fields the motion is essentially determined by the generalized Pauli equation (3.12), which also serves as a basis for understanding the role of the magnetic moment of a lepton on the classical level. As we will see, in the absence of electrical fields  $\mathbf{E}$  the quantum correction miraculously may be subsumed in a single number the anomalous magnetic moment, which is the result of relativistic quantum fluctuations, usually simply called *radiative corrections* (RC).

To study radiative corrections we have to extend the discussion of the preceding section and consider the full QED interaction Lagrangian

$$\mathcal{L}_{\text{int}}^{\text{QED}} = -e\bar{\psi}\gamma^\mu\psi A_\mu \tag{3.13}$$

in the case the photon field is part of the dynamics but has an external classical component  $A_\mu^{\text{ext}}$

$$A_\mu \rightarrow A_\mu + A_\mu^{\text{ext}} . \tag{3.14}$$

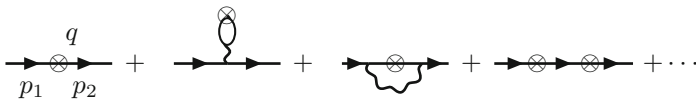
We are thus dealing with QED exhibiting an additional external field insertion “vertex”:

$$\text{⊗} = -ie \gamma^\mu \tilde{A}_\mu^{\text{ext}} .$$

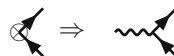
Gauge invariance (2.89) requires that a gauge transformation of the external field

$$A_\mu^{\text{ext}}(x) \rightarrow A_\mu^{\text{ext}}(x) - \partial_\mu\alpha(x) , \tag{3.15}$$

for an arbitrary scalar classical field  $\alpha(x)$ , leaves physics invariant. The motion of the lepton in the external field is described by a simultaneous expansion in the fine structure constant  $\alpha = \frac{e^2}{4\pi}$  and in the external field  $A_\mu^{\text{ext}}$  assuming the latter to be weak



In the following we will use the more customary graphic representation



of the external vertex, just as an amputated photon line at zero momentum.

The gyromagnetic ratio of the muon is defined by the ratio of the magnetic moment which couples to the magnetic field in the Hamiltonian and the spin operator in units of  $\mu_0 = e\hbar/2m_\mu c$

$$\boldsymbol{\mu} = g_\mu \frac{e\hbar}{2m_\mu c} \mathbf{s} ; \quad g_\mu = 2(1 + a_\mu) \quad (3.16)$$

and as indicated has a tree level part, the Dirac moment  $g_\mu^{(0)} = 2$  [3], and a higher order part the muon anomaly or anomalous magnetic moment

$$a_\mu = \frac{1}{2}(g_\mu - 2) . \quad (3.17)$$

In general, the anomalous magnetic moment of a lepton is related to the gyromagnetic ratio by

$$a_\ell = \mu_\ell/\mu_B - 1 = \frac{1}{2}(g_\ell - 2) \quad (3.18)$$

where the precise value of the Bohr magneton is given by

$$\mu_B = \frac{e\hbar}{2m_e c} = 5.788381804(39) \times 10^{-11} \text{ MeVT}^{-1} . \quad (3.19)$$

Here T as a unit stands for 1 Tesla =  $10^4$  Gauss. It is the unit in which the magnetic field  $B$  usually is given. In QED  $a_\mu$  may be calculated in perturbation theory by considering the matrix element

$$\mathcal{M}(x; p) = \langle \mu^-(p_2, r_2) | j_{\text{em}}^\mu(x) | \mu^-(p_1, r_1) \rangle$$

of the electromagnetic current for the scattering of an incoming muon  $\mu^-(p_1, r_1)$  of momentum  $p_1$  and 3rd component of spin  $r_1$  to a muon  $\mu^-(p_2, r_2)$  of momentum  $p_2$  and 3rd component of spin  $r_2$ , in the classical limit of zero momentum transfer  $q^2 = (p_2 - p_1)^2 \rightarrow 0$ . In momentum space, by virtue of space–time translational invariance  $j_{\text{em}}^\mu(x) = e^{iP \cdot x} j_{\text{em}}^\mu(0) e^{-iP \cdot x}$  and the fact that the lepton states are eigenstates of four–momentum  $e^{-iP \cdot x} | \mu^-(p_i, r_i) \rangle = e^{-i p_i \cdot x} | \mu^-(p_i, r_i) \rangle$  ( $i = 1, 2$ ), we find

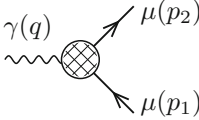
$$\begin{aligned} \tilde{\mathcal{M}}(q; p) &= \int d^4x e^{-iq \cdot x} \langle \mu^-(p_2, r_2) | j_{\text{em}}^\mu(x) | \mu^-(p_1, r_1) \rangle \\ &= \int d^4x e^{i(p_2 - p_1 - q) \cdot x} \langle \mu^-(p_2, r_2) | j_{\text{em}}^\mu(0) | \mu^-(p_1, r_1) \rangle \\ &= (2\pi)^4 \delta^{(4)}(q - p_2 + p_1) \langle \mu^-(p_2, r_2) | j_{\text{em}}^\mu(0) | \mu^-(p_1, r_1) \rangle , \end{aligned}$$

proportional to the  $\delta$ -function of four–momentum conservation. The  $T$ -matrix element is then given by

$$\langle \mu^-(p_2) | j_{\text{em}}^\mu(0) | \mu^-(p_1) \rangle .$$



In QED it has a relativistic covariant decomposition of the form



$$= (-ie) \bar{u}(p_2) \left[ \gamma^\mu F_E(q^2) + i \frac{\sigma^{\mu\nu} q_\nu}{2m_\mu} F_M(q^2) \right] u(p_1), \quad (3.20)$$

where  $q = p_2 - p_1$  and  $u(p)$  denote the Dirac spinors.  $F_E(q^2)$  is the electric charge or Dirac form factor and  $F_M(q^2)$  is the magnetic or Pauli form factor. Note that the matrix  $\sigma^{\mu\nu} = \frac{i}{2}[\gamma^\mu, \gamma^\nu]$  represents the spin 1/2 angular momentum tensor. In the static (classical) limit we have (see (2.210))

$$F_E(0) = 1, \quad F_M(0) = a_\mu, \quad (3.21)$$

where the first relation is the *charge renormalization condition* (in units of the physical positron charge  $e$ , which by definition is taken out as a factor in (3.20)), while the second relation is the finite prediction for  $a_\mu$ , in terms of the form factor  $F_M$  the calculation of which will be described below. The leading order (LO) contribution (2.215) we have been calculating already in Sect. 2.6.3.

Note that in higher orders the form factors in general acquire an imaginary part. One may write therefore an effective dipole moment Lagrangian with complex “coupling”

$$\mathcal{L}_{\text{eff}}^{\text{DM}} = -\frac{1}{2} \left\{ \bar{\psi} \sigma^{\mu\nu} \left[ D_\mu \frac{1 + \gamma_5}{2} + D_\mu^* \frac{1 - \gamma_5}{2} \right] \psi \right\} F_{\mu\nu} \quad (3.22)$$

with  $\psi$  the muon field and

$$\text{Re } D_\mu = a_\mu \frac{e}{2m_\mu}, \quad \text{Im } D_\mu = d_\mu = \frac{\eta_\mu}{2} \frac{e}{2m_\mu}, \quad (3.23)$$

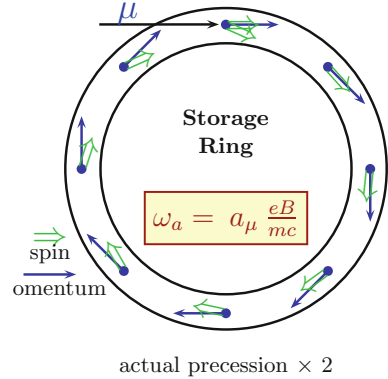
(see (3.84) and (3.85) below). Thus the imaginary part of  $F_M(0)$  corresponds to an electric dipole moment. The latter is non-vanishing only if we have T violation. For some more details we refer to Sect. 3.3.

As illustrated in Fig. 3.1, when polarized muons travel on a circular orbit in a constant magnetic field, then  $a_\mu$  is responsible for the *Larmor precession* of the direction of the spin of the muon, characterized by the angular frequency  $\omega_a$ . At the magic energy of about  $\sim 3.1$  GeV, the latter is directly proportional to  $a_\mu$ :

$$\omega_a = \frac{e}{m} \left[ a_\mu \mathbf{B} - \left( a_\mu - \frac{1}{\gamma^2 - 1} \right) \boldsymbol{\beta} \times \mathbf{E} \right]_{\text{at "magic } \gamma}^{E \sim 3.1 \text{ GeV}} \simeq \frac{e}{m} [a_\mu \mathbf{B}]. \quad (3.24)$$

Electric quadrupole fields  $\mathbf{E}$  are needed for focusing the beam and they affect the precession frequency in general.  $\gamma = E/m_\mu = 1/\sqrt{1 - \beta^2}$  is the relativistic Lorentz factor with  $\beta = v/c$  the velocity of the muon in units of the speed of light  $c$ . The magic

**Fig. 3.1** Spin precession in the  $g - 2$  ring ( $\sim 12^\circ/\text{circle}$ )



energy  $E_{\text{mag}} = \gamma_{\text{mag}} m_\mu$  is the energy  $E$  for which  $\frac{1}{\gamma_{\text{mag}}^2 - 1} = a_\mu$ . The existence of a solution is due to the fact that  $a_\mu$  is a positive constant in competition with an energy dependent factor of opposite sign (as  $\gamma \geq 1$ ). The second miracle, which is crucial for the feasibility of the experiment, is the fact that  $\gamma_{\text{mag}} = \sqrt{(1 + a_\mu)/a_\mu} \simeq 29.378$  is large enough to provide the time dilatation factor for the unstable muon boosting the life time  $\tau_\mu \simeq 2.197 \times 10^{-6}$  s to  $\tau_{\text{in flight}} = \gamma \tau_\mu \simeq 6.454 \times 10^{-5}$  s, which allows the muons, traveling at  $v/c = 0.99942\dots$ , to be stored in a ring of reasonable size (diameter  $\sim 14$  m).

This provided the basic setup for the  $g - 2$  experiments at the *Muon Storage Rings* at CERN and at BNL as well as for the upcoming new experiment at Fermilab. The oscillation frequency  $\omega_a$  can be measured very precisely. Also the precise tuning to the magic energy is not the major problem. The most serious challenge is to manufacture a precisely known constant magnetic field  $B$  (magnetic flux density), as the latter directly enters the experimental extraction of  $a_\mu$  via (3.24). Of course one also needs high enough statistics to get sharp values for the oscillation frequency. The basic principle of the measurement of  $a_\mu$  is a measurement of the ‘‘anomalous’’ frequency difference  $\omega_a = |\omega_a| = \omega_s - \omega_c$ , where  $\omega_s = g_\mu (e\hbar/2m_\mu) B/\hbar = g_\mu/2 \times e/m_\mu B$  is the muon spin–flip *precession frequency* in the applied magnetic field and  $\omega_c = e/m_\mu B$  is the muon *cyclotron frequency*. Instead of eliminating the magnetic field by measuring  $\omega_c$ ,  $B$  is determined from proton *Nuclear Magnetic Resonance* (NMR) measurements. This procedure requires the value of  $\mu_\mu/\mu_p$  to extract  $a_\mu$  from the data. Fortunately, a high precision value for this ratio is available from the measurement of the hyperfine splitting (HFS) in muonium. One obtains<sup>3</sup>

$$a_\mu^{\text{exp}} = \frac{\bar{R}}{|\mu_\mu/\mu_p| - \bar{R}}, \quad (3.25)$$

<sup>3</sup>E-821 has measured  $\bar{R} = \omega_a/\tilde{\omega}_p = 0.003\,707\,206\,4(20)$  while using  $\lambda = \mu_\mu/\mu_p = 3.18334539(10)$  from muonium HFS. The new CODATA 2011 recommended value is  $\lambda = 3.183345107(84)$ , such that the updated  $a_\mu^{\text{exp}} = (11\,659\,208.9 \pm 5.4 \pm 3.3[6.3]) \times 10^{-10}$ .

where  $\bar{R} = \omega_a/\bar{\omega}_p$  and  $\bar{\omega}_p = (e/m_p c)\langle B \rangle$  is the free-proton NMR frequency corresponding to the average magnetic field seen by the muons in their orbits in the storage ring. We mention that for the electron a *Penning trap* is employed to measure  $a_e$  rather than a storage ring. The  $B$  field in this case can be eliminated via a measurement of the cyclotron frequency. The CODATA group [4] recommends to use

$$a_\mu^{\text{exp}} = \frac{g_e \omega_a m_\mu \mu_p}{2 \bar{\omega}_p m_e \mu_e} \quad (3.26)$$

as a representation in terms of precisely measured ratios which multiply the extremely precisely measured electron  $g_e$  value.<sup>4</sup> Both representations derive from  $a_\mu = \frac{e}{m} B$ ,  $B = \frac{\hbar\omega_p}{2\mu_p}$  and  $\mu_\mu = (1 + a_\mu) \frac{e\hbar}{2m_\mu c}$  and  $\mu_e = \frac{g_e}{2} \frac{e\hbar}{2m_e c}$  used in the second form.

On the theory side, the crucial point is that  $a_\ell$  is dimensionless, just a number, and must vanish at tree level in any renormalizable theory. As an effective interaction it would look like

$$\delta\mathcal{L}_{\text{eff}}^{\text{AMM}} = -\frac{\delta g}{2} \frac{e}{4m} \left\{ \bar{\psi}_L(x) \sigma^{\mu\nu} F_{\mu\nu}(x) \psi_R(x) + \bar{\psi}_R(x) \sigma^{\mu\nu} F_{\mu\nu}(x) \psi_L(x) \right\} \quad (3.27)$$

where  $\psi_L$  and  $\psi_R$  are Dirac fields of negative (left-handed  $L$ ) and positive (right-handed  $R$ ) chirality and  $F_{\mu\nu} = \partial_\mu A_\nu - \partial_\nu A_\mu$  is the electromagnetic field strength tensor. This Pauli term has dimension 5 ( $=2 \times 3/2$  for the two Dirac fields plus 1 for the photon plus 1 for the derivative included in  $F$ ) and thus would spoil renormalizability. In a renormalizable theory, however,  $a_\mu$  is a finite unambiguous prediction of that theory. It is testing the rate of helicity flip transition and is one of the most precisely measured electroweak observables. Of course the theoretical prediction only may agree with the experimental result to the extent that we know the complete theory of nature, within the experimental accuracy.

Before we start discussing the theoretical prediction for the magnetic moment anomaly, we will specify the parameters which we will use for the numerical evaluations below.

Since the lowest order result for  $a_\ell$  is proportional to  $\alpha$ , obviously, the most important basic parameter for calculating  $a_\mu$  is the fine structure constant  $\alpha$ . It is best determined now from the very recent extraordinary precise measurement of the electron anomalous magnetic moment [4–7]

$$a_e^{\text{exp}} = 0.001\,159\,652\,180\,76(27) [0.24 \text{ ppb}] \quad (3.28)$$

<sup>4</sup>The values are from the electron  $g - 2$ :  $g_e = -2.002\,319\,304\,361\,53(53)$  [0.26 ppt], from E821  $\bar{R} = \omega_a/\bar{\omega}_p = 0.003\,707\,206\,4(20)$  [0.54 ppm], from Muonium HFS experiments  $m_\mu/m_e = 206.768\,2843(52)$  [25 ppb] and  $\mu_p/\mu_e = -0.001519270384(12)$  [8 ppb].

which, confronted with its theoretical prediction as a series in  $\alpha$  (see Sect. 3.2.2 below) determines [6, 8–11]

$$\alpha^{-1}(a_e) = 137.035\,999\,1657(342) [0.25 \text{ ppb}] .$$

This new value has an uncertainty 20 times smaller than any preceding independent determination of  $\alpha$ . We will use the updated value

$$\alpha^{-1}(a_e) = 137.035\,999\,139(31) [0.25 \text{ ppb}] , \quad (3.29)$$

recommended by [4, 12], throughout in the calculation of  $a_\mu$ .

All QED contributions associated with diagrams with lepton-loops, where the “internal” lepton has mass different from the mass of the external one, depend on the corresponding mass ratio. These mass-dependent contributions differ for  $a_e$ ,  $a_\mu$  and  $a_\tau$ , such that lepton universality is broken:  $a_e \neq a_\mu \neq a_\tau$ . Lepton universality is broken in any case by the difference in the masses and whatever depends on them. Such mass-ratio dependent contributions start at two loops. For the evaluation of these contributions precise values for the lepton masses are needed. We will use the following values for the muon–electron and muon–tau mass ratios, and lepton masses [4, 7, 12–14]

$$\begin{aligned} m_\mu/m_e &= 206.768\,2826(46) , & m_\mu/m_\tau &= 0.059\,4649(54) \\ m_e &= 0.510\,998\,9461(31) \text{ MeV} , & m_\mu &= 105.658\,3745(24) \text{ MeV} \\ & & m_\tau &= 1776.82(16) \text{ MeV} . \end{aligned} \quad (3.30)$$

Note that the primary determination of the electron and muon masses come from measuring the ratio with respect to the mass of a nucleus and the masses are obtained in atomic mass units (amu). The conversion factor to MeV is more uncertain than the mass of the electron and muon in amu. The ratio of course does not suffer from the uncertainty of the conversion factor.

Other physical constants which we will need later for evaluating the weak contributions are the Fermi constant

$$G_\mu = 1.1663787(6) \times 10^{-5} \text{ GeV}^{-2} , \quad (3.31)$$

the weak mixing parameter<sup>5</sup> (here defined by  $\sin^2 \Theta_W = 1 - M_W^2/M_Z^2$ )

$$\sin^2 \Theta_W = 0.22290(29) \quad (3.32)$$

and the masses of the intermediate gauge bosons  $Z$  and  $W$

$$M_Z = 91.1876 \pm 0.0021 \text{ GeV} , \quad M_W = 80.385 \pm 0.015 \text{ GeV} . \quad (3.33)$$

---

<sup>5</sup>The effective value  $\sin^2 \Theta_{\text{eff}} = 0.23155(5)$  is determined from the vector to axialvector  $Zf\bar{f}$  coupling ratios in  $e^+e^- \rightarrow f\bar{f}$ .

For the Standard Model (SM) Higgs boson, recently discovered [15] by ATLAS [16] and CMS [17] at the LHC at CERN, the mass has been measured to be [12]

$$m_H = 125.09 \pm 0.21 \text{ (syst)} \pm 0.11 \text{ (stat)} \text{ GeV} . \tag{3.34}$$

We also mention here that virtual pion–pair production is an important contribution to the photon vacuum polarization and actually yields the leading hadronic contribution to the anomalous magnetic moment. For the dominating  $\pi^+\pi^-$  channel, the threshold is at  $2m_\pi$  with the pion mass given by

$$m_{\pi^\pm} = 139.570 \text{ 18 (35)} \text{ MeV} . \tag{3.35}$$

There is also a small contribution from  $\pi^0\gamma$  with threshold at  $m_{\pi^0}$  which has the value

$$m_{\pi^0} = 134.976 \text{ 6 (6)} \text{ MeV} . \tag{3.36}$$

Later we will also need the pion decay constant

$$F_\pi \simeq 92.21(14) \text{ MeV} . \tag{3.37}$$

For the quark masses needed in some cases we use running current quark masses in the  $\overline{\text{MS}}$  scheme [12, 13] with renormalization scale parameter  $\mu$ . For the light quarks  $q = u, d, s$  we give  $m_q = \bar{m}_q(\mu = 2 \text{ GeV})$ , for the heavier  $q = c, b$  the values at the mass as a scale  $m_q = \bar{m}_q(\mu = \bar{m}_q)$  and for  $q = t$  the pole mass:

$$\begin{aligned} m_u &= 2.3_{-0.5}^{+0.7} \text{ MeV} & m_d &= 4.8_{-0.5}^{+0.7} \text{ MeV} & m_s &= 95 \pm 5 \text{ MeV} \\ m_c &= 1.275 \pm 0.025 \text{ GeV} & m_b &= 4.18 \pm 0.03 \text{ GeV} & M_t &= 173.21 \pm 0.87 \text{ GeV} . \end{aligned} \tag{3.38}$$

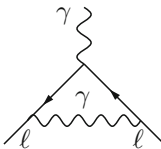
Within the SM the  $\overline{\text{MS}}$  mass of the top quark  $m_t(m_t)$  essentially agrees with the pole mass:  $m_t(m_t) \simeq M_t$  [18, 19].

This completes the list of the most relevant parameters and we may discuss the various contributions in turn now. This also can be read as an update of [20].

The profile of the most important contributions may be outlined as follows:

**(1) QED universal part:**

The by far largest QED/SM contribution comes from the one–loop QED diagram [21]



$$: a_e^{(2)} = a_\mu^{(2)} = a_\tau^{(2)} = \frac{\alpha}{2\pi} \tag{Schwinger 1948}$$

which we have calculated in Sect. 2.6.3, and which is universal for all charged leptons. As it is customary we indicate the perturbative order in powers of  $e$ , i.e.,  $a^{(n)}$  denotes an  $O(e^n)$  term, in spite of the fact that the perturbation expansion is usually represented as an expansion in  $\alpha = e^2/4\pi$ . Typically, analytic results for higher order terms may be expressed in terms of the Riemann zeta function

$$\zeta(n) = \sum_{k=1}^{\infty} \frac{1}{k^n} \quad (3.39)$$

and of the polylogarithmic integrals<sup>6</sup>

$$\text{Li}_n(x) = \frac{(-1)^{n-1}}{(n-2)!} \int_0^1 \frac{\ln^{n-2}(t) \ln(1-tx)}{t} dt = \sum_{k=1}^{\infty} \frac{x^k}{k^n}, \quad (3.40)$$

where  $\text{Li}_2(x)$  is often referred to as the Spence function  $\text{Sp}(x)$  (see (2.208) in Sect. 2.6.3 and [23] and references therein). Special  $\zeta(n)$  values we will need are

$$\zeta(2) = \frac{\pi^2}{6}, \quad \zeta(3) = 1.202\,056\,903\dots, \quad \zeta(4) = \frac{\pi^4}{90}, \quad \zeta(5) = 1.036\,927\,755\dots \quad (3.41)$$

Also the constants

$$\begin{aligned} \text{Li}_n(1) &= \zeta(n), \quad \text{Li}_n(-1) = -[1 - 2^{1-n}] \zeta(n) \\ a_4 &\equiv \text{Li}_4\left(\frac{1}{2}\right) = \sum_{n=1}^{\infty} 1/(2^n n^4) = 0.517\,479\,061\,674\dots, \end{aligned} \quad (3.42)$$

related to polylogarithms, will be needed later for the evaluation of analytical results. Since  $a_\mu$  is a number all QED contributions calculated in “one flavor QED”, with just one species of lepton, which exhibits *one* physical mass scale only, equal to the mass of the external lepton, are universal. The following universal contributions (one flavor QED) are known:

- 2-loop diagrams [7 diagrams] with one type of fermion lines yield

$$a_\ell^{(4)} = \left[ \frac{197}{144} + \frac{\pi^2}{12} - \frac{\pi^2}{2} \ln 2 + \frac{3}{4} \zeta(3) \right] \left( \frac{\alpha}{\pi} \right)^2. \quad (3.43)$$

The first calculation performed by Karplus and Kroll (1950) [24] later was recalculated and corrected by Petermann (1957) [25] and, independently, by Sommerfield

---

<sup>6</sup>The appearance of transcendental numbers like  $\zeta(n)$  and higher order polylogarithms  $\text{Li}_n(x)$  or so called harmonic sums is directly connected to the number of loops of a Feynman diagram. Typically, 2-loop results exhibit  $\zeta(3)$  3-loop ones  $\zeta(5)$  etc. of increasing transcendentality [22].

(1957) [26]. An instructive compact calculation based on the dispersion theoretic approach is due to Terentev (1962) [27].

- 3-loop diagrams [72 diagrams] with common fermion lines

$$\begin{aligned}
 a_\ell^{(6)} = & \left[ \frac{28259}{5184} + \frac{17101}{810} \pi^2 - \frac{298}{9} \pi^2 \ln 2 + \frac{139}{18} \zeta(3) \right. \\
 & + \frac{100}{3} \left\{ \text{Li}_4 \left( \frac{1}{2} \right) + \frac{1}{24} \ln^4 2 - \frac{1}{24} \pi^2 \ln^2 2 \right\} \\
 & \left. - \frac{239}{2160} \pi^4 + \frac{83}{72} \pi^2 \zeta(3) - \frac{215}{24} \zeta(5) \right] \left( \frac{\alpha}{\pi} \right)^3
 \end{aligned} \tag{3.44}$$

This is the famous analytical result of Laporta and Remiddi (1996) [28], which largely confirmed an earlier numerical result of Kinoshita [29]. For the evaluation of (3.44) one needs the constants given in (3.41) and (3.42) before.

- 4-loop diagrams [891 diagrams] with common fermion lines so far have been calculated by numerical methods mainly by Kinoshita and collaborators. The status had been summarized by Kinoshita and Marciano (1990) [30] some time ago. Since then, the result has been further improved by Kinoshita and his collaborators (2002/2005/2007/2012/2014) [9, 10, 31–33]. They find

$$- 1.91298(84) \left( \frac{\alpha}{\pi} \right)^4 ,$$

by improving earlier results. In a seminal paper Laporta [11] obtained the high precision (quasi-exact) result

$$- 1.912\,245\,764\,9 \dots \left( \frac{\alpha}{\pi} \right)^4 ,$$

which agrees to  $0.9\sigma$  with the previous result from [10] and we will use in the following.

Recently, for the first time, the universal 5-loop result has been worked out in [10, 33–35]. An evaluation of all 12672 diagrams with the help of an automated code generator yields the result

$$7.795(336) \left( \frac{\alpha}{\pi} \right)^5 .$$

The error is due to the statistical fluctuation in the Monte-Carlo integration of the Feynman amplitudes by the VEGAS routine. With the new result for the universal 5-loop term the largest uncertainty in the prediction of  $a_e$  has reduced by a factor of 4.5 from the previous one.

Collecting the universal terms we have

$$\begin{aligned}
 a_\ell^{\text{uni}} &= 0.5 \left(\frac{\alpha}{\pi}\right) - 0.328\,478\,965\,579\,193\,78\dots \left(\frac{\alpha}{\pi}\right)^2 \\
 &\quad + 1.181\,241\,456\,587\dots \left(\frac{\alpha}{\pi}\right)^3 - 1.912\,245\,764\,9\dots \left(\frac{\alpha}{\pi}\right)^4 + 7.795(336) \left(\frac{\alpha}{\pi}\right)^5 \\
 &= 0.001\,159\,652\,176\,42(26)(4)[26]\dots \tag{3.45}
 \end{aligned}$$

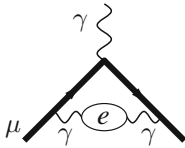
for the one-flavor QED contribution. The three errors are from the error of  $\alpha$  given in (3.29) and from the numerical uncertainties of the  $\alpha^5$  coefficients, respectively.

It is interesting to note that the first term  $a_\ell^{(2)} \simeq 0.00116141\dots$  contributes the first three significant digits. Thus the anomalous magnetic moment of a lepton is an effect of about 0.12%,  $g_\ell/2 \simeq 1.00116\dots$ , but in spite of the fact that it is so small we know  $a_e$  and  $a_\mu$  more precisely than most other precision observables.

**(2) QED mass dependent part:**

Since fermions, as demanded by the SM,<sup>7</sup> only interact via photons or other spin one gauge bosons, mass dependent corrections only may show up at the two-loop level via photon *vacuum polarization* effects. There are two different regimes for the mass dependent effects [36, 37]:

- LIGHT internal masses give rise to potentially large logarithms of mass ratios which get singular in the limit  $m_{\text{light}} \rightarrow 0$



$$a_\mu^{(4)}(\text{vap}, e) = \left[ \frac{1}{3} \ln \frac{m_\mu}{m_e} - \frac{25}{36} + O\left(\frac{m_e}{m_\mu}\right) \right] \left(\frac{\alpha}{\pi}\right)^2 .$$

Here we have a typical result for a light field which produces a large logarithm  $\ln \frac{m_\mu}{m_e} \simeq 5.3$ , such that the first term  $\sim 2.095$  is large relative to a typical constant second term  $-0.6944$ . Here<sup>8</sup> the exact two-loop result is

$$a_\mu^{(4)}(\text{vap}, e) \simeq 1.094\,258\,3092(72) \left(\frac{\alpha}{\pi}\right)^2 = 5.90406006(4) \times 10^{-6} .$$

The error is due to the uncertainty in the mass ratio ( $m_e/m_\mu$ ).

The kind of leading short distance log contribution just discussed, which is related to the UV behavior,<sup>9</sup> in fact may be obtained from a renormalization group type argument. In Sect. 2.6.5 (2.233) we have shown that if we replace in the one-loop result  $\alpha \rightarrow \alpha(m_\mu)$  we obtain

<sup>7</sup>Interactions are known to derive from a local gauge symmetry principle, which implies the structure of gauge couplings, which must be of vector (V) or axial-vector (A) type.

<sup>8</sup>The leading terms shown yield  $5.84199477 \times 10^{-6}$ .

<sup>9</sup>The muon mass  $m_\mu$  here serves as a UV cut-off, the electron mass as an IR cut-off, and the relevant integral reads



$$a_\mu = \frac{1}{2} \frac{\alpha}{\pi} \left( 1 + \frac{2}{3} \frac{\alpha}{\pi} \ln \frac{m_\mu}{m_e} \right), \tag{3.46}$$

which reproduces precisely the leading term of the two-loop result. RG type arguments, based on the related Callan–Symanzik (CS) equation approach, were further developed and refined in [38, 39]. The CS equation is a differential equation which quantifies the response of a quantity to a change of a physical mass like  $m_e$  relative to the renormalization scale which is  $m_\mu$  if we consider  $a_\mu$ . For the leading  $m_e$ -dependence of  $a_\mu$ , neglecting all terms which behave like powers of  $m_e/m_\mu$  for  $m_e \rightarrow 0$  at fixed  $m_\mu$ , the CS equation takes the simple homogeneous form

$$\left( m_e \frac{\partial}{\partial m_e} + \beta(\alpha) \alpha \frac{\partial}{\partial \alpha} \right) a_\mu^{(\infty)} \left( \frac{m_\mu}{m_e}, \alpha \right) = 0, \tag{3.47}$$

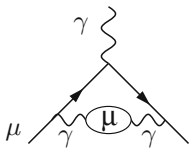
where  $a_\mu^{(\infty)}$  denotes the contribution to  $a_\mu$  from powers of logarithms  $\ln \frac{m_\mu}{m_e}$  and constant terms and  $\beta(\alpha)$  is the QED  $\beta$ -function. The latter governs the charge screening of the electromagnetic charge, which will be discussed below. The charge is running according to (resummed one-loop approximation)

$$\alpha(\mu) = \frac{\alpha}{1 - \frac{2}{3} \frac{\alpha}{\pi} \ln \frac{\mu}{m_e}} \tag{3.48}$$

which in linear approximation yields (3.46).

We continue with the consideration of the other contributions. For comparison we also give the result for the

- EQUAL internal masses case which yields a pure number and has been included in the  $a_\ell^{(4)}$  universal part (3.43) already:



$$a_\mu^{(4)}(\text{vap}, \mu) = \left[ \frac{119}{36} - \frac{\pi^2}{3} \right] \left( \frac{\alpha}{\pi} \right)^2.$$

This no scale result shows another typical aspect of perturbative answers. There is a rational term of size 3.3055... and a transcendental  $\pi^2$  term of very similar size 3.2899... but of opposite sign which yields as a sum a result which is only 0.5% of the individual terms:

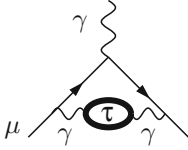
---

(Footnote 9 continued)

$$\int_{m_e}^{m_\mu} \frac{dE}{E} = \ln \frac{m_\mu}{m_e}.$$

$$a_\mu^{(4)}(\text{vap}, \mu) \simeq 0.015\,687\,4219 \left(\frac{\alpha}{\pi}\right)^2 = 8.464\,13319 \times 10^{-8}. \quad (3.49)$$

• HEAVY internal masses decouple<sup>10</sup> in the limit  $m_{\text{heavy}} \rightarrow \infty$  and thus only yield small power corrections



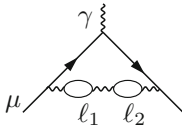
$$a_\mu^{(4)}(\text{vap}, \tau) = \left[ \frac{1}{45} \left(\frac{m_\mu}{m_\tau}\right)^2 + O\left(\frac{m_\mu^4}{m_\tau^4} \ln \frac{m_\tau}{m_\mu}\right) \right] \left(\frac{\alpha}{\pi}\right)^2.$$

Note that “heavy physics” contributions, from mass scales  $M \gg m_\mu$ , typically are proportional to  $m_\mu^2/M^2$ . This means that besides the order in  $\alpha$  there is an extra suppression factor, e.g.  $O(\alpha^2) \rightarrow Q(\alpha^2 \frac{m_\mu^2}{M^2})$  in our case. To unveil new heavy states thus requires a corresponding high precision in theory and experiment. For the  $\tau$  the contribution is relatively tiny

$$a_\mu^{(4)}(\text{vap}, \tau) \simeq 0.000\,078\,079(14) \left(\frac{\alpha}{\pi}\right)^2 = 4.2127(8) \times 10^{-10},$$

with error from the mass ratio ( $m_\mu/m_\tau$ ). However, at the level of accuracy reached by the Brookhaven experiment ( $63 \times 10^{-11}$ ), the contribution is non-negligible.

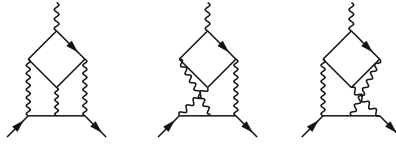
At the next higher order, in  $a^{(6)}$  up to two internal closed fermion loops show up. The photon vacuum polarization (VP) insertions into photon lines again yield mass dependent effects if one or two of the  $\mu$  loops of the universal contributions are replaced by an electron or a  $\tau$ . These contributions will be discussed in more detail in Chap. 4. Here we just give the numerical results for the coefficients of  $(\frac{\alpha}{\pi})^3$  [40–42]:



$$\begin{aligned} A_\mu^{(6)}(\text{vap}, e) &= 1.920\,455\,123(28), \\ A_\mu^{(6)}(\text{vap}, \tau) &= -0.001\,782\,61(27), \\ A_\mu^{(6)}(\text{vap}, e, \tau) &= 0.000\,527\,76(10). \end{aligned}$$

Besides these photon self-energy corrections, a new kind of contributions are the so called *light-by-light scattering* (LbL) insertions: closed fermion loops with four photons attached. Light-by-light scattering  $\gamma\gamma \rightarrow \gamma\gamma$  is a fermion-loop induced process between real on-shell photons. There are 6 diagrams which follow from the first one below, by permutation of the photon vertices on the external muon line:

<sup>10</sup>The decoupling-theorem 2.10 infers that in theories like QED or QCD, where couplings and masses are independent parameters of the Lagrangian, a heavy particle of mass  $M$  decouples from physics at lower scales  $E_0$  as  $E_0/M$  for  $M \rightarrow \infty$ .



plus the ones obtained by reversing the direction of the fermion loop. Remember that closed fermion loops with three photons vanish by Furry’s theorem. Again, besides the equal mass case  $m_{\text{loop}} = m_\mu$  there are two different regimes [43, 44]:

- LIGHT internal masses also in this case give rise to potentially large logarithms of mass ratios which get singular in the limit  $m_{\text{light}} \rightarrow 0$

$$a_\mu^{(6)}(\text{lbl}, e) = \left[ \frac{2}{3} \pi^2 \ln \frac{m_\mu}{m_e} + \frac{59}{270} \pi^4 - 3 \zeta(3) - \frac{10}{3} \pi^2 + \frac{2}{3} + O\left(\frac{m_e}{m_\mu} \ln \frac{m_\mu}{m_e}\right) \right] \left(\frac{\alpha}{\pi}\right)^3.$$

This again is a light loop which yields an unexpectedly large contribution

$$a_\mu^{(6)}(\text{lbl}, e) \simeq 20.947\,924\,85(14) \left(\frac{\alpha}{\pi}\right)^3 = 2.625\,351\,01(2) \times 10^{-7},$$

with error from the  $(m_e/m_\mu)$  mass ratio. Historically, it was calculated first numerically by Aldins et al. [45], after a  $1.7 \sigma$  discrepancy with the CERN measurement [46] in 1968 showed up.<sup>11</sup>

For comparison we also present the

- EQUAL internal masses case which yields a pure number which is included in the  $a_e^{(6)}$  universal part (3.44) already:

$$a_\mu^{(6)}(\text{lbl}, \mu) = \left[ \frac{5}{6} \zeta(5) - \frac{5}{18} \pi^2 \zeta(3) - \frac{41}{540} \pi^4 - \frac{2}{3} \pi^2 \ln^2 2 + \frac{2}{3} \ln^4 2 + 16a_4 - \frac{4}{3} \zeta(3) - 24\pi^2 \ln 2 + \frac{931}{54} \pi^2 + \frac{5}{9} \right] \left(\frac{\alpha}{\pi}\right)^3,$$

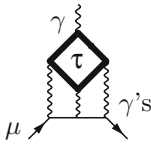
<sup>11</sup>The result of [45] was  $2.30 \pm 0.14 \times 10^{-7}$  pretty close to the “exact” answer above. The occurrence of such large terms of course has a physical interpretation [47]. Firstly, the large logs  $\ln(m_\mu/m_e)$  are due to a logarithmic UV divergence in the limit  $m_\mu \rightarrow \infty$ , i.e.,  $m_\mu$  serves as a UV cut-off, in conjunction with an IR singularity in the limit  $m_e \rightarrow 0$ , i.e.,  $m_e$  serves as an IR cut-off:  $\int_{m_e}^{m_\mu} \frac{dE}{E} = \ln \frac{m_\mu}{m_e}$ . The integral is large because of the large range  $[m_e, m_\mu]$  and an integrand with the property that it is contributing equally at all scales. Secondly, and this is the new point here, there is an unusual  $\pi^2 \sim 10$  factor in the coefficient of the large log. This enhancement arises from the LbL scattering sub-diagram where the electron is moving in the field of an almost static non-relativistic muon. A non-relativistic spin-flip interaction (required to contribute to  $a_\mu$ ) gets dressed by Coulomb interactions between muon and electron, which produces the large  $\pi^2$  factor.

where  $a_4$  is the constant defined in (3.42). The single scale QED contribution is much smaller

$$a_\mu^{(6)}(\text{lbl}, \mu) \simeq 0.371005292 \left(\frac{\alpha}{\pi}\right)^3 = 4.64971650 \times 10^{-9} \quad (3.50)$$

but is still a substantial contributions at the required level of accuracy.

• HEAVY internal masses again decouple in the limit  $m_{\text{heavy}} \rightarrow \infty$  and thus only yield small power correction



$$a_\mu^{(6)}(\text{lbl}, \tau) = \left[ \left[ \frac{3}{2} \zeta(3) - \frac{19}{16} \right] \left( \frac{m_\mu}{m_\tau} \right)^2 + O \left( \frac{m_\mu^4}{m_\tau^4} \ln^2 \frac{m_\tau}{m_\mu} \right) \right] \left( \frac{\alpha}{\pi} \right)^3 .$$

As expected this heavy contribution is power suppressed yielding

$$a_\mu^{(6)}(\text{lbl}, \tau) \simeq 0.00214324(38) \left(\frac{\alpha}{\pi}\right)^3 = 2.68607(48) \times 10^{-11} ,$$

and therefore would play a significant role at a next level of precision experiments only. Again the error is from the  $(m_\mu/m_\tau)$  mass ratio.

We mention that except for the mixed term  $A_\mu^{(6)}(\text{vap}, e, \tau)$ , which has been worked out as a series expansion in the mass ratios [41, 42], all contributions are known analytically in exact form [40, 43]<sup>12</sup> up to 3 loops. At 4 loops only a few terms are known analytically [49, 50]. Again the relevant 4-loop contributions have been evaluated by numerical integration methods by Kinoshita and Nio [31, 51]. The universal part is now superseded by Laporta's high-precision result [11]. After earlier estimates of the 5-loop term in [52–54], finally the pioneering complete 5-loop calculation by Aoyama, Hayakawa, Kinoshita and Nio [51] has been completed to contribute with  $A_2^{(10)}(m_\mu/m_e) = 663(20)$ . A number of partial results based on asymptotic expansion techniques have been obtained in [55]. More recent result have been presented in [39, 50, 56–58]. Results largely confirm the numerical calculations.

Combining the universal and the mass dependent terms discussed so far we arrive at the following QED result for  $a_\mu$

$$a_\mu^{\text{QED}} = \frac{\alpha}{2\pi} + 0.765857423(16) \left(\frac{\alpha}{\pi}\right)^2 + 24.05050982(28) \left(\frac{\alpha}{\pi}\right)^3 + 130.8734(60) \left(\frac{\alpha}{\pi}\right)^4 + 751.917(932) \left(\frac{\alpha}{\pi}\right)^5 . \quad (3.51)$$

<sup>12</sup>Explicitly, the papers present expansions in the mass ratios; some result have been extended in [44] and cross checked against the full analytic result in [48].

Growing coefficients in the  $\alpha/\pi$  expansion reflect the presence of large  $\ln \frac{m_\mu}{m_e} \simeq 5.3$  terms coming from electron loops. In spite of the strongly growing expansion coefficients the convergence of the perturbation series is excellent

# n of loops	$C_i [(\alpha/\pi)^n]$	$a_\mu^{\text{QED}} \times 10^{11}$
1	+ 0.5	116140973.242 (26)
2	+ 0.765 857 423 (16)	413217.627 (9)
3	+ 24.050 509 82 (28)	30141.9022 (4)
4	+ 130.8734 (60)	380.990 (17)
5	+ 751.917 (932)	5.0845 (63)
tot		116584718.859 (0.034)

because  $\alpha/\pi$  is a truly small expansion parameter.

Now we have to address the question what happens beyond QED. What is measured in an experiment includes effects from the real world and we have to include the contributions from all known particles and interactions such that from a possible deviation between theory and experiment we may get a hint of the yet unknown physics.

Going from QED of leptons to the SM the most important step is to include the hadronic effects mediated by the quarks, which in the SM sit in families together with the leptons and neutrinos. The latter being electrically neutral do not play any role, in contrast to the charged quarks. The *strong interaction effects* are showing up in particular through the hadronic structure of the photon via vacuum polarization starting at  $O(\alpha^2)$  or light-by-light scattering starting at  $O(\alpha^3)$ .

### (3) Hadronic VP effects:

Formally, these are the contributions obtained by replacing lepton-loops by quark-loops (see Fig. 3.2), however, the quarks are strongly interacting via gluons as described by the  $SU(3)_{\text{color}}$  gauge theory QCD [59] (see Sect. 2.8). While electromagnetic and weak interactions are weak in the sense that they allow us to perform perturbation expansions in the coupling constants, strong interactions are weak only at high energies as inferred by the property of asymptotic freedom (anti-screening).<sup>13</sup> At energies above about 2 GeV perturbative QCD (pQCD) may be applied as well. In the regime of interest to us here, however, perturbative QCD fails. The strength of the strong coupling “constant” increases dramatically as we approach lower energies. This is firmly illustrated by Fig. 3.3, which shows a compilation of measured strong coupling constants as a function of energy in comparison to perturbative QCD. The latter seems to describe very well the running of  $\alpha_s$  down to 2 GeV. Fortunately the leading order hadronic effects are vacuum polarization type corrections, which can

<sup>13</sup>Asymptotic freedom, discovered in 1973 by Politzer, Gross and Wilczek [60] (Nobel Prize 2004), is one of the key properties of QCD and explains why at high enough energies one observes quasi-free quarks, as in deep inelastic scattering (DIS) of electrons on protons. Thus, while quarks remain imprisoned inside color neutral hadrons (quark confinement), at high enough energies (so called hard subprocesses) the *quark parton model* (QPM) of free quarks may be a reasonable approximation, which may be systematically improved by including the perturbative corrections.

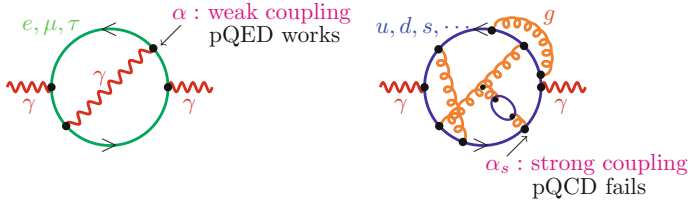


**Fig. 3.2** The hadronic analog of the lepton loops

**Fig. 3.3** A compilation of  $\alpha_s$  measurements in a plot from Ref. [12]. The lowest point shown is at the  $\tau$  lepton mass  $M_\tau = 1.78$  GeV where  $\alpha_s(M_\tau) = 0.322 \pm 0.030$ . Resource the Review of Particle Physics (2016)

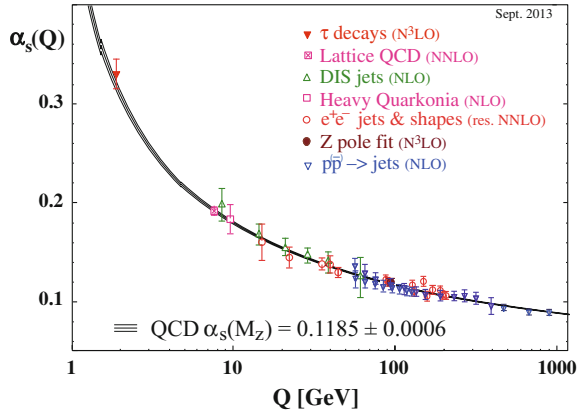
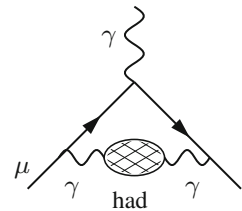


**Fig. 3.4** The leading order hadronic vacuum polarization diagram



be safely evaluated by exploiting causality (analyticity) and unitarity (optical theorem) together with experimental low energy data. The imaginary part of the photon self-energy function  $\Pi'_\gamma(s)$  (see Sect. 2.6.1) is determined via the optical theorem by the total cross section of hadron production in electron-positron annihilation:

$$\sigma(s)_{e^+e^- \rightarrow \gamma^* \rightarrow \text{hadrons}} = \frac{4\pi^2\alpha}{s} \frac{1}{\pi} \text{Im} \Pi_\gamma^{\text{had}}(s) . \quad (3.52)$$

The leading Hadronic Vacuum Polarization (HVP) contribution is represented by the diagram Fig. 3.4, which has a representation as a dispersion integral

$$a_\mu = \frac{\alpha}{\pi} \int_0^\infty \frac{ds}{s} \frac{1}{\pi} \text{Im} \Pi_\gamma^{\text{had}}(s) K(s) , \quad K(s) \equiv \int_0^1 dx \frac{x^2(1-x)}{x^2 + \frac{s}{m_\mu^2}(1-x)} . \quad (3.53)$$

As a result the leading non-perturbative hadronic contributions  $a_\mu^{\text{had}}$  can be obtained in terms of  $R_\gamma(s) \equiv \sigma^{(0)}(e^+e^- \rightarrow \gamma^* \rightarrow \text{hadrons})/\frac{4\pi\alpha^2}{3s}$  data via the dispersion integral:

$$a_\mu^{\text{had}} = \left(\frac{\alpha m_\mu}{3\pi}\right)^2 \left( \int_{m_{\pi^0}^2}^{E_{\text{cut}}^2} ds \frac{R_\gamma^{\text{data}}(s) \hat{K}(s)}{s^2} + \int_{E_{\text{cut}}^2}^{\infty} ds \frac{R_\gamma^{\text{pQCD}}(s) \hat{K}(s)}{s^2} \right), \quad (3.54)$$

where the rescaled kernel function  $\hat{K}(s) = 3s/m_\mu^2 K(s)$  is a smooth bounded function, increasing from 0.63... at  $s = 4m_\pi^2$  to 1 as  $s \rightarrow \infty$ . The  $1/s^2$  enhancement at low energy implies that the  $\rho \rightarrow \pi^+\pi^-$  resonance is dominating the dispersion integral ( $\sim 75\%$ ). Data can be used up to energies where  $\gamma - Z$  mixing comes into play at about  $E_{\text{cut}} = 40$  GeV. However, by the virtue of asymptotic freedom, perturbative Quantum Chromodynamics (see p. 145) (pQCD) gets the more reliable the higher the energy and, in fact, it may be used safely in regions away from the flavor thresholds, where resonances show up:  $\rho, \omega, \phi$ , the  $J/\psi$  series and the  $\Upsilon$  series. We thus use perturbative QCD [61, 62] from 5.2 to 9.6 GeV and for the high energy tail above 13 GeV, as recommended in [61–63].

Hadronic cross section measurements  $e^+e^- \rightarrow \text{hadrons}$  at electron-positron storage rings started in the early 1960's and continued up to date. Since our analysis [64] in 1995 data from MD1 [65], BES-II [66] and from CMD-2 [67] have lead to a substantial reduction in the hadronic uncertainties on  $a_\mu^{\text{had}}$ . More recently, KLOE [68], SND [69] and CMD-2 [70] published new measurements in the region below 1.4 GeV. My up-to-date evaluation of the leading order HVP yields [71–74]

$$a_\mu^{\text{had}(1)} = (688.77 \pm 3.38[688.07 \pm 4.14]) \times 10^{-10}. \quad (3.55)$$

The result also includes  $\tau$ -decay spectral data (the  $I=1$  part corrected for isospin breaking) in the range [0.63–0.96] GeV as estimated in [72] (see Chap. 5, Sect. 5.1.10). Table 3.1 gives more details about the origin of contributions and errors from different regions. A recent analysis [75] (also see [76, 77]) using the precise  $\pi\pi$  scattering data to constrain the low energy tail below 0.63 GeV (see (5.100) in Chap. 5) allows one to improve the estimate to

$$a_\mu^{\text{had}(1)} = (689.46 \pm 3.25) \times 10^{-10}. \quad (3.56)$$

A list of data based evaluations by different groups is presented in Table 3.2. The list documents the big efforts made by experiments within the past decade to provide more and more accurate data, which are the indispensable input for controlling non-perturbative strong interaction effects. Differences in errors come about mainly by utilizing more “theory-driven” concepts: use of selected data sets only, extended use of perturbative QCD in place of data [assuming local duality], sum rule methods, low

**Table 3.1** Contributions and errors from different energy ranges

Energy range	$a_\mu^{\text{had}} \times 10^{10}$ [in %]	(error) $\times 10^{10}$	rel. err. (%)	abs. err. (%)
$\rho, \omega$ ( $E < 2M_K$ )	541.25 [78.7%]	(2.84)	0.5	47.6
$2M_K < E < 2$ GeV	95.63 [13.9%]	(2.77)	3.1	45.2
$2$ GeV $< E < M_{J/\psi}$	21.63 [3.1%]	(0.93)	4.3	5.1
$M_{J/\psi} < E < 5.2$ GeV	20.34 [3.0%]	(0.59)	2.9	2.1
$5.2$ GeV $< E < M_\Upsilon$ pQCD	6.27 [0.9%]	(0.01)	0.1	0.0
$M_\Upsilon < E < E_{\text{cut}}$	0.98 [0.1%]	(0.05)	5.2	0.0
$E_{\text{cut}} < E$ pQCD	1.96 [0.3%]	(0.00)	0.0	0.0
$E < E_{\text{cut}}$ data	679.84 [98.8%]	(4.11)	0.6	100
Total	688.07 [100%]	(4.11)	0.6	100

energy effective methods [78]. Progress is essentially correlated with the availability of new data from Novosibirsk (NSK) [69, 70, 79], Frascati (KLOE) [80–82], SLAC (BaBar) [83] and Beijing (BES-III) [84].<sup>14</sup> In the last 15 years  $e^+e^-$  cross-section measurements have dramatically improved, from energy scans [69, 70, 79] (SCAN) at Novosibirsk (NSK) and later, using the radiative return mechanism, measurements via initial state radiation (ISR) at meson factories [80–84]. Still the most precise ISR measurements from KLOE and BaBar are in conflict and the new, although still somewhat less precise, ISR data from BES-III help to clarify this tension. The BES-III result for  $a_\mu^{\pi\pi, \text{LO}}$  (0.6 – 0.9 GeV) is found to be in good agreement with all KLOE values, while a  $1.7 \sigma$  lower value is observed with respect to the BaBar result. Other data recently collected, and published up to the end of 2014, include the  $e^+e^- \rightarrow 3(\pi^+\pi^-)$  data from CMD-3 [90], the  $e^+e^- \rightarrow \omega\pi^0 \rightarrow \pi^0\pi^0\gamma$  from SND [91] and several data sets collected by BaBar in the ISR mode<sup>15</sup> [92–94]. These data samples highly increase the available statistics for the annihilation channels opening above 1 GeV and lead to significant improvements. Recent/preliminary results also included are  $e^+e^- \rightarrow \pi^+\pi^-\pi^0$  from Belle,  $e^+e^- \rightarrow K^+K^-$  from CMD-3,  $e^+e^- \rightarrow K^+K^-$  from SND. The BES-III data sample is included in the last four entries of the table.

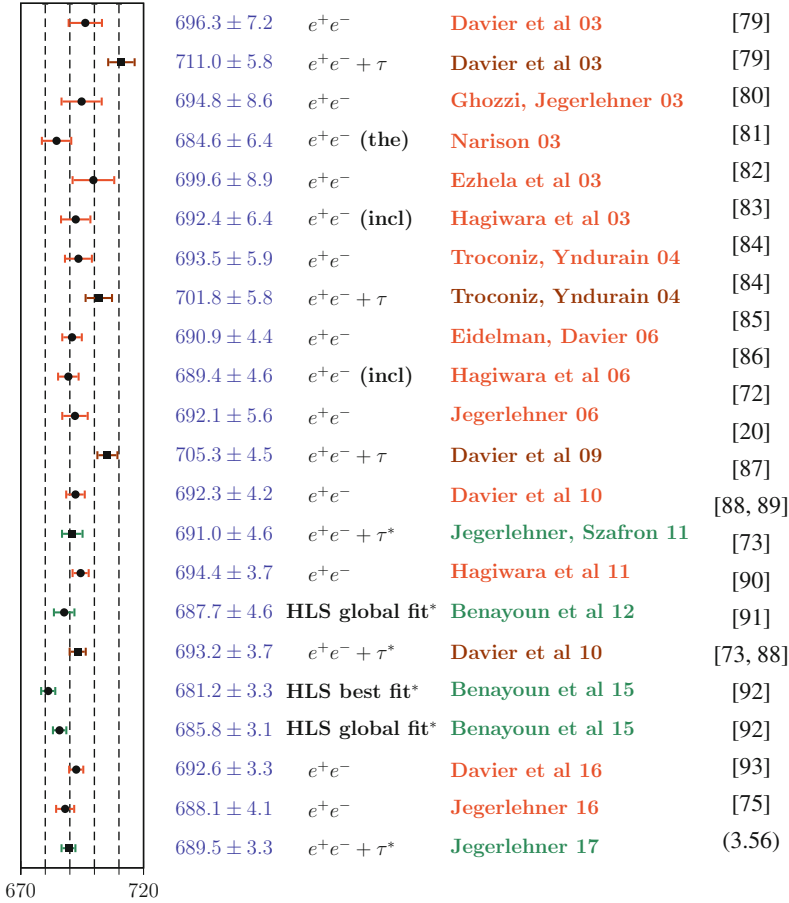
Besides the true  $e^+e^-$  data measured by energy scans and the ISR method, the  $I = 1$  isovector part of  $e^+e^- \rightarrow$  hadrons can be obtained in an alternative way by using the precise vector spectral functions from hadronic  $\tau$ -decays  $\tau \rightarrow \nu_\tau +$  hadrons via an isospin rotation [95]. For the dominating  $\pi\pi$  channel  $\tau$  decay spectra

<sup>14</sup>The analysis [85] does not include exclusive data in a range from 1.43 to 2 GeV; therefore also the important exclusive channels BaBar data are not included in that range. In [86–89] pQCD is used in the extended ranges 1.8–3.7 GeV and above 5.0 GeV and in [87] KLOE data are not included. More recently a reanalysis of the KLOE08 data were released as KLOE12 set, which was first included in the evaluation [73].

<sup>15</sup>Including the  $p\bar{p}$ ,  $K^+K^-$ ,  $K_L K_S$ ,  $K_L K_S \pi^+\pi^-$ ,  $K_S K_S \pi^+\pi^-$ ,  $K_S K_S K^+K^-$  final states.



**Table 3.2** Some recent evaluations of  $a_\mu^{\text{had}(1)}$  (in units  $10^{-10}$ ). The Table illustrates the progress since 2003, when precise data from Novosibirsk became available. Further progress has been possible with the data obtained by the ISR method at the  $\phi$ -factory Daphne at Frascati (KLOE detector) and the  $B$ -factory PEP-II at SLAC (BaBar detector) and with the BEPC storage ring at Beijing (BES detector)



have been measured by the ALEPH, OPAL, CLEO and Belle experiments [96–100]. After isospin violating corrections, due to photon radiation and the mass splitting  $m_d - m_u \neq 0$ , have been applied, there remains an unexpectedly large discrepancy between the  $e^+e^-$ - and the  $\tau$ -based determinations of  $a_\mu$  [86–89], as may be seen in Table 3.2. This  $\tau$  versus  $e^+e^-$  data puzzle has been persisting for several years. Possible explanations are so far unaccounted isospin breaking [101] or experimental problems with the data. Since the  $e^+e^-$ -data are more directly related to what is required in the dispersion integral, one usually advocates to use the  $e^+e^-$  data only.

The puzzle at the end disappeared, after isospin breaking by  $\gamma - \rho^0$  mixing, missing in the charged  $\tau$  channel, has been accounted for [72]. The point is the correct modeling of the Vector Meson Dominance (VMD) mechanism, which, by including  $\rho$ ,  $\omega$ ,  $\phi$  as well results in the Hidden Local Symmetry (HLS) model parametrization of the low energy data [73, 102] [up to including the  $\phi$  resonance]. This a low effective Lagrangian field theory approach, which includes the VMD model in accord with low energy structure of QCD. A ‘‘HLS best fit’’ is obtained for the data configuration NSK+KLOE10+KLOE12+BES-III+ $\tau$ . The ‘‘HLS global fit’’ includes the BaBar  $\pi\pi$  spectrum as well. In Table 3.2 results including  $\tau$  corrected for the  $\gamma - \rho^0$  mixing are marked by the asterisk \*. A comprehensive analysis of the hadronic effects will be presented in Chap. 5, Sect. 5.1. See also the comments to Fig. 7.1.

At next-to-leading order (NLO),  $O(\alpha^3)$ , diagrams of the type shown in Fig. 3.5a–c have to be calculated, where the first diagram stands for a class of higher order hadronic contributions obtained if one replaces in any of the first 6 two-loop diagrams of Fig. 4.2, one internal photon line by a dressed one. The relevant kernels for the corresponding dispersion integrals have been calculated analytically in [103] and appropriate series expansions were given in [104] (for earlier estimates see [105, 106]). Based on my recent compilation of the  $e^+e^-$  data [74] I obtain

$$a_\mu^{(6)}(\text{vap, had}) = -99.27(0.87) \times 10^{-11},$$

in accord with previous evaluations [95, 104, 106, 107] (see Table 5.7). The errors include statistical and systematic errors added in quadrature. Very recently the relevant next-to-next-to-leading order (NNLO),  $O(\alpha^4)$ , hadronic contributions, represented by diagrams of the type also shown in Fig. 3.5a–h, have been estimated [108, 109]

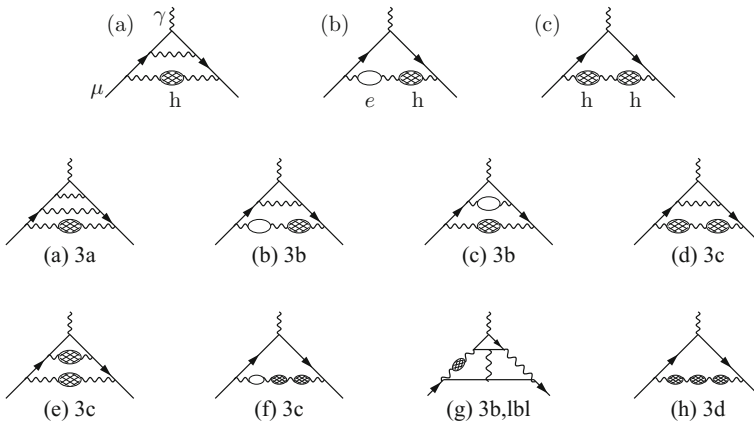


**Fig. 3.5** Higher order (HO) vacuum polarization contributions

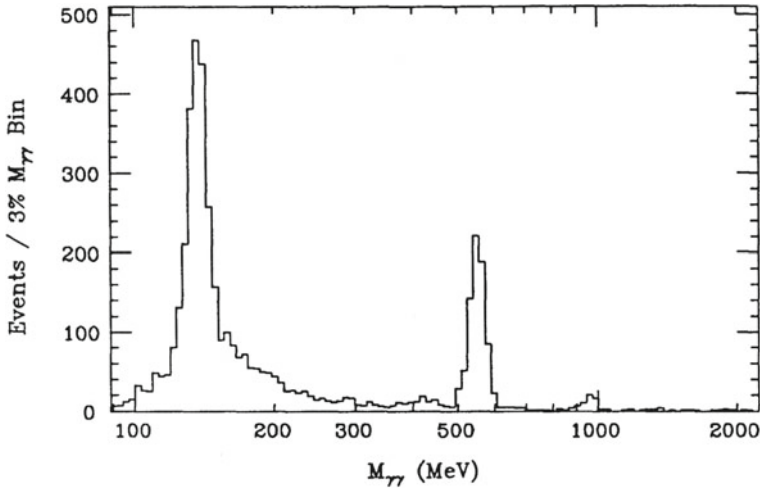


**Fig. 3.6** The spectrum of invariant  $\gamma\gamma$  masses obtained with the Crystal Ball detector [110]. The three rather pronounced spikes seen are the  $\gamma\gamma \rightarrow$  pseudoscalar (PS)  $\rightarrow \gamma\gamma$  excitations: PS =  $\pi^0, \eta, \eta'$

$$a_\mu^{(8)}(\text{vap, had}) = 12.21(0.10) \times 10^{-11},$$

which amounts to a 10% reduction of the NLO HVP result.

#### (4) Hadronic LbL effects:

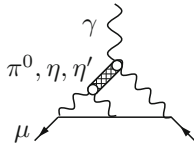
A much more problematic set of hadronic corrections are those related to hadronic light-by-light scattering, which sets in only at order  $O(\alpha^3)$ , fortunately. However, we already know from the leptonic counterpart that this contribution could be dramatically enhanced. It was estimated for the first time in [105]. Even for real-photon light-by-light scattering, perturbation theory is far from being able to describe reality, as the reader may convince himself by a glance at Fig. 3.6, showing sharp spikes of  $\pi^0, \eta$  and  $\eta'$  production, while pQCD predicts a smooth continuum.<sup>16</sup> As a contribution to the anomalous magnetic moment three of the four photons are virtual and to be integrated over all four-momentum space, such that a direct experimental input for the non-perturbative dressed four-photon correlator is not available. In this case one has to resort to the low energy effective descriptions of QCD like *Chiral Perturbation Theory* (CHPT) extended to include vector-mesons. This Resonance Lagrangian Approach (RLA) is realizing vector-meson dominance ideas in accord with the low energy structure of QCD [111]. Other effective theories are the Extended Nambu-Jona-Lasinio (ENJL) model [112] (see also [113]) or the very

<sup>16</sup>The pion which gives the by far largest contribution is a quasi Goldstone boson. In the chiral limit of vanishing light quark masses  $m_u = m_d = m_s = 0$  pions and Kaons are true Goldstone bosons which exist due to the spontaneous breakdown of the chiral  $U(N_f)_V \otimes U_A(N_f)$  ( $N_f = 3$ ) symmetry, which is a non-perturbative phenomenon, absent in pQCD.

similar HLS model [114, 115]; approaches more or less accepted as a framework for the evaluation of the hadronic LbL effects. The amazing fact is that the interactions involved in the hadronic LbL scattering process are the parity conserving QED and QCD interactions while the process is dominated by the parity odd pseudoscalar meson-exchanges. This means that the effective  $\pi^0\gamma\gamma$  interaction vertex exhibits the parity violating  $\gamma_5$  coupling, which of course in  $\gamma\gamma \rightarrow \pi^0 \rightarrow \gamma\gamma$  must appear twice (an even number of times). The process indeed is associated with the parity odd Wess-Zumino-Witten (WZW) effective interaction term

$$\mathcal{L}^{(4)} = -\frac{\alpha N_c}{12\pi F_0} \varepsilon_{\mu\nu\rho\sigma} F^{\mu\nu} A^\rho \partial^\sigma \pi^0 + \dots \quad (3.57)$$

which reproduces the Adler-Bell-Jackiw (ABJ) anomaly and which plays a key role in estimating the leading hadronic LbL contribution.  $F_0$  denotes the pion decay constant  $F_\pi$  in the chiral limit of massless light quarks ( $F_\pi \simeq 92.4$  MeV). The constant WZW form factor yields a divergent result, applying a cut-off  $\Lambda$  one obtains the leading term



$$a_\mu^{(6)}(\text{lbl}, \pi^0) = \left[ \frac{N_c^2}{48\pi^2} \frac{m_\mu^2}{F_\pi^2} \ln^2 \frac{\Lambda}{m_\mu} + \dots \right] \left( \frac{\alpha}{\pi} \right)^3$$

with a universal coefficient  $C = N_c^2 m_\mu^2 / (48\pi^2 F_\pi^2)$  [116]; in the VMD dressed cases  $M_V$  represents the cut-off  $\Lambda \rightarrow M_V$ .<sup>17</sup>

Based on refined effective field theory (EFT) models, two major efforts in evaluating the full  $a_\mu^{\text{LbL}}$  contribution were made by Hayakawa, Kinoshita and Sanda (HKS 1995) [114], Bijmans, Pallante and Prades (BPP 1995) [112] and Hayakawa and Kinoshita (HK 1998) [115] (see also Kinoshita, Nizic and Okamoto (KNO 1985) [106]). Although the details of the calculations are quite different, which results in a different splitting of various contributions, the results are in good agreement and essentially given by the  $\pi^0$ -pole contribution, which was taken with the wrong sign, however. In order to eliminate the cut-off dependence in separating long distance (L.D.) and short distance (S.D.) physics, more recently it became favorable to use quark-hadron duality, as it holds in the large- $N_c$  limit of QCD [117, 118], for modeling of the hadronic amplitudes [113]. The infinite series of narrow vector states known to show up in the large  $N_c$  limit is then approximated by a suitable lowest meson dominance (LMD+V) ansatz [119], assumed to be saturated by known low lying physical states of appropriate quantum numbers. This approach was adopted in a reanalysis by Knecht and Nyffeler (KN 2001) [116, 120–122] in 2001, in which they discovered a sign mistake in the dominant  $\pi^0, \eta, \eta'$  exchange contribution, which

<sup>17</sup>Since the leading term is divergent and requires UV subtraction, we expect this term to drop from the physical result, unless a physical cut-off tames the integral, like the physical  $\rho$  in effective theories which implement the VMD mechanism.

changed the central value by  $+167 \times 10^{-11}$ , a  $2.8 \sigma$  shift, and which reduces a larger discrepancy between theory and experiment. More recently Melnikov and Vainshtein (MV 2004) [123] found additional problems in previous calculations, this time in the short distance constraints (QCD/OPE) used in matching the high energy behavior of the effective models used for the  $\pi^0$ ,  $\eta$ ,  $\eta'$  exchange contribution. Another important change concerns the contributions from the axialvector exchanges which have been modeled in [123] violating the Landau–Yang theorem. We will elaborate on this in much more detail in Sect. 5.2.

We advocate to use consistently dressed form factors as inferred from the resonance Lagrangian approach. However, other effects which were first considered in [123] must be taken into account: (i) the constraint on the twist four ( $1/q^4$ )-term in the OPE requires  $h_2 = -10 \text{ GeV}^2$  in the Knecht-Nyffeler form factor [120]:  $\delta a_\mu \simeq +5 \pm 0$  relative to  $h_2 = 0$ , (ii) the contributions from the  $f_1$  and  $f'_1$  isoscalar axial–vector mesons:  $\delta a_\mu \simeq +6 \pm 2$  (using dressed photons, and implementing the Landau–Yang condition), (iii) for the remaining effects, scalars ( $f_0$ ) + dressed  $\pi^\pm$ ,  $K^\pm$  loops + dressed quark loops:  $\delta a_\mu \simeq -5 \pm 13$ . Note that this last group of terms have been evaluated in [112, 114] only. The splitting into the different terms is model dependent and only the sum should be considered; the results read  $-5 \pm 13$  (BPP) and  $5.2 \pm 13.7$  (HKS) and hence the contribution remains unclear.<sup>18</sup> As an estimate based on [112, 114, 120, 123, 124] we adopt  $\pi^0$ ,  $\eta$ ,  $\eta'$  [ $95 \pm 12$ ] + axial–vector [ $8 \pm 3$ ] + scalar [ $-6 \pm 1$ ] +  $\pi$ ,  $K$  loops [ $-20 \pm 5$ ] + quark loops [ $22 \pm 4$ ] + tensor [ $1 \pm 0$ ] + NLO [ $3 \pm 2$ ] which yields

$$a_\mu^{(6)}(\text{lbl, had}) = (103 \pm 29) \times 10^{-11} .$$

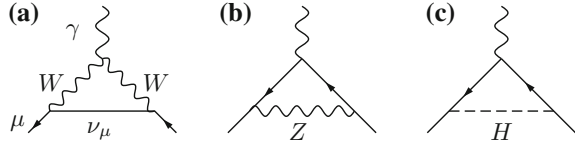
The result differs little from the “agreed” value  $(105 \pm 26) \times 10^{-11}$  presented in [125] and  $(116 \pm 39) \times 10^{-11}$  estimated in [20]. Both included a wrong, too large, Landau–Yang theorem violating axial–vector contribution from [123], correcting for this we obtain our reduced value relative to [20].

### (5) Weak interaction corrections:

The last set of corrections are due to the weak interaction as described by the electroweak SM. The weak corrections are those mediated by the weak currents which couple to the heavy spin 1 gauge bosons, the charged  $W^\pm$  or the neutral “heavy light” particle  $Z$  or by exchange of a Higgs particle  $H$  (see Fig. 3.7; masses are given in (3.33), (3.34)). What is most interesting is the occurrence of the first diagram of Fig. 3.7, which exhibits a non–Abelian triple gauge vertex and the corresponding contribution provides a test of the Yang–Mills structure involved. It is of course not surprising that the photon couples to the charged  $W$  boson the way it is dictated by electromagnetic gauge invariance. In spite of the fact that the contribution is of leading one–loop order, it is vastly suppressed by the fact that the corrections are mediated by the exchange of very heavy states which makes them suppressed by

<sup>18</sup>We adopt the result of [112] as the sign has to be negative in any case (see [121]).

**Fig. 3.7** The leading weak contributions to  $a_\ell$ ; diagrams in the physical unitary gauge



$O(2\frac{\alpha}{\pi} \frac{m_\mu^2}{M^2}) \sim 5 \times 10^{-9}$  for  $M$  of about 100 GeV. The gauge boson contributions up to negligible terms of order  $O(\frac{m_\mu^2}{M_{W,Z}^2})$  are given by (the Higgs contribution is negligible) [126]

$$a_\mu^{(2)\text{EW}} = [5 + (-1 + 4 \sin^2 \Theta_W)^2] \frac{\sqrt{2}G_\mu m_\mu^2}{48\pi^2} \simeq (194.82 \pm 0.02) \times 10^{-11} . \tag{3.58}$$

The error comes from the uncertainty in  $\sin^2 \Theta_W$  [see (3.32)].

Electroweak two-loop calculations started 1992 with Kukhto et al [127], who observed potentially large terms proportional to  $\sim G_F m_\mu^2 \frac{\alpha}{\pi} \ln \frac{M_Z}{m_\mu}$  enhanced by a large logarithm. The most important diagrams are triangle fermion-loops:

$$a_\mu^{(4)\text{EW}}([f]) \simeq \frac{\sqrt{2}G_\mu m_\mu^2 \alpha}{16\pi^2} \frac{\alpha}{\pi} 2T_{3f} N_{cf} Q_f^2 \left[ 3 \ln \frac{M_Z^2}{m_{f'}^2} + C_f \right]$$

where  $T_{3f}$  is the 3rd component of the weak isospin,  $Q_f$  the charge and  $N_{cf}$  the color factor, 1 for leptons, 3 for quarks. The mass  $m_{f'}$  is  $m_\mu$  if  $m_f < m_\mu$  and  $m_f$  if  $m_f > m_\mu$ , and  $C_e = 5/2$ ,  $C_\mu = 11/6 - 8/9 \pi^2$ ,  $C_\tau = -6$  [127]. Note that triangle fermion-loops cannot contribute in QED due to Furry's theorem. However, the weak interactions are parity violating and if one of the three vector vertices  $V^\mu = \gamma^\mu$  is replaced by an axial vertex  $A^\mu = \gamma^\mu \gamma_5$  one gets a non-vanishing contribution. This is what happens if we replace one of the photons by a “heavy light” particle  $Z$ . However, these diagrams are responsible for the Adler-Bell-Jackiw anomaly [128] which is leading to a violation of axial current conservation and would spoil renormalizability. The anomalous terms must cancel and in the SM this happens by lepton quark duality: leptons and quarks have to live in families and for each family  $\sum_f N_{cf} Q_f^2 T_{3f} = 0$ , which is the anomaly cancellation condition in the  $SU(3)_c \otimes SU(2)_L \otimes U(1)_Y$  gauge theory. This is again one of the amazing facts, that at the present level of precision one starts to be sensitive to the anomaly cancellation mechanism. This anomaly cancellation leads to substantial cancellations between the individual fermion contributions. The original results therefore get rectified by taking into account the family structure of SM fermions [129–131].

For more sophisticated analyses we refer to [129, 130, 132] which was corrected and refined in [131, 133]. Including subleading effects yields  $-5.0 \times 10^{-11}$  for the first two families. The 3rd family of fermions including the heavy top quark can be treated in perturbation theory and was worked out to be  $-8.2 \times 10^{-11}$  in [134]. Subleading fermion loops contribute  $-5.3 \times 10^{-11}$ . There are many more diagrams contributing, in particular the calculation of the bosonic contributions (1678 diagrams) is a formidable task and has been performed 1996 by Czarnecki, Krause and Marciano as an expansion in  $(m_\mu/M_V)^2$  and  $(M_V/m_H)^2$  [135]. Later complete calculations, valid also for lighter Higgs masses, were performed [136, 137], which confirmed the previous result  $-22.3 \times 10^{-11}$ . The 2-loop result reads<sup>19</sup>

$$a_\mu^{(4)\text{EW}} = -41(1) \times 10^{-11} .$$

The complete weak contribution may be summarized by [133]

$$\begin{aligned} a_\mu^{\text{EW}} &= \frac{\sqrt{2}G_\mu m_\mu^2}{16\pi^2} \left\{ \frac{5}{3} + \frac{1}{3} (1 - 4 \sin^2 \Theta_W)^2 - \frac{\alpha}{\pi} [155.5(4)(2)] \right\} \\ &= (154 \pm 1[\text{had}] \pm 0.4[m_H, m_t, 3 - \text{loop}]) \times 10^{-11} \end{aligned} \quad (3.59)$$

with errors from triangle quark-loops. For the Higgs we use the recent LHC observation  $m_H \simeq 125.1 \pm 0.3$  GeV. The 3-loop effect has been estimated to be small [131, 133] (see (4.124)).

This closes our overview of the various contributions to the anomalous magnetic moment of the muon. More details about the higher order QED corrections as well as the weak and strong interaction corrections will be discussed in detail in the next Chap. 4. First we give a brief account of the status of the theory in comparison to the experiments. We will consider the electron and the muon in turn.

### 3.2.2 The Anomalous Magnetic Moment of the Electron

The electron magnetic moment anomaly likely is the experimentally most precisely known quantity. For almost 20 years the value was based on the extraordinary precise measurements of electron and positron anomalous magnetic moments

---

<sup>19</sup>The authors of [127] reported

$$a_\mu^{(4)\text{EW}} = -42 \times 10^{-11}$$

for what they thought was the leading correction, which is very close to the complete weak two-loop corrections, however, this coincidence looks to be a mere accident. Nevertheless, the sign and the order of magnitude turned out to be correct.

$$\begin{aligned} a_{e^-}^{\text{exp}} &= 0.001\,159\,652\,188\,4(43), \\ a_{e^+}^{\text{exp}} &= 0.001\,159\,652\,187\,9(43), \end{aligned} \quad (3.60)$$

by Van Dyck et al. (1987) [138]. The experiment used the ion trap technique, which has made it possible to study a single electron with extreme precision.<sup>20</sup> The result impressively confirms the conservation of CPT:  $a_{e^+} = a_{e^-}$ . Being a basic prediction of any QFT, CPT symmetry will be assumed to hold in the following. This allows us to average the electron and positron values with the result [14]

$$a_e = \mu_e/\mu_B - 1 = (g_e - 2)/2 = 1.159\,652\,1883(42) \times 10^{-3}. \quad (3.61)$$

The relative standard uncertainty is 3.62 ppb. A big step forward has been achieved more recently by Gabrielse et al. [5, 6, 139] in an experiment at Harvard University using a one-electron quantum cyclotron. The new result is

$$a_e = 1.159\,652\,180\,73(28)[0.24 \text{ ppb}] \times 10^{-3}, \quad (3.62)$$

with an accuracy nearly 15 times better than (3.61) and shifting down the central value of  $a_e$  by 1.8 standard deviations.

The measurements of  $a_e$  not only played a key role in the history of precision tests of QED in particular, and of QFT concepts in general, today we may use the anomalous magnetic moment of the electron to get the most precise indirect measurement of the fine structure constant  $\alpha$ . This possibility of course hangs on our ability to pin down the theoretical prediction with very high accuracy. Indeed  $a_e$  is much safer to predict reliably than  $a_\mu$ . The reason is that non-perturbative hadronic effects as well as the sensitivity to unknown physics beyond the SM are suppressed by the large factor  $m_\mu^2/m_e^2 \simeq 42\,753$  in comparison to  $a_\mu$ . This suppression has to be put into perspective with the 2250 times higher precision with which we know  $a_e$ . We thus can say that effectively  $a_e$  is a factor 19 less sensitive to model dependent physics than  $a_\mu$ .

The reason why it is so interesting to have such a precise measurement of  $a_e$  of course is that it can be calculated with comparable accuracy in theory. The prediction is given by a perturbation expansion of the form

$$a_e = \sum_{n=1}^N C_n (\alpha/\pi)^n, \quad (3.63)$$

---

<sup>20</sup>The ion trap technique was introduced and developed by Paul and Dehmelt, whom was awarded the Nobel Prize in 1989. The ion traps utilize electrical quadrupole fields obtained with hyperboloid shaped electrodes. The Paul trap works with dynamical trapping using r.f. voltage, the Penning trap used by Dehmelt works with d.c. voltage and a magnetic field in  $z$ -direction.



with terms up to five loops,  $N = 5$ , under consideration. The experimental precision of  $a_e$  requires the knowledge of the coefficients with accuracies  $\delta C_2 \sim 5 \times 10^{-8}$ ,  $\delta C_3 \sim 2 \times 10^{-5}$ ,  $\delta C_4 \sim 1 \times 10^{-2}$  and  $\delta C_5 \sim 4$ . Actually, Aoyama, Hayakawa, Kinoshita and Nio [10, 33] not long ago achieved remarkable progress in calculating missing four- and five-loop QED contributions. Besides the leading universal  $C_5$  term, which we already included in (3.45), also so far missing mass-dependent  $\mu$  and  $\tau$  lepton contributions have been evaluated. Concerning the mass-dependent contributions, the situation for the electron is quite different from the muon. Since the electron is the lightest of the leptons a potentially large “light internal loop” contribution is absent. For  $a_e$  the muon is a heavy particle  $m_\mu \gg m_e$  and its contribution is of the type “heavy internal loops” which is suppressed by an extra power of  $m_e^2/m_\mu^2$ . In fact the  $\mu$ -loops tend to decouple and therefore only yield small terms. We may evaluate them by just replacing  $m_\mu \rightarrow m_e$  and  $m_\tau \rightarrow m_\mu$  in the formula for the  $\tau$ -loop contributions to  $a_\mu$ . Corrections due to internal  $\mu$ -loops are suppressed as  $O(2\alpha/\pi m_e^2/m_\mu^2) \simeq 1.1 \times 10^{-7}$  relative to the leading term and the  $\tau$ -loops practically play no role at all.

Collecting the results we have<sup>21</sup>

$$a_e^{\text{QED}} = a_e^{\text{uni}} + a_e(\mu) + a_e(\tau) + a_e(\mu, \tau) \quad (3.64)$$

with universal term given by (3.45) and

$$\begin{aligned} a_e(\mu) &= 5.197\,386\,76(26) \times 10^{-7} \left(\frac{\alpha}{\pi}\right)^2 - 7.373\,941\,70(27) \times 10^{-6} \left(\frac{\alpha}{\pi}\right)^3 \\ &\quad + 9.161\,970\,703(373) \times 10^{-4} \left(\frac{\alpha}{\pi}\right)^4 - 0.00382(39) \times 10^{-6} \left(\frac{\alpha}{\pi}\right)^5 \\ a_e(\tau) &= 1.83798(33) \times 10^{-9} \left(\frac{\alpha}{\pi}\right)^2 - 6.5830(11) \times 10^{-8} \left(\frac{\alpha}{\pi}\right)^3 \\ &\quad + 7.429\,24(118) \times 10^{-6} \left(\frac{\alpha}{\pi}\right)^4 \\ a_e(\mu, \tau) &= 0.190982(34) \times 10^{-12} \left(\frac{\alpha}{\pi}\right)^3 + 7.4687(28) \times 10^{-7} \left(\frac{\alpha}{\pi}\right)^4. \end{aligned}$$

<sup>21</sup>The order  $\alpha^3$  terms are given by two parts which cancel partly

$$\begin{aligned} A_2^{(6)}(m_e/m_\mu) &= -7.373\,941\,70(27) \times 10^{-6} \\ &= -2.17684018(10) \times 10^{-5} \Big|_{\mu\text{-vap}} + 1.439446007(72) \times 10^{-5} \Big|_{\mu\text{-lbl}} \\ A_2^{(6)}(m_e/m_\tau) &= -6.5830(11) \times 10^{-8} \\ &= -1.16744(20) \times 10^{-7} \Big|_{\tau\text{-vap}} + 0.50914(9) \times 10^{-7} \Big|_{\tau\text{-lbl}}. \end{aligned}$$

The errors are due to the errors in the mass ratios. They are completely negligible in comparison to the other errors.

Altogether the perturbative expansion for the QED prediction of  $a_e$  is given by

$$\begin{aligned}
 a_e^{\text{QED}} &= \frac{\alpha}{2\pi} - 0.328\,478\,444\,002\,54(33) \left(\frac{\alpha}{\pi}\right)^2 \\
 &\quad + 1.181\,234\,016\,816(11) \left(\frac{\alpha}{\pi}\right)^3 \\
 &\quad - 1.91134(182) \left(\frac{\alpha}{\pi}\right)^4 \\
 &\quad + 7.791(580) \left(\frac{\alpha}{\pi}\right)^5.
 \end{aligned} \tag{3.65}$$

The improvement of the coefficient  $C_4$  and knowing  $C_5$  now are important for the precise determination of  $\alpha$  from  $a_e^{\text{exp}}$  below. For our accurate value for the fine structure constant (3.29), which has been determined by matching the SM prediction of  $a_e$  below with  $a_e^{\text{exp}}$ , we obtain

$$a_e^{\text{QED}} = a_e^{\text{uni}} + 0.0000000000268 = 0.00115965217910(26)(0)(4)[26], \tag{3.66}$$

which shows that the QED part of the SM prediction of  $a_e$  is overwhelmingly dominated by the universal part (3.45).

What still is missing are the hadronic and weak contributions, which both are substantially reduced relative to  $a_\mu$ . One should note that these contributions do not scale by the  $(m_e/m_\mu)^2$  factor as one could naively guess. Estimates yield  $a_e^{\text{had}} = 1.697(12) \times 10^{-12}$  and  $a_e^{\text{weak}} = 0.030 \times 10^{-12}$ , respectively [74].<sup>22</sup> With the improved experimental result for  $a_e$  and the improved QED calculations available, the hadronic contribution now start to be significant, however, unlike in  $a_\mu^{\text{had}}$  for the muon,  $a_e^{\text{had}}$  is known with sufficient accuracy and is not the limiting factor here. As a result  $a_e$  essentially only depends on perturbative QED, while hadronic, weak and new physics (NP) contributions are suppressed by  $(m_e/M)^2$ , where  $M$  is a weak, hadronic or new physics scale. As a consequence  $a_e$  at this level of accuracy is theoretically well under control (almost a pure QED object) and therefore is an excellent observable for extracting  $\alpha_{\text{QED}}$  based on the SM prediction

$$a_e^{\text{SM}} = a_e^{\text{QED}}[\text{Eq. (3.65)}] + 1.721(12) \times 10^{-12} \text{ (hadronic \& weak)}. \tag{3.67}$$

---

<sup>22</sup>The precise procedure of evaluating the hadronic contributions will be discussed extensively in Chap. 5 for the muon, for which the effects are much more sizable. As expected, corresponding calculations for the electron give small contributions only. We find  $a_e^{\text{had, LO}} = 1.8465(121) \times 10^{-12}$  for the leading HVP contribution,  $a_e^{\text{had, NLO}} = -0.2210(14) \times 10^{-12}$  for the next to leading and  $a_e^{\text{had, NNLO}} = 0.0279(2) \times 10^{-12}$  for the next-to-next leading order [108]. For the hadronic light-by-light scattering contribution we estimate  $a_e^{\text{had, LbL}} = 0.037(5) \times 10^{-12}$ . An early relatively accurate evaluation  $a_e^{(4)}(\text{vap, had}) = 1.884(41) \times 10^{-12}$  for the leading term has been obtained in 1995 [64] and illustrates the progress since.

We now compare this result with the very recent extraordinary precise measurement of the electron anomalous magnetic moment [6]

$$a_e^{\text{exp}} = 0.001\,159\,652\,180\,73(28) \quad (3.68)$$

which yields

$$\alpha^{-1}(a_e) = 137.035\,999\,1547(331)(0)(27)(14)[333] ,$$

which is close [55  $\rightarrow$  39 in  $10^{-9}$ ] to the value (3.29) [10] given earlier. If one adopts the CODATA recommended value  $a_e^{\text{exp}} = 0.001\,159\,652\,180\,76(27)$  as an input one obtains

$$\alpha^{-1}(a_e) = 137.035\,999\,1512(320)(0)(27)(14)[321] . \quad (3.69)$$

The first error is the experimental one of  $a_e^{\text{exp}}$ , the second and third are the numerical uncertainties of the  $\alpha^4$  and  $\alpha^5$  terms, respectively. The last one is the hadronic uncertainty, which is completely negligible. This is now the by far most precise determination of  $\alpha$  and we will use the recommended variant (3.29) throughout in the calculation of  $a_\mu$ , below.

A different strategy is to use  $a_e$  for a precision test of QED. For a theoretical prediction of  $a_e$  we then need the best determinations of  $\alpha$  which do not depend on  $a_e$ . They are [140–142]<sup>23</sup>

$$\alpha^{-1}(\text{Cs06}) = 137.03600000(110)[8.0 \text{ ppb}] , \quad (3.70)$$

$$\alpha^{-1}(\text{Rb11}) = 137.035999037(91)[0.66 \text{ ppb}] , \quad (3.71)$$

and have been determined by atomic interferometry. The new much improved value (3.71) is obtained from the measurement of  $h/m_{\text{Rb}}$ , combined with the very precisely known Rydberg constant and the new value for  $m_{\text{Rb}}/m_e$  [10, 142].

In terms of  $\alpha(\text{Cs06})$  one gets  $a_e = 0.00115965217359(929)$  which agrees well with the experimental value  $a_e^{\text{exp}} - a_e^{\text{the}} = 7.14(9.30) \times 10^{-12}$ ; With the new value  $\alpha(\text{Rb11})$  the prediction is  $a_e = 0.00115965218172(77)$ , again in good agreement with experiment:  $a_e^{\text{exp}} - a_e^{\text{the}} = -0.99(0.82) \times 10^{-12}$ . The error is completely dominated by the error of the input value of  $\alpha$  used. The precision reached is close to become interesting for testing new physics scenarios [150, 151]. The following Table 3.3 collects the typical contributions to  $a_e$  evaluated in terms of Eqs. (3.70) and (3.71). The new results [10] imply that the theory error is reduced by almost a factor 5. In spite of the fact that the best non- $a_e$  determinations of  $\alpha$  also improved by

---

<sup>23</sup>The results rely upon a number of other experimental quantities. One is the measured Rydberg constant [143], others are the Cesium (Cs) and Rubidium (Rb) masses in atomic mass units (amu) [144] and the electron mass in amu [145–147]. The  $\hbar/M_{\text{Cs}}$  needed comes from an optical measurement of the Cs D1 line [140, 148] and the preliminary recoil shift in an atom interferometer [149], while  $\hbar/M_{\text{Rb}}$  comes from a measurement of an atom recoil of a Rb atom in an optical lattice [140].

**Table 3.3** Contributions to  $a_e(h/M)$  in units  $10^{-6}$ . The three errors given in the universal contribution come from the experimental uncertainty in  $\alpha$ , from the  $\alpha^4$  term and from the  $\alpha^5$  term, respectively

Contribution	$\alpha(h/M_{Cs06})$	$\alpha(h/M_{Rb11})$
Universal	1159.652 169 15(929)(0)(4)	1159.652 177 28(77)(0)(4)
$\mu$ -loops	0.000 002 738 (0)	0.000 002 738 (0)
$\tau$ -loops	0.000 000 009 (0)	0.000 000 009 (0)
Hadronic	0.000 001 690 (13)	0.000 001 690 (13)
Weak	0.000 000 030 (0)	0.000 000 030 (0)
Theory	1159.652 173 59(929)	1159.652 181 72(77)
Experiment	1159.652 180 73 (28)	1159.652 180 73 (28)
$a_e^{\text{exp}} - a_e^{\text{the}}$	$7.14(9.30) \times 10^{-12}$	$-0.99(0.82) \times 10^{-12}$

a factor 10 the error is still dominated by the uncertainty of  $\alpha^{-1}(\text{Rb11})$ . An improvement by a factor 10 would allow a much more stringent test of QED, and therefore would be very important. At present, assuming that  $|\Delta a_e^{\text{New Physics}}| \simeq m_e^2/\Lambda^2$  where  $\Lambda$  approximates the scale of ‘‘New Physics’’, the agreement between  $\alpha^{-1}(a_e)$  and  $\alpha^{-1}(\text{Rb11})$  probes the scale  $\Lambda \lesssim O(400 \text{ GeV})$ . To access the much more interesting range of  $\Lambda \sim O(1 \text{ TeV})$  would require primarily a substantially more precise  $\alpha$ . The tenth order QED calculations by Aoyama, Hayakawa, Kinoshita and Nio mark a new milestone in accuracy and in complexity of theoretical predictions in quantum field theory. They put g-2 calculations on a much safer basis for what concerns the perturbative part. Still, independent cross checks of both the  $O(\alpha^4)$  and the  $O(\alpha^5)$  QED calculations are highly desirable, even though we have no doubts that the new results are reliable. Important semi-analytic cross checks so far confirm the numerical calculations [50, 57]. The new quasi-analytic  $O(\alpha^4)$  result by Laporta [11] is certainly a milestone in consolidating the QED part  $a_e^{\text{QED}}$ .

As a summary, we note that with

$$a_e^{\text{exp}} - a_e^{\text{the}} = -0.99(0.82) \times 10^{-12}, \quad (3.72)$$

theory and experiment are in excellent agreement. We know that the sensitivity to new physics is reduced by  $(m_\mu/m_e)^2 \cdot \delta a_e^{\text{exp}}/\delta a_\mu^{\text{exp}} \simeq 19$  relative to  $a_\mu$ . Nevertheless, one has to keep in mind that  $a_e$  is suffering less from hadronic uncertainties and thus may provide a safer test. One should also keep in mind that experiments determining  $a_e$  on the one hand and  $a_\mu$  on the other hand are very different with different systematics. While  $a_e$  is determined in an ultra cold environment  $a_\mu$  has been determined with ultra relativistic (magic  $\gamma$ ) muons so far. Presently, the  $a_e$  prediction is limited by the, by a factor  $\delta\alpha(\text{Rb11})/\delta\alpha(a_e) \simeq 5.3$  less precise,  $\alpha$  available. Combining all uncertainties  $a_\mu$  is about a factor 43 more sensitive to new physics at present.

**Table 3.4** QED contributions to  $a_\mu$  in units  $10^{-6}$ 

Term	Universal	$e$ -loops	$\tau$ -loops	$e \times \tau$ -loops
$a^{(4)}$	-1.772 305 06 (0)	5.904 060 07 (4)	0.000 421 28 (8)	–
$a^{(6)}$	0.014 804 20 (0)	0.286 603 69 (0)	0.000 004 52 (0)	0.000 006 61 (0)
$a^{(8)}$	-0.000 055 67 (0)	0.003 862 64 (18)	0.000 001 23 (0)	0.000 001 83 (0)
$a^{(10)}$	0.000 000 62 (4)	0.000 050 19 (6)	-0.000 000 01 (0)	0.000 000 14 (0)

Recently, the possible non-perturbative QED effect of order  $\alpha^5$  of the positronium exchange  $\gamma^* \rightarrow [e^+e^-]_{\text{bound state}} \rightarrow \gamma^*$ , in the virtual photon line of the LO diagram of the electron  $g-2$ , was pointed out in [152, 153], but has been shown to be absent as an additional contribution [153–156], in accord with earlier studies [157, 158].

### 3.2.3 The Anomalous Magnetic Moment of the Muon

The muon magnetic moment anomaly is defined by

$$a_\mu = \frac{1}{2}(g_\mu - 2) = \frac{\mu_\mu}{e\hbar/2m_\mu} - 1, \quad (3.73)$$

where  $g_\mu = 2\mu_\mu/(e\hbar/2m_\mu)$  is the  $g$ -factor and  $\mu_\mu$  the magnetic moment of the muon. The different higher order QED contributions are collected in Table 3.4. We thus arrive at a QED prediction of  $a_\mu$  given by

$$a_\mu^{\text{QED}} = 116\,584\,718.859(0.026)(0.009)(0.017)(0.006)[0.034] \times 10^{-11} \quad (3.74)$$

where the first error is the uncertainty of  $\alpha$  in (3.29), the second one combines in quadrature the uncertainties due to the errors in the mass ratios (3.30), the third and fourth are the numerical uncertainties of the  $O(\alpha^4)$  and  $O(\alpha^5)$  terms, respectively. With the spectacular progress achieved with the calculation of the complete  $O(\alpha^5)$  term [10, 51] the error is essentially given by the input error of  $\alpha[a_e]$  in spite of the fact that this error has been reduced as well due to the  $O(\alpha^5)$  result on  $a_e$ .

The following Table 3.5 collects the typical contributions to  $a_\mu$  evaluated in terms of  $\alpha$  (3.29) determined via  $a_e$ .

The world average experimental muon magnetic anomaly, dominated by the very precise BNL result, is now [7, 159]

$$a_\mu^{\text{exp}} = 1.16592091(63) \times 10^{-3} \quad (3.75)$$

(relative uncertainty  $5.4 \times 10^{-7}$ ), which confronts the SM prediction

$$a_\mu^{\text{the}} = 1.16591783(35) \times 10^{-3}. \quad (3.76)$$

**Table 3.5** The various types of contributions to  $a_\mu$  in units  $10^{-6}$ , ordered according to their size (L.O. lowest order, H.O. higher order, LbL light-by-light). The gray band shows the present experimental result with its uncertainty. The hatched overlay illustrates the expected uncertainty (for the same central value) which will be reached in the coming years. “Theory  $\tau$ ” shows the result from [88] where  $\tau$ -data have been taken into account, before taking into care of  $\rho^0 - \gamma$  mixing. This result is outdated. The LbL result’s history is also shown. Results are from: 1995 [112, 114, 115], 2001 [KN] [120], 2003 [MV] [123], and 2015 [JN] [20, 74, 125]

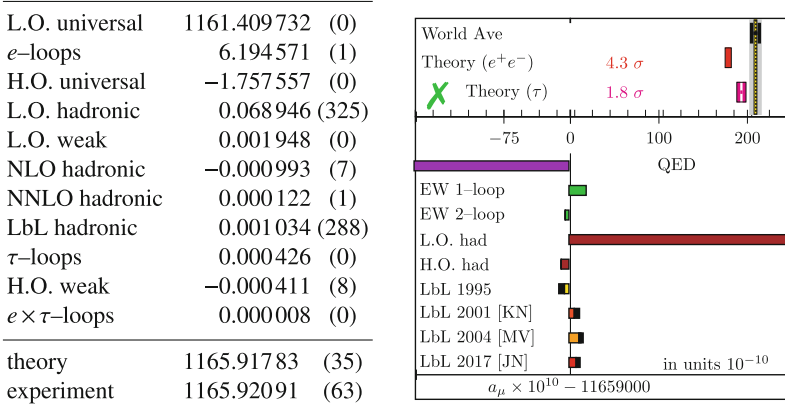


Figure 3.8 illustrates the sensitivity to various contributions and how it developed in history. The high sensitivity of  $a_\mu$  to physics from not too high scales  $M$  above  $m_\mu$ , which is scaling like  $(m_\mu/M)^2$ , and the more than one order of magnitude improvement of the experimental accuracy has brought many SM effects into the focus of the interest. Not only are we testing now the 4-loop QED contribution, higher order HVP effects, the infamous hadronic LbL contribution and the weak loops, we are reaching or limiting possible New Physics at a level of sensitivity which caused and still causes a lot of excitement. “New Physics” is displayed in the figure as the ppm deviation of

$$a_\mu^{\text{exp}} - a_\mu^{\text{the}} = (306 \pm 72) \times 10^{-11}, \quad (3.77)$$

which is  $4.3 \sigma$ . We note that the theory error is now smaller than the experimental one. It is fully dominated by the uncertainty of the hadronic low energy cross section data, which determine the hadronic vacuum polarization and, partially, from the uncertainty of the hadronic light-by-light scattering contribution.

As we notice, the enhanced sensitivity to “heavy” physics is somehow good news and bad news at the same time: the sensitivity to “New Physics” we are always hunting for at the end is enhanced due to

$$a_\ell^{\text{NP}} \sim \left( \frac{m_\ell}{M_{\text{NP}}} \right)^2$$

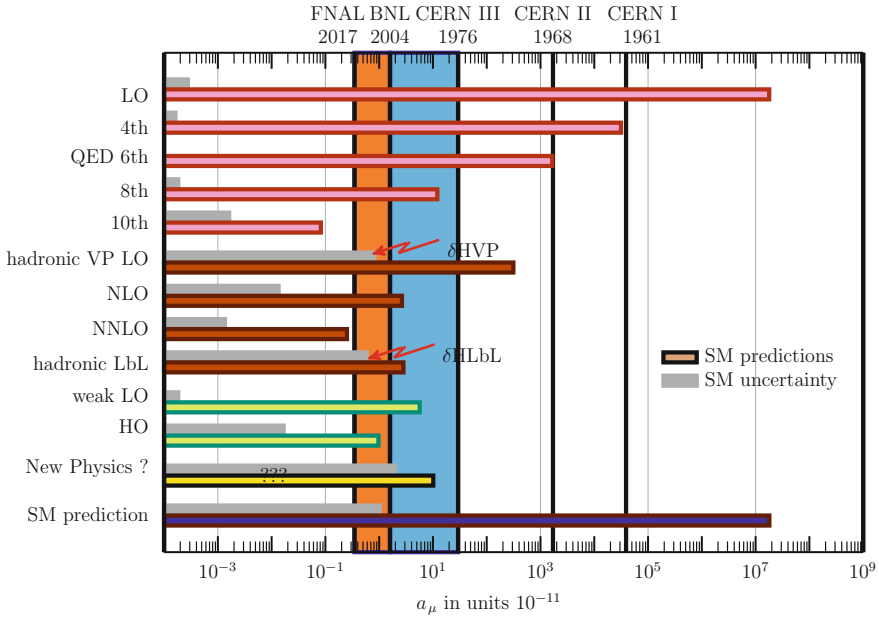


**Fig. 3.8** History of the muon  $g - 2$  experiments and the sensitivity to various contributions. The increase in precision with the BNL  $g - 2$  experiment is shown as a blue vertical band. New Physics is illustrated by the deviation  $(a_\mu^{\text{exp}} - a_\mu^{\text{the}})/a_\mu^{\text{exp}}$ . The left orange vertical band shows the sensitivity band which will be reached with the upcoming muon  $g - 2$  experiment at Fermilab [160]. Arrows point to what is limiting theory precision presently: the Hadronic Vacuum Polarization (HVP) and Hadronic Light-by-Light (HLbL) contributions

by the mentioned mass ratio square, but at the same time also scale dependent SM effects are dramatically enhanced, and the hadronic ones are not easy to estimate with the desired precision.

The perspectives for future developments will be discussed at the end of Chap. 7.

After this summary of the current status of  $a_\mu$  and  $a_e$ , we will now go on and present basic techniques and tools used in calculating the various effects, before we are going to present a more detailed account of the individual contributions in the next chapter.

### 3.3 Structure of the Electromagnetic Vertex in the SM

Here we want to discuss the lepton moments beyond QED in the more general context of the SM, in which parity P as well as CP are broken by the weak interactions. We again start from the relevant matrix element of the electromagnetic current between lepton states

$$i\Gamma_{\gamma\ell\ell}^{\mu}(p_1, p_2; r_1, r_2) = \langle \ell^-(p_2, r_2) | j_{\text{em}}^{\mu}(0) | \ell^-(p_1, r_1) \rangle = i\bar{u}(p_2, r_2)\Pi_{\gamma\ell\ell}^{\mu}u(p_1, r_1) \quad (3.78)$$

and look for the additional form factors showing up if P and C are violated. Again  $q = p_2 - p_1$  is the momentum transfer.  $u(p_1, r_1)$  is the Dirac spinor, the wave function of the incoming lepton, with momentum  $p_1$  and 3rd component of spin  $r_1 (= \pm \frac{1}{2})$ , and  $\bar{u} = u^+\gamma^0$  is the adjoint spinor representing the wave function of the outgoing lepton.  $\Pi_{\gamma\ell\ell}^{\mu}$  is a Hermitian  $4 \times 4$  matrix in spinor space and a Lorentz four-vector.

Besides the Dirac matrix  $\gamma^{\mu}$  we have two further independent four-vectors, the momenta  $p_1$  and  $p_2$  or linear combinations of them. It is convenient to choose the orthogonal vectors  $P = p_1 + p_2$  and  $q = p_2 - p_1$  (with  $Pq = 0$ ). The general covariant decomposition for on-shell leptons in the SM then may be written in the form

$$\Pi_{\gamma\ell\ell}^{\mu} = \gamma^{\mu}A_1 + \frac{P^{\mu}}{2m}A_2 + \frac{q^{\mu}}{2m}A_3 + \gamma^{\mu}\gamma_5A_4 + \frac{q^{\mu}}{2m}\gamma_5A_5 + i\frac{P^{\mu}}{2m}\gamma_5A_6 \quad (3.79)$$

where the scalar amplitudes  $A_i(p_1, p_2)$  are functions of the scalar products  $p_1^2$ ,  $p_2^2$  and  $p_1p_2$ . Since the lepton is on the mass shell  $p_1^2 = p_2^2 = m^2$  and using  $q^2 = 2m^2 - 2p_1p_2$ , the dimensionless amplitudes depend on the single kinematic variable  $q^2$  and on all the parameters of the theory: the fine structure constant  $\alpha = e^2/4\pi$  and all physical particle masses. We will simply write  $A_i = A_i(q^2)$  in the following.

When writing (3.79) we already have made use of the Gordon identities

$$\begin{aligned} i\sigma^{\mu\nu}q_{\nu} &= -P^{\mu} + 2m\gamma^{\mu}, & i\sigma^{\mu\nu}P_{\nu} &= -q^{\mu}, \\ i\sigma^{\mu\nu}q_{\nu}\gamma_5 &= -P^{\mu}\gamma_5, & i\sigma^{\mu\nu}P_{\nu}\gamma_5 &= -q^{\mu}\gamma_5 + 2m\gamma^{\mu}\gamma_5, \end{aligned} \quad (3.80)$$

which hold if sandwiched between the spinors like  $\bar{u}(p_2) \cdots u(p_1)$ . In QED due to parity conservation the terms proportional to  $\gamma_5$  are absent.

The electromagnetic current still is conserved:

$$\partial_{\mu}j_{\text{em}}^{\mu} = 0. \quad (3.81)$$

On a formal level, this may be considered as a trivial consequence of the inhomogeneous Maxwell equation (see [161] for a manifestly gauge invariant formulation in the SM)

$$\partial_{\mu}F^{\mu\nu} = -e j_{\text{em}}^{\nu} \quad \text{with} \quad F_{\mu\nu} = \partial_{\mu}A_{\nu} - \partial_{\nu}A_{\mu}$$

since  $\partial_{\nu}\partial_{\mu}F^{\mu\nu} = -e \partial_{\nu}j_{\text{em}}^{\nu} \equiv 0$  as  $\partial_{\nu}\partial_{\mu}$  is symmetric in  $\mu \leftrightarrow \nu$  while  $F^{\mu\nu}$  is antisymmetric. As a consequence we must have  $q_{\mu}\bar{u}_2\Pi_{\gamma\ell\ell}^{\mu}u_1 = 0$ . By the Dirac equations  $\not{p}_i u_i = m u_i$  ( $i = 1, 2$ ) we have  $\bar{u}_2 \not{q} u_1 = 0$ , while  $\bar{u}_2 \not{q} \gamma_5 u_1 = -2m\bar{u}_2\gamma_5 u_1$ , furthermore,  $qP = 0$  while keeping  $q^2 \neq 0$  at first. Hence current conservation requires  $A_3 = 0$  and  $A_5 = -4m^2/q^2 A_4$  such that we remain with four



physical form factors<sup>24</sup>

$$\bar{u}_2 \Pi_{\gamma\ell\ell}^\mu u_1 = \bar{u}_2 \left( \gamma^\mu A_1 + \frac{P^\mu}{2m} A_2 + \left( \gamma^\mu - \frac{2mq^\mu}{q^2} \right) \gamma_5 A_4 + i \frac{P^\mu}{2m} \gamma_5 A_6 \right) u_1 .$$

This shows that the two amplitudes  $A_3$  and  $A_6$  are redundant for physics, however, they show up in actual calculations at intermediate steps and/or for contributions from individual Feynman diagrams. By virtue of the Gordon decomposition

$$\bar{u}(p_2) \frac{P^\mu}{2m} u(p_1) \equiv \bar{u}(p_2) \left( \gamma^\mu - i \frac{\sigma^{\mu\nu} q_\nu}{2m} \right) u(p_1)$$

we finally obtain for the form factor

$$\Pi_{\gamma\ell\ell}^\mu = \gamma^\mu F_E(q^2) + \left( \gamma^\mu - \frac{2mq^\mu}{q^2} \right) \gamma_5 F_A + i \sigma^{\mu\nu} \frac{q_\nu}{2m} F_M(q^2) + \sigma^{\mu\nu} \frac{q_\nu}{2m} \gamma_5 F_D(q^2) \quad (3.82)$$

With  $F_E = A_1 + A_2$  the electric charge form factor, normalized by charge renormalization to  $F_E(0) = 1$ ,  $F_A = A_4$  the *anapole moment* [162–166] which is P violating and vanishing at  $q^2 = 0$ :  $F_A(0) = 0$ . The magnetic form factor is  $F_M = -A_2$  which yields the anomalous magnetic moment as  $a_\ell = F_M(0)$ . The last term with  $F_D = A_6$  represents the CP violating *electric dipole moment* (EDM)

$$d_\ell = - \frac{F_D(0)}{2m} . \quad (3.83)$$

Note that (3.82) is the most general Lorentz covariant answer, which takes into account current conservation (3.81) and the on-shell conditions for the leptons (Dirac equation for the spinors).

In the SM at the tree level  $F_E(q^2) = 1$ , while  $F_i(q^2) = 0$  for ( $i = M, A, D$ ).

The anomalous magnetic moment  $a_\ell$  is a dimensionless quantity, just a number, and corresponds to an effective interaction term

$$\delta \mathcal{L}_{\text{eff}}^{\text{AMM}} = - \frac{e_\ell a_\ell}{4m_\ell} \bar{\psi}(x) \sigma^{\mu\nu} \psi(x) F_{\mu\nu}(x) , \quad (3.84)$$

with classical low energy limit

$$-\delta \mathcal{L}_{\text{eff}}^{\text{AMM}} \Rightarrow \mathcal{H}_m \simeq \frac{e_\ell a_\ell}{2m_\ell} \boldsymbol{\sigma} \mathbf{B} ,$$

<sup>24</sup>In the SM the proper definition of the form factors is highly non-trivial. The conventional definition of the photon field has to be replaced by one which satisfies Maxwell's equations to all orders. This has been investigated extensively in [161]. Since we are interested only in the form factors in the classical limit here, we need not go further into this discussion.

written as a Hamiltonian in 2–spinor space à la Pauli. Note that a term (3.84), if present in the fundamental Lagrangian, would spoil renormalizability of the theory and contribute to  $F_i(q^2)$  ( $i=M,D$ ) at the tree level. In addition it is not  $SU(2)_L$  gauge invariant, because gauge invariance only allows minimal couplings via the covariant derivative: vector and/or axial–vector terms. The emergence of an anomalous magnetic moment term in the SM is a consequence of the symmetry breaking by the Higgs mechanism,<sup>25</sup> which provides the mass to the physical particles and allows for helicity flip processes like the anomalous magnetic moment transitions. In any renormalizable theory the anomalous magnetic moment term must vanish at tree level, which also means that there is no free parameter associated with it. It is thus a finite prediction of the theory to all orders of the perturbation expansion.

The EDM term only can be non–vanishing if both parity P and time–reversal T are violated [167, 168]. It corresponds to an effective interaction

$$\delta\mathcal{L}_{\text{eff}}^{\text{EDM}} = -\frac{d_\ell}{2} \bar{\psi}(x) i \sigma^{\mu\nu} \gamma_5 \psi(x) F_{\mu\nu}(x), \quad (3.85)$$

which in the non–relativistic limit becomes

$$-\delta\mathcal{L}_{\text{eff}}^{\text{EDM}} \Rightarrow \mathcal{H}_e \simeq -d_\ell \boldsymbol{\sigma} \mathbf{E}, \quad (3.86)$$

again written as a Hamiltonian in 2–spinor space. Again a term (3.85) is non–renormalizable and it is not  $SU(2)_L$  gauge invariant and thus can be there only because the symmetry is broken in the Higgs phase. In the framework of a QFT where CPT is conserved T violation directly corresponds to CP violation, which is small (0.3 %) in the light particle sector and can come in at second order at best [169].<sup>26</sup> This is the reason why the EDM is so much smaller than its magnetic counterpart. The experimental limit for the electron is  $|d_e| < 1.6 \times 10^{-27} e \cdot \text{cm}$  at 90% C.L. [171]. The direct test for the muon gave  $d_\mu = 3.7 \pm 3.4 \times 10^{-19} e \cdot \text{cm}$  at 90% C.L. [172]. New much more precise experiments for  $d_\mu$  are under discus-

---

<sup>25</sup>Often the jargon *spontaneously broken gauge symmetry* (or the like) is used for the Higgs mechanism. The formal similarity to true *spontaneous symmetry breaking*, like in the Goldstone model, which requires the existence of physical zero mass Goldstone bosons, only shows up on an unphysical state space which is including the Higgs ghosts (would be Goldstone bosons). In fact it is the discrete  $Z_2$  symmetry  $H \leftrightarrow -H$  of the physical Higgs field (in the unitary gauge) which is spontaneously broken. This also explains the absence of physical Goldstone bosons.

<sup>26</sup>CP–violation in the SM arises from the complex phase  $\delta$  in the CKM matrix, which enters the interactions of the quarks with the  $W^\pm$  gauge bosons. The magnitude in the 3 family SM is given by the Jarlskog invariant [170]

$$J = \cos\theta_1 \cos\theta_2 \cos\theta_3 \sin^2\theta_1 \sin\theta_2 \sin\theta_3 \sin\delta = (2.88 \pm 0.33) \times 10^{-5} \quad (3.87)$$

where the  $\theta_i$  are the 3 mixing angles and  $\delta$  is the phase in the CKM matrix. Note that  $J$  is very small. In addition, only diagrams with at least one quark–loop with at least four CC vertices can give a contribution. This requires 3–loop diagrams exhibiting four virtual  $W$ –boson lines inside. Such contributions are highly suppressed. Expected CP violation in the neutrino mixing matrix are expected to yield even much smaller effects.

sion [173]. Theory expects  $d_e^{\text{the}} \sim 10^{-28} e \cdot \text{cm}$  [169], 10 times smaller than the present limit. For a theoretical review I refer to [174] or [35]. If we assume that  $\eta_\mu \sim (m_\mu/m_e)^2 \eta_e$  (see (1.5)), i.e.,  $\eta_\ell$  scales like heavy particle (X) effects in  $\delta a_\ell(X) \propto (m_\ell/M_X)^2$ , as they do in many new physics scenarios, we expect that  $d_\mu \sim (m_\mu/m_e) d_e$ , and thus  $d_\mu \sim 3.2 \times 10^{-25} e \cdot \text{cm}$ . This is too small to affect the extraction of  $a_\mu$ , for example, as we will see.

### 3.4 Dipole Moments in the Non-Relativistic Limit

Here we are interested in the non-relativistic limits of the effective dipole moment interaction terms (3.84)

$$\delta \mathcal{L}_{\text{eff}}^{\text{AMM}} = -\frac{e_\ell a_\ell}{4m_\ell} \bar{\psi}(x) \sigma^{\mu\nu} \psi(x) F_{\mu\nu}(x),$$

and (3.85)

$$\delta \mathcal{L}_{\text{eff}}^{\text{EDM}} = -\frac{d_\ell}{2} \bar{\psi}(x) i \sigma^{\mu\nu} \gamma_5 \psi(x) F_{\mu\nu}(x),$$

when the electron is moving in a classical external field described by  $F_{\mu\nu}^{\text{ext}}$ . The relevant expansion may be easily worked out as follows: since the antisymmetric electromagnetic field strength tensor  $F_{\mu\nu}$  exhibits the magnetic field in the spatial components  $F_{ik}: B^l = \frac{1}{2} \epsilon^{ikl} F_{ik}$  and the electric field in the mixed time-space part:  $E^i = F_{0i}$ , we have to work out  $\sigma^{\mu\nu}$  for the corresponding components:

$$\begin{aligned} \sigma^{ik} &= \frac{i}{2} (\gamma^i \gamma^k - \gamma^k \gamma^i) \\ &= \frac{i}{2} \left( \begin{pmatrix} 0 & \sigma^i \\ -\sigma^i & 0 \end{pmatrix} \begin{pmatrix} 0 & \sigma^k \\ -\sigma^k & 0 \end{pmatrix} - \begin{pmatrix} 0 & \sigma^k \\ -\sigma^k & 0 \end{pmatrix} \begin{pmatrix} 0 & \sigma^i \\ -\sigma^i & 0 \end{pmatrix} \right) \\ &= -\frac{i}{2} \begin{pmatrix} [\sigma^i, \sigma^k] & 0 \\ 0 & [\sigma^i, \sigma^k] \end{pmatrix} = \epsilon^{ikl} \begin{pmatrix} \sigma^l & 0 \\ 0 & \sigma^l \end{pmatrix} \\ \sigma^{0i} \gamma_5 &= \frac{i}{2} (\gamma^0 \gamma^i - \gamma^i \gamma^0) \gamma_5 \\ &= \frac{i}{2} \left( \begin{pmatrix} 1 & 0 \\ 0 & -1 \end{pmatrix} \begin{pmatrix} 0 & \sigma^i \\ -\sigma^i & 0 \end{pmatrix} - \begin{pmatrix} 0 & \sigma^i \\ -\sigma^i & 0 \end{pmatrix} \begin{pmatrix} 1 & 0 \\ 0 & -1 \end{pmatrix} \right) \gamma_5 \\ &= i \begin{pmatrix} 0 & \sigma^i \\ \sigma^i & 0 \end{pmatrix} \begin{pmatrix} 0 & 1 \\ 1 & 0 \end{pmatrix} = i \begin{pmatrix} \sigma^i & 0 \\ 0 & \sigma^i \end{pmatrix}. \end{aligned}$$

Note that the  $\gamma_5$  here is crucial to make the matrix block diagonal, because, only block diagonal terms contribute to the leading order in the non-relativistic expansion, as we will see now.

In the rest frame of the electron the spinors have the form

$$u(p, r) = \frac{1}{\sqrt{p^0 + m}} (\not{p} + m) \tilde{u}(0, r) \simeq \tilde{u}(0, r)$$

with

$$\tilde{u}(0, r) = \begin{pmatrix} U(r) \\ 0 \end{pmatrix}, \quad U\left(\frac{1}{2}\right) = \begin{pmatrix} 1 \\ 0 \end{pmatrix}, \quad U\left(-\frac{1}{2}\right) = \begin{pmatrix} 0 \\ 1 \end{pmatrix}.$$

We first work out the magnetic dipole term

$$\begin{aligned} \bar{u}_2 \sigma^{\mu\nu} u_1 F_{\mu\nu} &\simeq (U^T(r_2), 0) \sigma^{\mu\nu} \begin{pmatrix} U(r_1) \\ 0 \end{pmatrix} F_{\mu\nu} \\ &= (U^T(r_2), 0) \sigma^{ik} \begin{pmatrix} U(r_1) \\ 0 \end{pmatrix} F_{ik} \\ &= \epsilon^{ikl} (U^T(r_2), 0) \begin{pmatrix} \sigma^l & 0 \\ 0 & \sigma^l \end{pmatrix} \begin{pmatrix} U(r_1) \\ 0 \end{pmatrix} F_{ik} \\ &= 2U^T(r_2) \boldsymbol{\sigma} U(r_1) \mathbf{B} = 2(\boldsymbol{\sigma})_{r_2, r_1} \mathbf{B}. \end{aligned}$$

The other non-diagonal terms do not contribute in this static limit. Similarly, for the electric dipole term

$$\begin{aligned} \bar{u}_2 \sigma^{\mu\nu} \gamma_5 u_1 F_{\mu\nu} &\simeq (U^T(r_2), 0) \sigma^{\mu\nu} \gamma_5 \begin{pmatrix} U(r_1) \\ 0 \end{pmatrix} F_{\mu\nu} \\ &= 2(U^T(r_2), 0) \sigma^{0i} \gamma_5 \begin{pmatrix} U(r_1) \\ 0 \end{pmatrix} F_{0i} \\ &= 2i(U^T(r_2), 0) \begin{pmatrix} \sigma^i & 0 \\ 0 & \sigma^i \end{pmatrix} \begin{pmatrix} U(r_1) \\ 0 \end{pmatrix} F_{0i} \\ &= 2iU^T(r_2) \boldsymbol{\sigma} U(r_1) \mathbf{E} = 2i(\boldsymbol{\sigma})_{r_2, r_1} \mathbf{E}. \end{aligned}$$

In the low energy expansion matrix elements of the form  $\bar{v}_2 \Gamma_i u_1$  or  $\bar{u}_2 \Gamma_i v_1$  pick out off-diagonal  $2 \times 2$  sub-matrices mediating electron-positron creation or annihilation processes, which have thresholds  $\sqrt{s} \geq 2m$  and thus are genuinely relativistic effects. The leading terms are the known classical low energy effective terms

$$-\delta \mathcal{L}_{\text{eff}}^{\text{AMM}} \Rightarrow \mathcal{H}_m \simeq \frac{e_\ell a_\ell}{2m_\ell} \boldsymbol{\sigma} \mathbf{B},$$

and

$$-\delta \mathcal{L}_{\text{eff}}^{\text{EDM}} \Rightarrow \mathcal{H}_e \simeq -d_\ell \boldsymbol{\sigma} \mathbf{E},$$

written as  $2 \times 2$  matrix Hamiltonian, as given before.

### 3.5 Projection Technique

Especially the calculations of the anomalous magnetic moment in higher orders require most efficient techniques to perform such calculations. As we have seen in Chap. 2 the straightforward calculation of the electromagnetic form factors turns out to be quite non-trivial at the one-loop level already. In particular the occurrence of higher order tensor integrals (up to second rank) makes such calculations rather tedious. Here we outline a projection operator technique which appears to be a much more clever set up for such calculations. Calculations turn out to simplify considerably as we will see.

The tensor integrals showing up in the direct evaluation of the Feynman integrals may be handled in a different way, which allows us to deal directly with the individual amplitudes appearing in the covariant decomposition (3.79). With the matrix element of the form (3.78) we may construct projection operators  $\mathcal{P}_{\mu i}$  such that the amplitudes  $A_i$  are given by the trace

$$A_i = \text{Tr} \left\{ \mathcal{P}_{\mu i} \Pi_{\gamma\ell\ell}^\mu \right\}. \quad (3.88)$$

Since we assume parity P and CP symmetry here (QED) and we have to form a scalar amplitude, a projection operator has to be of a form like (3.79) but with different coefficients which have to be chosen such that the individual amplitudes are obtained. An additional point we have to take into account is the following: since we are working on the physical mass shell (off-shell there would be many more amplitudes), we have to enforce that contributions to  $\Pi_{\gamma\ell\ell}^\mu$  of the form  $\delta\Pi_{\gamma\ell\ell}^\mu = \dots (\not{p}_1 - m) + (\not{p}_2 - m) \dots$  give vanishing contribution as  $\bar{u}_2 \delta\Pi_{\gamma\ell\ell}^\mu u_1 = 0$ . This is enforced by applying the projection matrices  $\not{p}_1 + m$  from the right and  $\not{p}_2 + m$  from the left, respectively, such that the general form of the projector of interest reads

$$\mathcal{P} = (\not{p}_1 + m) \left( \gamma^\mu c_1 + \frac{P^\mu}{2m} c_2 + \frac{q^\mu}{2m} c_3 + \gamma^\mu \gamma_5 c_4 + \frac{q^\mu}{2m} \gamma_5 c_5 - i \frac{P^\mu}{2m} \gamma_5 c_6 \right) (\not{p}_2 + m). \quad (3.89)$$

It indeed yields

$$\text{Tr} \left\{ \mathcal{P}_\mu \delta\Pi_{\gamma\ell\ell}^\mu \right\} = 0$$

for arbitrary values of the constants  $c_i$ , because  $(\not{p}_2 + m)(\not{p}_2 - m) = p_2^2 - m^2 = 0$  if we set  $p_2^2 = m^2$  and making use of the cyclicity of the trace, similarly,  $(\not{p}_1 - m)(\not{p}_1 + m) = p_1^2 - m^2 = 0$  if we set  $p_1^2 = m^2$ . In order to find the appropriate sets of constants which allow us to project to the individual amplitudes we compute  $\text{Tr} \mathcal{P}_\mu \Pi_{\gamma\ell\ell}^\mu$  and obtain

$$\text{Tr} \left\{ \mathcal{P}_\mu \Pi_{\gamma\ell\ell}^\mu \right\} = \sum_{i=1}^6 g_i A_i \quad (3.90)$$

$$\begin{aligned}
\sum_{i=1}^6 g_i A_i &= A_1 \left[ c_1(2ds - 4s + 8m^2) + c_2(-2s + 8m^2) \right] \\
&+ A_2 \left[ c_1(-2s + 8m^2) + c_2(-4s + 1/2s^2m^{-2} + 8m^2) \right] \\
&+ A_3 \left[ c_3(2s - 1/2s^2m^{-2}) \right] \\
&+ A_4 \left[ c_4(2ds - 8dm^2 - 4s + 8m^2) + c_5(2s) \right] \\
&+ A_5 \left[ c_4(-2s) + c_5(1/2s^2m^{-2}) \right] \\
&+ A_6 \left[ c_6(2s - 1/2s^2m^{-2}) \right]
\end{aligned}$$

where  $s = q^2$ . We observe, firstly, that each of the amplitudes  $A_3$  and  $A_6$  does not mix with any other amplitude and hence may be projected out in a trivial way setting  $c_3 = 1$  or  $c_6 = 1$ , respectively, with all others zero in (3.89). Secondly, the parity violating amplitudes  $A_i$   $i = 4, 5, 6$  do not interfere of course with the parity conserving ones  $A_i$   $i = 1, 2, 3$  which are the only ones present in QED. To disentangle  $A_1$  and  $A_2$  we have to choose  $c_1/c_2$  such that the coefficient of  $A_2$  or the one of  $A_1$  is vanishing, and correspondingly for  $A_4$  and  $A_5$ . The coefficient of the projected amplitude  $A_i$  has to be normalized to unity, such that the requested projector yields (3.88).

Thus,  $\mathcal{P}_i$  is obtained by choosing  $c_j$  such that  $g_i = 1$  and  $g_j = 0$  for all  $j \neq i$ . The following table lists the non-zero coefficients required for the corresponding projector:

$$\begin{aligned}
\mathcal{P}_1 : c_1 &= c_2 \frac{s - 4m^2}{4m^2} & c_2 &= \frac{1}{(d-2)f_1(d)} \frac{2m^2}{s(s - 4m^2)} \\
\mathcal{P}_2 : c_2 &= c_1 \frac{(d-2)s + 4m^2}{s - 4m^2} & c_1 &= \frac{1}{(d-2)f_1(d)} \frac{2m^2}{s(s - 4m^2)} \\
\mathcal{P}_3 : & & c_3 &= \frac{1}{f_1(d)} \frac{2m^2}{s(s-4m^2)} \\
\mathcal{P}_4 : c_4 &= c_5 \frac{s}{4m^2} & c_5 &= \frac{1}{(d-2)f_1(d)} \frac{2m^2}{s(s - 4m^2)} \\
\mathcal{P}_5 : c_5 &= -c_4 \frac{(d-2)(s - 4m^2) - 4m^2}{s} & c_4 &= \frac{1}{(d-2)f_1(d)} \frac{2m^2}{s(s - 4m^2)} \\
\mathcal{P}_6 : & & c_6 &= -i \frac{1}{f_1(d)} \frac{2m^2}{s(s-4m^2)}
\end{aligned}$$

with  $f_1(d)$  we denote  $f(d)/f(d=4)$  where  $f(d) \doteq \text{Tr } 1 = 2^{(d/2)}$  ( $\lim_{d \rightarrow 4} f(d) = 4$ ). As discussed in Sect. 2.4.2, p. 68 physics is not affected by the way  $f(d=4) = 4$  is extrapolated to  $d \neq 4$ , provided one sticks to a given convention, like setting  $f(d) = 4$  for arbitrary  $d$  which means we may take  $f_1(d) = 1$  everywhere as a convention. For the amplitudes we are interested in the following we have

$$\begin{aligned}
\mathcal{P}_1^\mu &= \frac{1}{2f_1(d)(d-2)} (\not{p}_1 + m) \left( \gamma^\mu + \frac{4m^2}{s(s-4m^2)} \frac{P^\mu}{2m} \right) (\not{p}_2 + m), \\
\mathcal{P}_2^\mu &= \frac{2m^2/s}{f_1(d)(d-2)(s-4m^2)} (\not{p}_1 + m) \left( \gamma^\mu + \frac{(d-2)s + 4m^2}{(s-4m^2)} \frac{P^\mu}{2m} \right) (\not{p}_2 + m), \\
\mathcal{P}_3^\mu &= \frac{1}{f_1(d)} \frac{2m^2/s}{(s-4m^2)} (\not{p}_1 + m) \left( \frac{q^\mu}{2m} \right) (\not{p}_2 + m). \tag{3.91}
\end{aligned}$$

All projectors are of the form

$$\mathcal{P}_i^\mu = (\not{p}_1 + m) \Lambda_i^\mu(p_2, p_1) (\not{p}_2 + m), \quad (3.92)$$

for example, in the projector for  $A_2$  taking  $f_1(d) = 1$  we have

$$\Lambda_2^\mu(p_2, p_1) = \frac{2m^2}{(d-2)s(s-4m^2)} \left( \gamma^\mu + \frac{(d-2)s+4m^2}{s-4m^2} \frac{P^\mu}{2m} \right). \quad (3.93)$$

This projector we will need later for calculating higher order contributions to the anomalous magnetic moment in an efficient manner.

The amplitudes  $A_i$  at one-loop are now given by the integrals

$$A_i = e^2 \int \frac{d^d k}{(2\pi)^d} \frac{f_i(k)}{((p_2 - k)^2 - m^2)((p_1 - k)^2 - m^2)(k^2)} \quad (3.94)$$

with

$$\begin{aligned} f_1(k) &= (4m^2 - 2s) - 4kP + (d-4)k^2 + \frac{2(kq)^2}{s} - \frac{2(kP)^2}{(s-4m^2)} \\ f_2(k) &= -\frac{8m^2}{s-4m^2} \left( kP + k^2 + (d-1) \frac{(kP)^2}{(s-4m^2)} - \frac{(kq)^2}{s} \right) \\ f_3(k) &= \frac{8m^2}{s} kq \left( 1 - (d-2) \frac{kP}{(s-4m^2)} \right). \end{aligned} \quad (3.95)$$

Again we use the relations  $2kP = 2[k^2] - [(p_1 - k)^2 - m^2] - [(p_2 - k)^2 - m^2]$  and  $2kq = [(p_1 - k)^2 - m^2] - [(p_2 - k)^2 - m^2]$  when it is possible to cancel against the scalar propagators  $\frac{1}{(1)}$ ,  $\frac{1}{(2)}$  and  $\frac{1}{(3)}$  where (1)  $\doteq (p_1 - k)^2 - m^2$ , (2)  $\doteq (p_2 - k)^2 - m^2$ , (3)  $\doteq k^2$ :

$$\begin{aligned} f_1(k) &= (4m^2 - 2s) + (d-8)(3) + 2(1) + 2(2) \\ &\quad + \frac{(kq)}{s} [(1) - (2)] - \frac{(kP)}{(s-4m^2)} [2(3) - (1) - (2)] \\ f_2(k) &= -\frac{4m^2}{s-4m^2} \left( 4(3) - (1) - (2) \right) \\ &\quad + (d-1) \frac{(kP)}{(s-4m^2)} [2(3) - (1) - (2)] - \frac{(kq)}{s} [(1) - (2)] \\ f_3(k) &= \frac{4m^2}{s} [(1) - (2)] \left( 1 - (d-2) \frac{kP}{(s-4m^2)} \right). \end{aligned} \quad (3.96)$$

We observe that besides the first term in  $f_1$  which yields a true vertex correction (three point function) all other terms have at least one scalar propagator (1), (2) or (3) in the numerator which cancels against one of the denominators and hence

only yields a much simpler two point function. In particular  $f_i$   $i = 2, 3$  are completely given by two point functions and the remaining  $k$  dependence in the numerator is at most linear (first rank tensor) and only in combination of two point functions. This is a dramatic simplification in comparison to the most frequently applied direct method presented before. With  $\int_k \frac{1}{(1)(2)(3)} = -C_0$ ,  $\int_k \frac{1}{(1)(2)} = B_0(m, m; s)$ ,  $\int_k \frac{1}{(1)(3)} = \int_k \frac{1}{(2)(3)} = B_0(0, m; m^2)$ ,  $\int_k \frac{k^\mu}{(1)(3)} = p_1^\mu \frac{A_0(m)}{2m^2}$ ,  $\int_k \frac{k^\mu}{(2)(3)} = p_2^\mu \frac{A_0(m)}{2m^2}$ ,  $\int_k \frac{k^\mu}{(1)(2)} = 0$ ,  $\int_k \frac{1}{(1)} = \int_k \frac{1}{(3)} = -A_0(m)$  and  $\int_k \frac{1}{(3)} = 0$  we easily find

$$\begin{aligned} A_1 &= \frac{e^2}{16\pi^2} \left\{ (2s - 4m^2) C_0(m_\gamma, m, m) \right. \\ &\quad \left. - 3 B_0(m, m; s) + 4 B_0(0, m; m^2) - 2 \right\} \\ A_2 &= \frac{e^2}{16\pi^2} \left\{ \frac{-4m^2}{s - 4m^2} (B_0(m, m; s) - B_0(0, m; m^2)) \right\} \\ A_3 &= 0 \end{aligned} \quad (3.97)$$

in agreement with (2.204).

For our main goal of calculating the muon anomaly  $a_\mu = F_M(0) = -A_2(0)$  we may work out the classical limit  $s = q^2 \rightarrow 0$

$$a_\mu = \lim_{q^2 \rightarrow 0} \text{Tr} \left\{ (\not{p}_1 + m) \Lambda_2^\mu(p_2, p_1) (\not{p}_2 + m) \Pi_\mu(P, q) \right\} \quad (3.98)$$

explicitly. Because of the singular factor  $1/q^2$  in front of the projector  $\Lambda_2$  (3.93) we are required to expand the amplitude  $\Pi^\mu(P, q)$  to first order for small  $q$ ,

$$\Pi_\mu(P, q) \simeq \Pi_\mu(P, 0) + q^\nu \frac{\partial}{\partial q^\nu} \Pi_\mu(P, q) \Big|_{q=0} \equiv V_\mu(p) + q^\nu T_{\nu\mu}(p), \quad (3.99)$$

where for  $q = 0$  we have  $p = P/2 = p_1$ . Other factors of  $q$  come from expanding the other factors in the trace by setting  $p_2 = (P + q)/2$  and  $p_1 = (P - q)/2$  and performing an expansion in  $q = p_2 - p_1$  for fixed  $P = p_2 + p_1$ . We note that due to the on-shell condition  $p_2^2 = p_1^2 = m^2$  we have  $Pq = 2pq + q^2 = 0$ . The only relevant  $q^\mu$  dependence left are the terms linear and quadratic in  $q$ , proportional to  $q^\mu$  and  $q^\mu q^\nu$ . Since the trace under consideration projects to a scalar, we may average the residual  $q$  dependence over all spatial directions without changing the result. Since  $P$  and  $q$  are two independent and orthogonal vectors, averaging is relative to the direction of  $P$ . For the linear term we have

$$\overline{q^\mu} \equiv \int \frac{d\Omega(P, q)}{4\pi} q^\mu = 0 \quad (3.100)$$



because the integrand is an odd function, while

$$\overline{q^\mu q^\nu} \equiv \int \frac{d\Omega(P, q)}{4\pi} q^\mu q^\nu = \alpha g^{\mu\nu} + \beta \frac{P^\mu P^\nu}{P^2}$$

must be a second rank tensor in  $P$ . Since  $Pq = 0$ , the contraction with  $P_\mu$  is vanishing, which requires

$$\beta = -\alpha .$$

The other possible contraction with  $g_{\mu\nu}$  yields  $q^2$ :

$$\int \frac{d\Omega(P, q)}{4\pi} q^2 = q^2 \int \frac{d\Omega(P, q)}{4\pi} = q^2 = \alpha d + \beta = (d-1) \alpha$$

and hence

$$\alpha = \frac{q^2}{(d-1)}$$

or

$$\overline{q^\mu q^\nu} = \frac{q^2}{(d-1)} \left( g^{\mu\nu} - \frac{P^\mu P^\nu}{P^2} \right) . \quad (3.101)$$

Using these averages we may work out the limit which yields

$$\begin{aligned} a_\mu &= \frac{1}{8(d-2)(d-1)m} \text{Tr} \{ (\not{p} + m) [\gamma^\mu, \gamma^\nu] (\not{p} + m) T_{\nu\mu}(p) \} \\ &+ \frac{1}{4(d-1)m^2} \text{Tr} \{ [m^2 \gamma^\mu - (d-1)m p^\mu - d \not{p} p^\mu] V_\mu(p) \} \Big|_{p^2=m^2} \end{aligned} \quad (3.102)$$

as a master formula for the calculation of  $a_\mu$  [103]. The form of the first term is obtained upon anti-symmetrization in the indices  $[\mu\nu]$ . The amplitudes  $V_\mu(p)$  and  $T_{\nu\mu}(p)$  depend on one on-shell momentum  $p$ , only, and thus the problem reduces to the calculation of on-shell self-energy type diagrams shown in Fig. 3.9.

In  $T_{\nu\mu}$  the extra vertex is generated by taking the derivative of the internal muon propagators

$$\frac{\partial}{\partial q^\nu} \frac{i}{\not{p} - \not{k} \mp q/2 - m} \Big|_{q=0} = \mp \frac{1}{2} \frac{i}{\not{p} - \not{k} - m} (-i \gamma_\nu) \frac{i}{\not{p} - \not{k} - m} .$$

Usually, writing the fermion propagators in terms of scalar propagators

$$\frac{i}{\not{p}_i - \not{k} - m} = \frac{i(\not{p}_i - \not{k} + m)}{(p_i - k)^2 - m^2}$$

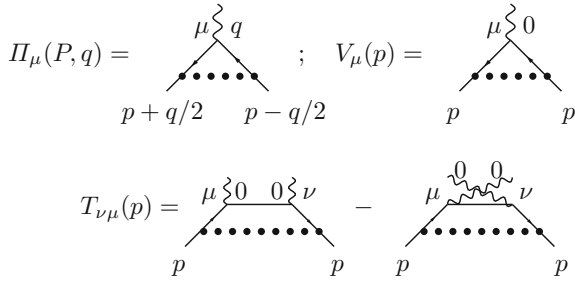


**Fig. 3.9** To calculate  $a_\mu$  one only needs the on-shell vertex  $V_\mu(p) = \Pi_\mu(P, q)|_{q=0}$  and its  $\mu \leftrightarrow \nu$  anti-symmetrized derivative  $T_{\nu\mu} = \frac{\partial}{\partial q^\nu} \Pi_\mu(P, q)|_{q=0}$  at zero momentum transfer. Illustrated here for the lowest order diagram; the dotted line may be a photon or a heavy “photon” as needed in the dispersive approach to be discussed below

as done in (2.203), only the expansion of the numerators contributes to  $T_{\nu\mu}$ , while expanding the product of the two scalar propagators

$$\frac{1}{(p_2 - k)^2 - m^2} \frac{1}{(p_1 - k)^2 - m^2} = \frac{1}{((p - k)^2 - m^2)^2} + Q(q^2)$$

gives no contribution linear in  $q$ , as the linear terms coming from the individual propagators cancel in the product. Looking at (2.203), for the lowest order contribution we thus have to calculate the trace (3.102) with

$$V_\mu \rightarrow v_\mu = \gamma^\rho (\not{p} - \not{k} + m) \gamma_\mu (\not{p} - \not{k} + m) \gamma_\rho$$

$$T_{\nu\mu} \rightarrow t_{\nu\mu} = \frac{1}{2} \gamma^\rho (\gamma_\nu \gamma_\mu (\not{p} - \not{k} + m) - (\not{p} - \not{k} + m) \gamma_\mu \gamma_\nu) \gamma_\rho .$$

The trace yields

$$2k^2 \left( \frac{1}{d-1} - 1 \right) - 4kp + \frac{(2kp)^2}{2m^2} \left( d - 1 - \frac{1}{d-1} \right)$$

which is to be integrated as in (2.203). The result is (see Sect. 2.6.3 p. 116)

$$a_\mu = \frac{e^2}{16\pi^2} \frac{2}{3} \{ B_0(0, m; m^2) - B_0(m, m; 0) + 1 \} = \frac{\alpha}{\pi} \frac{1}{2}$$

as it should be. Note that the result differs in structure from (3.97) because integration and taking the limit is interchanged. Since we are working throughout with dimensional regularization, it is crucial to take the dimension  $d$  generic until after integration. In particular setting  $d = 4$  in the master formula (3.102) would lead to a wrong constant term in the above calculation. In fact, the constant term would just be absent.

The projection technique just outlined provides an efficient tool for calculating individual on-shell amplitudes directly. One question may be addressed here, however. The muon is an unstable particle and mass and width are defined via the resonance pole in the complex  $p^2$ -plane. In this case the projection technique as presented above has its limitation. However, the muon width is so many orders of magnitude smaller than the muon mass, that at the level of accuracy which is of any practical interest, this is not a matter of worry, i.e. the muon as a quasi stable particle may be safely approximated to be stable in calculations of  $a_\mu$ .

### 3.6 Properties of the Form Factors

We again consider the interaction of a lepton in an external field: the relevant  $T$ -matrix element is

$$T_{fi} = e \mathcal{J}_{fi}^\mu \tilde{A}_\mu^{\text{ext}}(q) \quad (3.103)$$

with

$$\mathcal{J}_{fi}^\mu = \bar{u}_2 \Gamma^\mu u_1 = \langle f | j_{\text{em}}^\mu(0) | i \rangle = \langle \ell^-(p_2) | j_{\text{em}}^\mu(0) | \ell^-(p_1) \rangle . \quad (3.104)$$

By the crossing property we have the following channels:

- Elastic  $\ell^-$  scattering:  $s = q^2 = (p_2 - p_1)^2 \leq 0$
- Elastic  $\ell^+$  scattering:  $s = q^2 = (p_1 - p_2)^2 \leq 0$
- Annihilation (or pair-creation) channel:  $s = q^2 = (p_1 + p_2)^2 \geq 4m_\ell^2$

The domain  $0 < s < 4m_\ell^2$  is unphysical. A look at the unitarity condition

$$i \{ T_{if}^* - T_{fi} \} = \sum_n \int (2\pi)^4 \delta^{(4)}(P_n - P_i) T_{nf}^* T_{ni} , \quad (3.105)$$

which derives from (2.96), (2.103), taking  $\langle f | S^+ S | i \rangle$  and using (3.128) below, tells us that for  $s < 4m_\ell^2$  there is no physical state  $|n\rangle$  allowed by energy and momentum conservation and thus

$$T_{fi} = T_{if}^* \quad \text{for} \quad s < 4m_\ell^2 , \quad (3.106)$$

which means that the current matrix element is Hermitian. As the electromagnetic potential  $A_\mu^{\text{ext}}(x)$  is real its Fourier transform satisfies

$$\tilde{A}_\mu^{\text{ext}}(-q) = \tilde{A}_\mu^{*\text{ext}}(q) \quad (3.107)$$

and hence

$$\mathcal{J}_{fi}^\mu = \mathcal{J}_{if}^{\mu*} \quad \text{for} \quad s < 4m_\ell^2 . \quad (3.108)$$

If we interchange initial and final state the four-vectors  $p_1$  and  $p_2$  are interchanged such that  $q$  changes sign:  $q \rightarrow -q$ . The unitarity relation for the form factor decomposition of  $\bar{u}_2 \Pi_{\gamma\ell\ell}^\mu u_1$  (3.82) thus reads ( $u_i = u(p_i, r_i)$ )

$$\begin{aligned} & \bar{u}_2 \left( \gamma^\mu F_E(q^2) + [\gamma^\mu - \frac{2mq^\mu}{q^2}] \gamma_5 F_A + i\sigma^{\mu\nu} \frac{q_\nu}{2m} F_M(q^2) + \sigma^{\mu\nu} \frac{q_\nu}{2m} \gamma_5 F_D \right) u_1 \\ &= \left\{ \bar{u}_1 \left( \gamma^\mu F_E(q^2) + [\gamma^\mu + \frac{2mq^\mu}{q^2}] \gamma_5 F_A - i\sigma^{\mu\nu} \frac{q_\nu}{2m} F_M(q^2) - \sigma^{\mu\nu} \frac{q_\nu}{2m} \gamma_5 F_D \right) u_2 \right\}^* \\ &= u_2^+ \left( \gamma^{\mu+} F_E^*(q^2) + \gamma_5^+ [\gamma^{\mu+} + \frac{2mq^\mu}{q^2}] F_A^* + i\sigma^{\mu\nu+} \frac{q_\nu}{2m} F_M^*(q^2) - \gamma_5^+ \sigma^{\mu\nu+} \frac{q_\nu}{2m} F_D^* \right) \bar{u}_1^+ \\ &= \bar{u}_2 \left( \gamma^\mu F_E^*(q^2) + [\gamma^\mu - \frac{2mq^\mu}{q^2}] \gamma_5 F_A^* + i\sigma^{\mu\nu} \frac{q_\nu}{2m} F_M^*(q^2) + \sigma^{\mu\nu} \frac{q_\nu}{2m} \gamma_5 F_D^* \right) u_1 . \end{aligned}$$

The last equality follows using  $u_2^+ = \bar{u}_2 \gamma^0$ ,  $\bar{u}_1^+ = \gamma^0 u_1$ ,  $\gamma_5^+ = \gamma_5$ ,  $\gamma^0 \gamma_5 \gamma^0 = -\gamma_5$ ,  $\gamma^0 \gamma^{\mu+} \gamma^0 = \gamma^\mu$  and  $\gamma^0 \sigma^{\mu\nu+} \gamma^0 = \sigma^{\mu\nu}$ . Unitarity thus implies that the form factors are real

$$\text{Im } F(s)_i = 0 \quad \text{for } s < 4m_e^2 \quad (3.109)$$

below the threshold of pair production  $s = 4m_e^2$ . For  $s \geq 4m_e^2$  the form factors are complex; they are analytic in the complex  $s$ -plane with a cut along the positive axis starting at  $s = 4m_e^2$  (see Fig. 3.10). In the annihilation channel ( $p_- = p_2$ ,  $p_+ = -p_1$ )

$$\langle 0 | j_{\text{em}}^\mu(0) | p_-, p_+ \rangle = \sum_n \langle 0 | j_{\text{em}}^\mu(0) | n \rangle \langle n | p_-, p_+ \rangle , \quad (3.110)$$

where the lowest state  $|n\rangle$  contributing to the sum is an  $e^+e^-$  state at threshold:  $E_+ = E_- = m_e$  and  $\mathbf{p}_+ = \mathbf{p}_- = 0$  such that  $s = 4m_e^2$ . Because of the causal  $i\epsilon$ -prescription in the time-ordered Green functions the imaginary parts of the analytic amplitudes change sign when  $s \rightarrow s^*$  and hence

$$F_i(s^*) = F_i^*(s) , \quad (3.111)$$

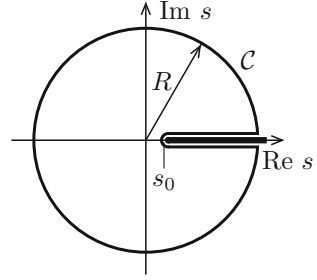
which is the Schwarz reflection principle.

### 3.7 Dispersion Relations

Causality together with unitarity imply analyticity of the form factors in the complex  $s$ -plane except for the cut along the positive real axis starting at  $s \geq 4m_e^2$ . Cauchy's integral theorem tells us that the contour integral, for the contour  $\mathcal{C}$  shown in Fig. 3.10, satisfies

$$F_i(s) = \frac{1}{2\pi i} \oint_{\mathcal{C}} \frac{ds' F(s')}{s' - s} . \quad (3.112)$$

**Fig. 3.10** Analyticity domain and Cauchy contour  $\mathcal{C}$  for the lepton form factor (vacuum polarization).  $\mathcal{C}$  is a circle of radius  $R$  with a cut along the positive real axis for  $s > s_0 = 4m^2$  where  $m$  is the mass of the lightest particles which can be pair-produced



Since  $F^*(s) = F(s^*)$  the contribution along the cut may be written as

$$\lim_{\epsilon \rightarrow 0} (F(s + i\epsilon) - F(s - i\epsilon)) = 2i \operatorname{Im} F(s) ; \quad s \text{ real}, s > 0$$

and hence for  $R \rightarrow \infty$

$$F(s) = \lim_{\epsilon \rightarrow 0} F(s + i\epsilon) = \frac{1}{\pi} \lim_{\epsilon \rightarrow 0} \int_{4m^2}^{\infty} ds' \frac{\operatorname{Im} F(s')}{s' - s - i\epsilon} + \mathcal{C}_{\infty} .$$

In all cases where  $F(s)$  falls off sufficiently rapidly as  $|s| \rightarrow \infty$  the boundary term  $\mathcal{C}_{\infty}$  vanishes and the integral converges. This may be checked order by order in perturbation theory. In this case the “un-subtracted” dispersion relation (DR)

$$F(s) = \frac{1}{\pi} \lim_{\epsilon \rightarrow 0} \int_{4m^2}^{\infty} ds' \frac{\operatorname{Im} F(s')}{s' - s - i\epsilon} \tag{3.113}$$

uniquely determines the function by its imaginary part. A technique based on DRs is frequently used for the calculation of Feynman integrals, because the calculation of the imaginary part is simpler in general. The real part which actually is the object to be calculated is given by the principal value ( $\mathcal{P}$ ) integral

$$\operatorname{Re} F(s) = \frac{1}{\pi} \mathcal{P} \int_{4m^2}^{\infty} ds' \frac{\operatorname{Im} F(s')}{s' - s} , \tag{3.114}$$

which is also known under the name Hilbert transform.

For our form factors the fall off condition is satisfied for the Pauli form factor  $F_M$  but not for the Dirac form factor  $F_E$ . In the latter case the fall off condition is not satisfied because  $F_E(0) = 1$  (charge renormalization condition = subtraction condition). However, performing a subtraction of  $F_E(0)$  in (3.113), one finds that  $(F_E(s) - F_E(0))/s$  satisfies the “subtracted” dispersion relations

$$\frac{F(s) - F(0)}{s} = \frac{1}{\pi} \lim_{\varepsilon \rightarrow 0} \int_{4m^2}^{\infty} ds' \frac{\text{Im } F(s')}{s'(s' - s - i\varepsilon)}, \quad (3.115)$$

which exhibits one additional power of  $s'$  in the denominator and hence improves the damping of the integrand at large  $s'$  by one additional power. Order by order in perturbation theory the integral (3.115) is convergent for the Dirac form factor. A very similar relation is satisfied by the vacuum polarization amplitude which we will discuss in the following section.

### 3.7.1 Dispersion Relations and the Vacuum Polarization

Dispersion relations play an important role for taking into account the photon propagator contributions. The related photon self-energy, obtained from the photon propagator by the amputation of the external photon lines, is given by the correlator of two electromagnetic currents and may be interpreted as vacuum polarization for the following reason: as we have seen in Sect. 2.6.3 charge renormalization in QED, according to (2.212), is caused solely by the photon self-energy correction; the fundamental electromagnetic fine structure constant  $\alpha$  in fact is a function of the energy scale  $\alpha \rightarrow \alpha(E)$  of a process due to charge screening. The latter is a result of the fact that a naked charge is surrounded by a cloud of virtual particle-antiparticle pairs (dipoles mostly) which line up in the field of the central charge and such lead to a vacuum polarization which screens the central charge. This is illustrated in Fig. 3.11. From long distances (classical charge) one thus sees less charge than if one comes closer, such that one sees an increasing charge with increasing energy. Figure 3.12 shows the usual diagrammatic representation of a vacuum polarization effect.

**Fig. 3.11** Vacuum polarization causing charge screening by virtual pair creation and re-annihilation. The effective charge seen by a test charge at distance  $r = \hbar/E$  ( $E$  the collision energy) is given by the charge inside the ball of radius  $r$

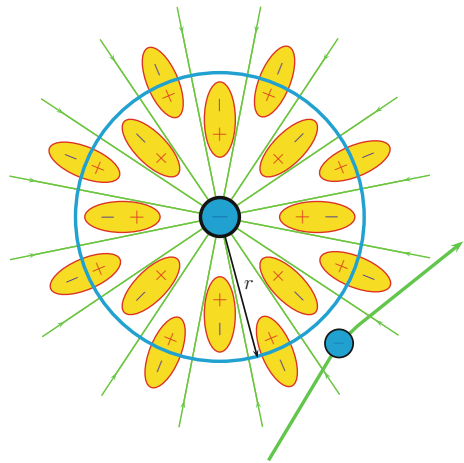
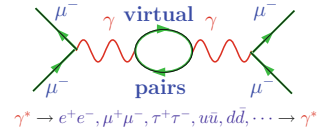


**Fig. 3.12** Feynman diagram describing the vacuum polarization in muon scattering



As discussed in Sect. 2.6.1 the vacuum polarization affects the photon propagator in that the full or dressed propagator is given by the geometrical progression of self-energy insertions  $-i\Pi_\gamma(q^2)$ . The corresponding Dyson summation implies that the free propagator is replaced by the dressed one

$$iD_\gamma^{\mu\nu}(q) = \frac{-ig^{\mu\nu}}{q^2 + i\epsilon} \rightarrow iD'_\gamma{}^{\mu\nu}(q) = \frac{-ig^{\mu\nu}}{q^2 + \Pi_\gamma(q^2) + i\epsilon} \tag{3.116}$$

modulo unphysical gauge dependent terms. By  $U(1)_{em}$  gauge invariance the photon remains massless and hence we have  $\Pi_\gamma(q^2) = \Pi_\gamma(0) + q^2 \Pi'_\gamma(q^2)$  with  $\Pi_\gamma(0) \equiv 0$ . As a result we obtain

$$iD'_\gamma{}^{\mu\nu}(q) = \frac{-ig^{\mu\nu}}{q^2 (1 + \Pi'_\gamma(q^2))} + \text{gauge terms} \tag{3.117}$$

where the “gauge terms” will not contribute to gauge invariant physical quantities, and need not be considered further.

Including a factor  $e^2$  and considering the renormalized propagator (wave function renormalization factor  $Z_\gamma$ ) we have

$$i e^2 D'_\gamma{}^{\mu\nu}(q) = \frac{-ig^{\mu\nu} e^2 Z_\gamma}{q^2 (1 + \Pi'_\gamma(q^2))} + \text{gauge terms} \tag{3.118}$$

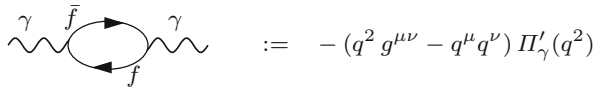
which in effect means that the charge has to be replaced by a **running charge**

$$e^2 \rightarrow e^2(q^2) = \frac{e^2 Z_\gamma}{1 + \Pi'_\gamma(q^2)} \tag{3.119}$$

The wave function renormalization factor  $Z_\gamma$  is fixed by the condition that at  $q^2 \rightarrow 0$  one obtains the classical charge (charge renormalization in the *Thomson limit*; see also (2.170)). Thus the renormalized charge is

$$e^2 \rightarrow e^2(q^2) = \frac{e^2}{1 + (\Pi'_\gamma(q^2) - \Pi'_\gamma(0))} \tag{3.120}$$

where the lowest order diagram in perturbation theory which contributes to  $\Pi'_\gamma(q^2)$  is



$$:= - (q^2 g^{\mu\nu} - q^\mu q^\nu) \Pi'_\gamma(q^2)$$

and describes the virtual creation and re-absorption of fermion pairs  $\gamma^* \rightarrow e^+ e^-$ ,  $\mu^+ \mu^-$ ,  $\tau^+ \tau^-$ ,  $u\bar{u}$ ,  $d\bar{d}$ ,  $\dots \rightarrow \gamma^*$ , In terms of the fine structure constant  $\alpha = \frac{e^2}{4\pi}$  (3.120) reads<sup>27</sup>

$$\alpha(q^2) = \frac{\alpha}{1 - \Delta\alpha} \quad ; \quad \Delta\alpha = -\text{Re} (\Pi'_\gamma(q^2) - \Pi'_\gamma(0)) \quad . \quad (3.121)$$

The various contributions to the shift in the fine structure constant come from the leptons (lep =  $e$ ,  $\mu$  and  $\tau$ ) the 5 light quarks ( $u$ ,  $d$ ,  $s$ ,  $c$ , and  $b$  and the corresponding hadrons = had) and from the top quark:

$$\Delta\alpha = \Delta\alpha_{\text{lep}} + \Delta^{(5)}\alpha_{\text{had}} + \Delta\alpha_{\text{top}} + \dots \quad (3.122)$$

Also  $W$ -pairs contribute at  $q^2 > M_W^2$ . While the other contributions can be calculated order by order in perturbation theory the hadronic contribution  $\Delta^{(5)}\alpha_{\text{had}}$  exhibits low energy strong interaction effects and hence cannot be calculated by perturbative means. Here the dispersion relations play a key role. This will be discussed in detail in Sect. 5.1.7.

The leptonic contributions are calculable in perturbation theory. Using our result (2.176) for the renormalized photon self-energy, at leading order the free lepton loops yield

$$\begin{aligned} \Delta\alpha_{\text{lep}}(q^2) &= \\ &= \sum_{\ell=e,\mu,\tau} \frac{\alpha}{3\pi} \left[ -\frac{5}{3} - y_\ell + \left(1 + \frac{y_\ell}{2}\right) \sqrt{1 - y_\ell} \ln \left( \left| \frac{\sqrt{1 - y_\ell} + 1}{\sqrt{1 - y_\ell} - 1} \right| \right) \right] \\ &= \sum_{\ell=e,\mu,\tau} \frac{\alpha}{3\pi} \left[ -\frac{8}{3} + \beta_\ell^2 + \frac{1}{2}\beta_\ell(3 - \beta_\ell^2) \ln \left( \left| \frac{1 + \beta_\ell}{1 - \beta_\ell} \right| \right) \right] \\ &= \sum_{\ell=e,\mu,\tau} \frac{\alpha}{3\pi} \left[ \ln(|q^2|/m_\ell^2) - \frac{5}{3} + O(m_\ell^2/q^2) \right] \text{ for } |q^2| \gg m_\ell^2 \\ &\simeq 0.03142 \text{ for } q^2 = M_Z^2 \end{aligned} \quad (3.123)$$

where  $y_\ell = 4m_\ell^2/q^2$  and  $\beta_\ell = \sqrt{1 - y_\ell}$  are the lepton velocities. The two-loop QED contribution

<sup>27</sup>Later, in particular when discussing hadronic resonance contributions, we will also use a complex definition of the effective fine structure constant by including the imaginary part on the r.h.s of (3.121) as well.





has been calculated long time ago [175, 176]. Defining the conformal variable (2.182) (see Sect. 2.6.1)

$$q^2 \rightarrow \xi = \frac{\sqrt{1-y}-1}{\sqrt{1-y}+1} ; \quad y = \frac{4m^2}{q^2} = -\frac{4\xi}{(1-\xi)^2},$$

we may write the single fermion contribution to two loops for spacelike  $q^2 < 0$  ( $0 \leq \xi \leq 1$ ) as (in this from provided by M. Kalmykov)

$$\begin{aligned} \Delta^{(1)}\alpha(q^2) &= \frac{\alpha}{4\pi} \left[ -\frac{20}{9} + \frac{16}{3} \frac{\xi}{(1-\xi)^2} - \frac{4}{3} \frac{(1+\xi)(1-4\xi+\xi^2)}{(1-\xi)^3} \ln \xi \right], \\ \Delta^{(2)}\alpha(q^2) &= \frac{\alpha^2}{(4\pi)^2} \left\{ -\frac{10}{3} + \frac{104}{3} \frac{\xi}{(1-\xi)^2} + 16\zeta_3 \left( 1 - 4 \frac{\xi^2}{(1-\xi)^4} \right) \right. \\ &\quad - \frac{16}{3} \frac{1-4\xi+\xi^2}{(1-\xi)^4} [\ln(1-\xi) + 2\ln(1+\xi)] \ln \xi [(1+\xi^2)\ln \xi - 2(1-\xi^2)] \\ &\quad + \frac{8}{3} \xi \frac{2+7\xi-22\xi^2+6\xi^3}{(1-\xi)^4} \ln^2 \xi - 4 \frac{(1+\xi)(1-\xi)(1-8\xi+\xi^2)}{(1-\xi)^3} \ln \xi \\ &\quad + \frac{32}{3} \frac{(1-4\xi+\xi^2)}{(1-\xi)^4} [\text{Li}_2(\xi) + 2\text{Li}_2(-\xi)] [1-\xi^2 - 2(1+\xi^2)\ln \xi] \\ &\quad \left. + 32 \frac{(1-4\xi+\xi^2)}{(1-\xi)^4} (1+\xi^2) [\text{Li}_3(\xi) + 2\text{Li}_3(-\xi)] \right\}, \end{aligned} \quad (3.124)$$

The analytical continuation to  $q^2 > 4m^2$  ( $-1 \leq \xi \leq 0$ ) can be obtained using  $m^2 \rightarrow m^2 - i\varepsilon$ , i.e.

$$\xi = \frac{\sqrt{1 - \frac{4m^2}{q^2} + i\varepsilon} - 1}{\sqrt{1 - \frac{4m^2}{q^2} + i\varepsilon} + 1} \equiv \xi + i\varepsilon ; \quad \ln \xi = \ln |\xi| + i\pi.$$

In the unphysical region  $0 < q^2 < 4m^2$  ( $\xi = e^{i\varphi}$ ) one may use the parametrization (setting  $\varphi = 2\tau$ ):

$$\xi = \exp(i2\tau), \quad \frac{q^2}{4m^2} = \sin^2 \tau, \quad \ln \xi = i2\tau,$$

to obtain

$$\begin{aligned} \Delta\alpha^{(1)}(s) &= \frac{\alpha}{4\pi} \left\{ -\frac{20}{9} + \frac{4}{3} \frac{\tau \cos \tau}{\sin^3 \tau} (1 + 2 \sin^2 \tau) - \frac{4}{3} \frac{1}{\sin^2 \tau} \right\}, \\ \Delta\alpha^{(2)}(s) &= \frac{\alpha^2}{(4\pi)^2} \left\{ 16 \left[ 2\text{Cl}_3(2\tau) + 4\text{Cl}_3(\pi - 2\tau) + \zeta_3 \right] \left[ 1 - \frac{1}{4 \sin^4 \tau} \right] \right. \\ &+ \frac{16}{3} \left[ \text{Cl}_2(2\tau) - 2\text{Cl}_2(\pi - 2\tau) \right] \left[ 8\tau \left[ 1 - \frac{1}{4 \sin^4 \tau} \right] - \frac{\cos \tau (1 + 2 \sin^2 \tau)}{\sin^3 \tau} \right] \\ &+ \frac{32}{3} \left[ \ln(2 \sin \tau) + 2 \ln(2 \cos \tau) \right] \left[ 2\tau^2 \left[ 1 - \frac{1}{4 \sin^4 \tau} \right] - \frac{\tau \cos \tau (1 + 2 \sin^2 \tau)}{\sin^3 \tau} \right] \\ &\left. - \frac{10}{3} + 4 \frac{\tau \cos \tau (3 + 2 \sin^2 \tau)}{\sin^3 \tau} - \frac{26}{3} \frac{1}{\sin^2 \tau} + \frac{14}{3} \frac{\tau^2}{\sin^4 \tau} + \frac{16}{3} \frac{\tau^2}{\sin^2 \tau} - 32\tau^2 \right\}. \quad (3.125) \end{aligned}$$

The Clausen function is defined by  $\text{Cl}_n(\varphi) = \text{Im Li}_n(e^{i\varphi}) = \sum_{m=1}^{\infty} \frac{\sin(m\varphi)}{m^n}$ . The gluonic perturbative QCD correction is given by the same formulas multiplied by the color factor  $N_c = 3$  and the  $SU(3)$  Casimir coefficient  $C_F = 4/3$  [177].

For  $\alpha = 137.036$ ,  $m_e = 0.510998902$ ,  $m_\mu = 105.658357$ ,  $m_\tau = 1776.99$  we get

$\Delta\alpha(M_Z) \times 10^4$	$e$	$\mu$	$\tau$	$e + \mu + \tau$
1-loop	174.34669	91.78436	48.05954	314.19059
2-loop	0.379829	0.235999	0.160339	0.7761677

Thus the leading contribution is affected by small electromagnetic corrections only in the next to leading order. For large  $q^2$  the leptonic contribution is actually known to three loops [178] at which it takes the value

$$\Delta\alpha_{\text{leptons}}(M_Z^2) \simeq 314.98 \times 10^{-4}. \quad (3.126)$$

As already mentioned, in contrast, the corresponding free quark loop contribution gets substantially modified by low energy strong interaction effects, which cannot be calculated reliably by perturbative QCD. The evaluation of the hadronic contribution will be discussed later.

Vacuum polarization effects are large when large scale changes are involved (large logarithms) and because of the large number of light fermionic degrees of freedom (see (2.181)) as we infer from the asymptotic form in perturbation theory

$$\Delta\alpha^{\text{pert}}(q^2) \simeq \frac{\alpha}{3\pi} \sum_f Q_f^2 N_{cf} \left( \ln \frac{|q^2|}{m_f^2} - \frac{5}{3} \right); \quad |q^2| \gg m_f^2. \quad (3.127)$$

**Fig. 3.13** Shift of the effective fine structure constant  $\Delta\alpha$  as a function of the energy scale in the space-like region  $q^2 < 0$  ( $E = -\sqrt{-q^2}$ ). The vertical bars at selected points indicate the uncertainty

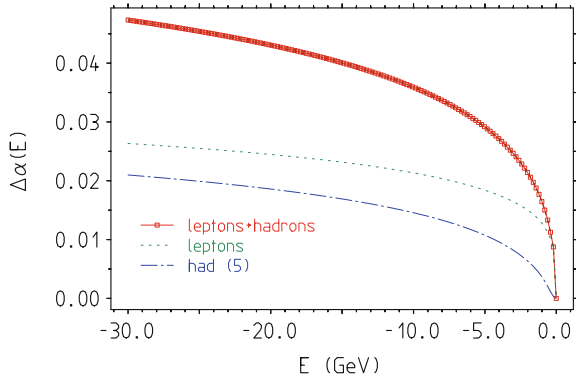


Figure 3.13 illustrates the running of the effective charges at lower energies in the space-like region.<sup>28</sup> Typical values are  $\Delta\alpha(5 \text{ GeV}) \sim 3\%$  and  $\Delta\alpha(M_Z) \sim 6\%$ , where about  $\sim 50\%$  of the contribution comes from leptons and about  $\sim 50\%$  from hadrons. Note the sharp increase of the screening correction at relatively low energies.

The vacuum polarization may be described alternatively as the vacuum expectation value of the time ordered product of two electromagnetic currents, which follows by amputation of the external photon lines of the photon propagator: at one loop order



One may represent the current correlator as a Källén–Lehmann representation [181] in terms of spectral densities. To this end, let us consider first the Fourier transform of the vacuum expectation value of the product of two currents. Using translation invariance and inserting a complete set of states  $n$  of momentum  $p_n$ ,<sup>29</sup> satisfying the completeness relation

$$\int \frac{d^4 p_n}{(2\pi)^3} \sum_n |n\rangle \langle n| = 1 \tag{3.128}$$

<sup>28</sup>A direct measurement is difficult because of the normalizing process involved in any measurement which itself depends on the effective charge. Measurements of the evolution of the electromagnetic coupling are possible in any case with an offset energy scale and results have been presented in [179] (see also [180]).

<sup>29</sup>Note that the intermediate states are multi-particle states, in general, and the completeness integral includes an integration over  $p_n^0$ , since  $p_n$  is not on the mass shell  $p_n^0 \neq \sqrt{m_n^2 + \mathbf{p}_n^2}$ . In general, in addition to a possible discrete part of the spectrum we are dealing with a continuum of states.

where  $\sum_n$  includes, for fixed total momentum  $p_n$ , integration over the phase space available to particles of all possible intermediate physical states  $|n\rangle$ , we have

$$\begin{aligned} i \int d^4x e^{iqx} \langle 0 | j^\mu(x) j^\nu(0) | 0 \rangle &= i \int \frac{d^4 p_n}{(2\pi)^3} \int d^4x e^{i(q-p_n)x} \sum_n \langle 0 | j^\mu(0) | n \rangle \langle n | j^\nu(0) | 0 \rangle \\ &= i \int \frac{d^4 p_n}{(2\pi)^3} \sum_n (2\pi)^4 \delta^{(4)}(q - p_n) \langle 0 | j^\mu(0) | n \rangle \langle n | j^\nu(0) | 0 \rangle \\ &= i 2\pi \sum_n \langle 0 | j^\mu(0) | n \rangle \langle n | j^\nu(0) | 0 \rangle \Big|_{p_n=q} . \end{aligned}$$

Key ingredient of the representation we are looking for is the **spectral function** tensor  $\rho^{\mu\nu}(q)$  defined by

$$\rho^{\mu\nu}(q) \doteq \sum_n \langle 0 | j^\mu(0) | n \rangle \langle n | j^\nu(0) | 0 \rangle \Big|_{p_n=q} . \quad (3.129)$$

Taking into account that  $q$  is the momentum of a physical state (spectral condition  $q^2 \geq 0$ ,  $q^0 \geq 0$ ), the relativistic covariant decomposition may be written as

$$\rho^{\mu\nu}(q) = \Theta(q^0)\Theta(q^2) \{ [q^\mu q^\nu - q^2 g^{\mu\nu}] \rho_1(q^2) + q^\mu q^\nu \rho_0(q^2) \} \quad (3.130)$$

and current conservation  $\partial_\mu j^\mu = 0 \Leftrightarrow q_\mu \rho^{\mu\nu} = 0$  implies  $\rho_0 \equiv 0$ , which is the transversality condition. For non-conserved currents, like the ones of the weak interactions, a longitudinal component  $\rho_0$  exists in addition to the transversal one  $\rho_1$ . Note that  $\Theta(p^2)$  may be represented as

$$\Theta(q^2) = \int_0^\infty dm^2 \delta(q^2 - m^2)$$

and therefore we may write

$$\begin{aligned} &i \int d^4x e^{iqx} \langle 0 | j^\mu(x) j^\nu(0) | 0 \rangle \quad (3.131) \\ &= \int_0^\infty dm^2 \{ [m^2 g^{\mu\nu} - q^\mu q^\nu] \rho_1(m^2) - q^\mu q^\nu \rho_0(m^2) \} \left( -2\pi i \Theta(q^0) \delta(q^2 - m^2) \right), \end{aligned}$$

which is the Källén–Lehmann representation for the positive frequency part of the current correlator. The latter, according to (2.141), is twice the imaginary part of the corresponding time-ordered current correlation function

$$\begin{aligned}
& i \int d^4x e^{iqx} \langle 0 | T j^\mu(x) j^\nu(0) | 0 \rangle \\
&= \int_0^\infty dm^2 \{ [m^2 g^{\mu\nu} - q^\mu q^\nu] \rho_1(m^2) - q^\mu q^\nu \rho_0(m^2) \} \left( \frac{1}{q^2 - m^2 + i\varepsilon} \right)
\end{aligned} \tag{3.132}$$

constrained to positive  $q^0$ .

In our case, for the conserved electromagnetic current, only the transversal amplitude is present: thus  $\rho_0 \equiv 0$  and we denote  $\rho_1$  by  $\rho$ , simply.<sup>30</sup> Thus, formally, in Fourier space we have

$$\begin{aligned}
i \int d^4x e^{iqx} \langle 0 | T j_{\text{em}}^\mu(x) j_{\text{em}}^\nu(0) | 0 \rangle &= \int_0^\infty dm^2 \rho(m^2) (m^2 g^{\mu\nu} - q^\mu q^\nu) \frac{1}{q^2 - m^2 + i\varepsilon} \\
&= -(q^2 g^{\mu\nu} - q^\mu q^\nu) \hat{\Pi}'_\gamma(q^2)
\end{aligned} \tag{3.133}$$

where  $\hat{\Pi}'_\gamma(q^2)$  up to a factor  $e^2$  is the **photon vacuum polarization function** introduced before (see (2.159) and (2.160)):

$$\Pi'_\gamma(q^2) = e^2 \hat{\Pi}'_\gamma(q^2) . \tag{3.134}$$

With this bridge to the photon self-energy function  $\Pi'_\gamma$  we can get its imaginary part by substituting

$$\frac{1}{q^2 - m^2 + i\varepsilon} \rightarrow -\pi i \delta(q^2 - m^2)$$

in (3.133), which if constrained to positive  $q^0$  yields back half of (3.131) with  $\rho_0 = 0$ . Thus contracting (3.131) with  $2\Theta(q^0)g_{\mu\nu}$  and dividing by  $g_{\mu\nu}(q^2 g^{\mu\nu} - q^\mu q^\nu) = 3q^2$  we obtain

$$\begin{aligned}
2\Theta(q^0) \text{Im} \hat{\Pi}'_\gamma(q^2) &= \Theta(q^0) 2\pi \rho(q^2) \\
&= -\frac{1}{3q^2} 2\pi \sum_n^f \langle 0 | j_{\text{em}}^\mu(0) | n \rangle \langle n | j_{\mu \text{em}}(0) | 0 \rangle \Big|_{p_n=q} .
\end{aligned} \tag{3.135}$$

Again causality implies analyticity and the validity of a dispersion relation. In fact the electromagnetic current correlator exhibits a logarithmic UV singularity and thus requires one subtraction such that from (3.133) we find

---

<sup>30</sup>In the case of a conserved current, where  $\rho_0 \equiv 0$ , we may formally derive that  $\rho_1(s)$  is real and positive  $\rho_1(s) \geq 0$ . To this end we consider the element  $\rho^{00}$

$$\rho^{00}(q) = \sum_n^f \langle 0 | j^0(0) | n \rangle \langle n | j^0(0) | 0 \rangle \Big|_{q=p_n} = \sum_n^f | \langle 0 | j^0(0) | n \rangle |_{q=p_n}^2 \geq 0 = \Theta(q^0) \Theta(q^2) \mathbf{q}^2 \rho_1(q^2)$$

from which the statement follows.

$$\Pi'_\gamma(q^2) - \Pi'_\gamma(0) = \frac{q^2}{\pi} \int_0^\infty ds \frac{\text{Im } \Pi'_\gamma(s)}{s(s - q^2 - i\varepsilon)}. \quad (3.136)$$

Unitarity (3.105) implies the *optical theorem*, which is obtained from this relation in the limit of elastic forward scattering  $|f\rangle \rightarrow |i\rangle$  where

$$2\text{Im } T_{ii} = \sum_{\mathbf{n}} (2\pi)^4 \delta^{(4)}(P_n - P_i) |T_{ni}|^2. \quad (3.137)$$

which tells us that the imaginary part of the photon propagator is proportional to the total cross section  $\sigma_{\text{tot}}(e^+e^- \rightarrow \gamma^* \rightarrow \text{anything})$  (“anything” means any possible state). The precise relationship reads (see Sect. 5.1.5)

$$\text{Im } \hat{\Pi}'_\gamma(s) = \frac{1}{12\pi} R(s) \quad (3.138)$$

$$\text{Im } \Pi'_\gamma(s) = e^2 \text{Im } \hat{\Pi}'_\gamma(s) = \frac{\alpha}{3} R(s) = \frac{\alpha s}{4\pi |\alpha(s)|^2} \sigma_{\text{tot}}(e^+e^- \rightarrow \gamma^* \rightarrow \text{anything})$$

where

$$R(s) = \sigma_{\text{tot}} / \frac{4\pi |\alpha(s)|^2}{3s}. \quad (3.139)$$

The normalization factor is the point cross section (tree level)  $\sigma_{\mu\mu}(e^+e^- \rightarrow \gamma^* \rightarrow \mu^+\mu^-)$  in the limit  $s \gg 4m_\mu^2$ . Taking into account the mass effects the  $R(s)$  which corresponds to the production of a lepton pair reads

$$R_\ell(s) = \sqrt{1 - \frac{4m_\ell^2}{s}} \left( 1 + \frac{2m_\ell^2}{s} \right), \quad (\ell = e, \mu, \tau) \quad (3.140)$$

which may be read of from the imaginary part given in (2.179). This result provides an alternative way to calculate the renormalized vacuum polarization function (2.176), namely, via the DR (3.136) which now takes the form

$$\Pi'_{\gamma \text{ ren}}{}^\ell(q^2) = \frac{\alpha q^2}{3\pi} \int_{4m_\ell^2}^\infty ds \frac{R_\ell(s)}{s(s - q^2 - i\varepsilon)} \quad (3.141)$$

yielding the vacuum polarization due to a lepton–loop.

In contrast to the leptonic part, the hadronic contribution cannot be calculated analytically as a perturbative series, but it can be expressed in terms of the cross section of the reaction  $e^+e^- \rightarrow \text{hadrons}$ , which is known from experiments. Via

$$R_{\text{had}}(s) = \sigma(e^+e^- \rightarrow \text{hadrons}) / \frac{4\pi |\alpha(s)|^2}{3s}. \quad (3.142)$$

we obtain the relevant hadronic vacuum polarization

$$\Pi'_{\gamma \text{ ren}}{}^{\text{had}}(q^2) = \frac{\alpha q^2}{3\pi} \int_{4m_\pi^2}^{\infty} ds \frac{R_{\text{had}}(s)}{s(s - q^2 - i\varepsilon)}. \quad (3.143)$$

Thus, including the five quarks  $u, d, s, c$  and  $b$  subject to non-perturbative QCD effects, we may evaluate

$$\Delta^{(5)}\alpha_{\text{had}}(q^2) = -\Pi'_{\gamma \text{ ren}}{}^{\text{had}}(q^2) = -\frac{\alpha q^2}{3\pi} \int_{4m_\pi^2}^{\infty} ds \frac{R_{\text{had}}(s)}{s(s - q^2 - i\varepsilon)}, \quad (3.144)$$

by utilizing experimental  $e^+e^-$ -data up to energies where  $\gamma - Z$  mixing comes into play, at about 20 GeV, and for the high energy tail we may use perturbative QCD by the virtue of asymptotic freedom. Note that real and imaginary parts are obtained by the identity

$$\frac{1}{s - q^2 - i\varepsilon} = \frac{\mathcal{P}}{s - q^2} + i\pi \delta(s - q^2)$$

where  $\mathcal{P}$  denotes the finite part prescription

$$\mathcal{P} \int_{4m_\pi^2}^{\infty} ds \frac{R_{\text{had}}(s)}{s(s - q^2 - i\varepsilon)} = \lim_{\varepsilon \rightarrow 0} \left\{ \int_{4m_\pi^2}^{q^2 - \varepsilon} ds \frac{R_{\text{had}}(s)}{s(s - q^2)} + \int_{q^2 + \varepsilon}^{\infty} ds \frac{R_{\text{had}}(s)}{s(s - q^2)} \right\}$$

and the imaginary part is indeed given by  $\text{Im} \Pi'_{\gamma \text{ ren}}{}^{\text{had}}(q^2) = \frac{\alpha}{3} R_{\text{had}}(q^2)$ , with the low energy  $\alpha$  as a factor, as claimed before. Corresponding relations hold for the leptonic and as well as other contributions.

At low energies, where the final state necessarily consists of two pions, the cross section is given by the square of the electromagnetic form factor of the pion (undressed from VP effects),

$$R_{\text{had}}(s) = \frac{1}{4} \left( 1 - \frac{4m_\pi^2}{s} \right)^{\frac{3}{2}} |F_\pi^{(0)}(s)|^2, \quad s < 9m_\pi^2, \quad (3.145)$$

which directly follows from the corresponding imaginary part (2.259) of the photon vacuum polarization. There are three differences between the pionic loop integral and those belonging to the lepton loops:

- the masses are different
- the spins are different
- the pion is composite – the Standard Model leptons are elementary

The compositeness manifests itself in the occurrence of the form factor  $F_\pi(s)$ , which generates an enhancement: at the  $\rho$  peak,  $|F_\pi(s)|^2$  reaches values about 45, while the quark parton model would give about 7. The remaining difference in the expressions for the quantities  $R_\ell(s)$  and  $R_h(s)$  in (3.140) and (3.145), respectively, originates

in the fact that the leptons carry spin  $\frac{1}{2}$ , while the spin of the pion vanishes. Near threshold, the angular momentum barrier suppresses the function  $R_h(s)$  by three powers of momentum, while  $R_\ell(s)$  is proportional to the first power. The suppression largely compensates the enhancement by the form factor – by far the most important property is the mass.

### 3.8 Dispersive Calculation of Feynman Diagrams

Dispersion relations (DR) may be used to calculate Feynman integrals in a way different from the Feynman parametric approach described in Sect. 2.5. The reason is simply because the imaginary part of an amplitude in general is much easier to calculate than the amplitude itself, which then follows from the imaginary part by a one-fold integral. The imaginary part in principle may be obtained by the unitarity relation of the form (3.105) which translate into *Cutkosky rules* [182], which may be obtained using Veltman's [183] largest time equation in coordinate space. The latter make use of the splitting of the Feynman propagator into real and imaginary part (2.141) and contributes to the imaginary part of a Feynman integral if the substitution

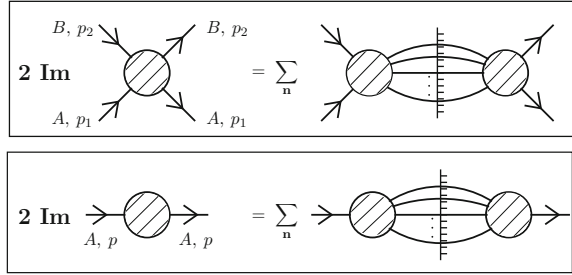
$$\frac{1}{p^2 - m^2 + i\epsilon} \rightarrow -\pi i \delta(p^2 - m^2)$$

replacing a virtual particle (un-cut line) by a physical state (cut line) is made for an odd number of propagators, and provided the corresponding state is physical, i.e., is admissible by energy-momentum conservation and all other physical conservation laws (charge, lepton number etc.). With a diagram we may associate a specific physical channel by specifying which external lines are in-coming and which are out-going. For a given channel then the imaginary part of the diagram is given by cutting internal lines of the diagram between the in-coming and the out-going lines in all possible ways into two disconnected parts. A cut contributes if the cut lines can be viewed as external lines of a real physical subprocess. On the right hand side of the cut the amplitude has to be taken complex conjugate, since the out-going state produced by the cut on the left hand side becomes the in-coming state on the right hand side. Due to the many extra  $\delta$ -functions (on-shell conditions) part of the integrations become phase space integrations, which in general are easier to do. As a rule, the complexity is reduced from  $n$ -loop to a  $n - 1$ -loop problem, on the expense that the last integration, a dispersion integral, still has to be done. A very instructive non-trivial example has been presented by Terentev [27] for the complete two-loop calculation of  $g - 2$  in QED.

Cut diagrams in conjunction with DRs play a fundamental role also beyond being just a technical trick for calculating Feynman integrals. They not only play a key role for the evaluation of non-perturbative hadronic effects but allows one to calculate numerically or sometimes analytically all kinds of VP effects in higher order diagrams as we will see. Before we discuss this in more detail, let us summarize the key ingredients of the method, which we have considered before, once more:



**Fig. 3.14** Optical theorem for scattering and propagation



□ *Optical theorem implied by unitarity*: maybe most familiar is its application to scattering processes: the imaginary part of the forward scattering amplitude of an elastic process  $A + B \rightarrow A + B$  is proportional to the sum over all possible final states  $A + B \rightarrow$  “anything” (see Fig. 3.14)

$$\text{Im } T_{\text{forward}} (A + B \rightarrow A + B) = \sqrt{\lambda (s, m_1^2, m_2^2)} \sigma_{\text{tot}} (A + B \rightarrow \text{anything})$$

for the photon propagator it implies

$$\text{Im} \Pi'_\gamma(s) = \frac{\alpha s}{4\pi |\alpha(s)|^2} \sigma_{\text{tot}}(e^+e^- \rightarrow \text{anything})$$

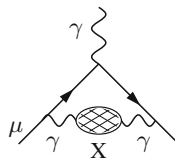
which we have been proving in the last section already.

□ *Analyticity*, implied by *causality*, may be expressed in form of a so-called (subtracted) dispersion relation

$$\Pi'_\gamma(k^2) - \Pi'_\gamma(0) = \frac{k^2}{\pi} \int_0^\infty ds \frac{\text{Im} \Pi'_\gamma(s)}{s (s - k^2 - i\epsilon)} . \tag{3.146}$$

The latter, together with the optical theorem, directly implies the validity of (3.143). Note that its validity is based on general principles and holds beyond perturbation theory. It is the basis of all non-perturbative evaluations of hadronic vacuum polarization effects in terms of experimental data. But more than that.

Within the context of calculating  $g - 2$  in the SM the maybe most important application of DRs concerns the vacuum polarization contribution related to diagrams of the type



where the “blob” is the full photon propagator, including all kinds of contributions as predicted by the SM and maybe additional yet unknown contributions from physics beyond the SM. The vacuum polarization amplitude satisfies a dispersion relation (3.136) and the spectral function is given by (3.139).

The contribution to the anomalous magnetic moment from graphs of the photon vacuum polarization type shown above can be obtained in a straightforward way as follows: The physics wise relevant  $g^{\mu\nu}$ -term of the full photon propagator, carrying loop momentum  $k$ , reads

$$\frac{-ig^{\mu\nu}}{k^2 (1 + \Pi'_\gamma(k^2))} \simeq \frac{-ig^{\mu\nu}}{k^2} \left( 1 - \Pi'_\gamma(k^2) + (\Pi'_\gamma(k^2))^2 - \dots \right) \quad (3.147)$$

and the renormalized photon self-energy may be written as

$$-\frac{\Pi'_{\gamma \text{ ren}}(k^2)}{k^2} = \int_0^\infty \frac{ds}{s} \frac{1}{\pi} \text{Im} \Pi'_\gamma(s) \frac{1}{k^2 - s} . \quad (3.148)$$

Note that the only  $k$  dependence under the convolution integral shows up in the last factor. Thus, the free photon propagator in the one-loop vertex graph discussed in Sect. 2.6.3 in the next higher order is replaced by

$$-ig_{\mu\nu}/k^2 \rightarrow -ig_{\mu\nu}/(k^2 - s)$$

which is the exchange of a photon of mass square  $s$ . The result afterward has to be convoluted with the imaginary part of the photon vacuum polarization. In a first step we have to calculate the contribution from the massive photon which may be calculated exactly as in the massless case. As discussed above  $F_M(0)$  most simply may be calculated using the projection method directly at  $q^2 = 0$ . The result is [184, 185]<sup>31</sup>

$$K_\mu^{(2)}(s) \equiv a_\mu^{(2) \text{ heavy } \gamma} = \frac{\alpha}{\pi} \int_0^1 dx \frac{x^2 (1-x)}{x^2 + (s/m_\mu^2)(1-x)} , \quad (3.149)$$

which is the second order contribution to  $a_\mu$  from an exchange of a photon with square mass  $s$ . Note that for  $s = 0$  we get the known Schwinger result.

---

<sup>31</sup>Replacing the heavy vector exchange by a heavy scalar exchange leads to the substitution

$$x^2 (1-x) \text{ (vector)} \rightarrow x^2 (1-x/2) \text{ (scalar)}$$

in the numerator of (3.149).

Utilizing this result and (3.148), the contribution from the “blob” to  $g - 2$  reads

$$a_\mu^{(X)} = \frac{1}{\pi} \int_0^\infty \frac{ds}{s} \operatorname{Im} \Pi_\gamma'^{(X)}(s) K_\mu^{(2)}(s). \quad (3.150)$$

If we exchange integrations and evaluating the DR we arrive at

$$\begin{aligned} a_\mu^{(X)} &= \frac{\alpha}{\pi} \int_0^1 dx (1-x) \int_0^\infty \frac{ds}{s} \frac{1}{\pi} \operatorname{Im} \Pi_\gamma'^{(X)}(s) \frac{x^2}{x^2 + (s/m_\mu^2)(1-x)} \\ &= \frac{\alpha}{\pi} \int_0^1 dx (1-x) \left[ -\Pi_\gamma'^{(X)}(s_x) \right] \end{aligned} \quad (3.151)$$

where

$$s_x = -\frac{x^2}{1-x} m_\mu^2.$$

The last simple representation in terms of  $\Pi_\gamma'^{(X)}(s_x)$  follows using

$$\frac{x^2}{x^2 + (s/m_\mu^2)(1-x)} = -s_x \frac{1}{s - s_x}.$$

In this context a convenient one-fold integral representation of the VP function is (2.177)

$$\Pi_{\gamma \text{ ren}}'^\ell \left( \frac{-x^2}{1-x} m_\mu^2 \right) = -\frac{\alpha}{\pi} \int_0^1 dz 2z (1-z) \ln \left( 1 + \frac{x^2}{1-x} \frac{m_\mu^2}{m_\ell^2} z (1-z) \right), \quad (3.152)$$

which together with (3.151) leads to a two-fold integral representation of the VP contribution by lepton loops at two-loop order.

This kind of dispersion integral representation can be generalized to higher order and sequential VP insertions corresponding to the powers of  $\Pi'(k^2)$  in (3.147).

Denoting  $\rho(s) = \operatorname{Im} \Pi_{\gamma \text{ ren}}'(s) / \pi$  we may write (3.148) in the form  $-\Pi_{\gamma \text{ ren}}'(k^2) = \int_0^\infty \frac{ds}{s} \rho(s) \frac{k^2}{k^2 - s}$  such that the  $n$ -th term of the propagator expansion (3.147) is given by

$$\begin{aligned} \left( -\Pi_{\gamma \text{ ren}}'(k^2) \right)^n / k^2 &= \frac{1}{k^2} \prod_{i=1}^n \int_0^\infty \frac{ds_i}{s_i} \rho(s_i) \frac{k^2}{k^2 - s_i} \\ &= \sum_{j=1}^n \int_0^\infty \frac{ds_j}{s_j} \rho(s_j) \frac{1}{k^2 - s_j} \prod_{i \neq j} \int_0^\infty \frac{ds_i}{s_i} \rho(s_i) \frac{s_j}{s_j - s_i}, \end{aligned}$$

where we have been applying the partial fraction decomposition

$$\frac{1}{k^2} \prod_{i=1}^n \frac{k^2}{k^2 - s_i} = \sum_{k=1}^n \frac{1}{k^2 - s_j} \prod_{i \neq j} \frac{s_j}{s_j - s_i} .$$

We observe that the integration over the loop momentum  $k$  of the one-loop muon vertex proceeds exactly as before, with the photon replaced by a single heavy photon of mass  $s_j$ . Thus, the contribution to  $a_\mu$  reads

$$\begin{aligned} a_\mu^{(X)} &= \frac{\alpha}{\pi} \int_0^1 dx (1-x) \sum_{j=1}^n \int_0^\infty \frac{ds_j}{s_j} \rho(s_j) \frac{-s_x}{s_j - s_x} \prod_{i \neq j} \int_0^\infty \frac{ds_i}{s_i} \rho(s_i) \frac{s_j}{s_j - s_i} \\ &= \frac{\alpha}{\pi} \int_0^1 dx (1-x) \left( \prod_{k=1}^n \int_0^1 \frac{ds_k}{s_k} \rho(s_k) \right) s_x \left( \sum_{j=1}^n \frac{1}{s_x - s_j} \prod_{i \neq j} \frac{s_j}{s_j - s_i} \right) . \end{aligned}$$

Under the integral, to the last factor, we may apply the above partial fraction decomposition backward

$$\sum_{j=1}^n \frac{1}{s_x - s_j} \prod_{i \neq j} \frac{s_j}{s_j - s_i} = \frac{1}{s_x} \prod_{i=1}^n \frac{s_x}{s_x - s_i}$$

which proves that the  $s_i$ -integrals factorize and we find [186]

$$\begin{aligned} a_\mu^{(X)} &= \frac{\alpha}{\pi} \int_0^1 dx (1-x) \left( \int_0^\infty \frac{ds}{s} \rho(s) \frac{-s_x}{s - s_x} \right)^n \\ &= \frac{\alpha}{\pi} \int_0^1 dx (1-x) \left( -\Pi'_{\gamma \text{ ren}}(s_x) \right)^n \end{aligned} \quad (3.153)$$

We are thus able to write formally the result for the one-loop muon vertex when we replace the free photon propagator by the full transverse propagator as [187]

$$\begin{aligned} a_\mu^{(X)} &= \frac{\alpha}{\pi} \int_0^1 dx (1-x) \left( \frac{1}{1 + \Pi'_{\gamma \text{ ren}}(s_x)} \right) \\ &= \frac{1}{\pi} \int_0^1 dx (1-x) \alpha(s_x) , \end{aligned} \quad (3.154)$$

which according to (3.120) is equivalent to the contribution of a free photon interacting with dressed charge (effective fine structure constant). However, since  $\Pi'_{\gamma \text{ ren}}(k^2)$  is negative and grows logarithmically with  $k^2$  the full photon propagator develops a so called *Landau pole* where the effective fine structure constant becomes infinite. Thus resumming the perturbation expansion under integrals may produce a problem and one better resorts to the order by order approach, by expanding the full propagator into its geometrical progression. Nevertheless (3.154) is a very useful bookkeeping device, collecting effects from different contributions and different orders. In particular if we expand the 1PI photon self-energy into order by order contributions

$$\Pi'_{\gamma \text{ ren}}(k^2) = \Pi'_{\gamma \text{ ren}}(2)(k^2) + \Pi'_{\gamma \text{ ren}}(4)(k^2) + \dots$$

and also write  $\rho = \rho^{(2)} + \rho^{(4)} + \dots$  for the spectral densities.

Coming back to the single VP insertion formula (3.151) we may use (3.152) as well as the second form given in (2.177) which reads

$$\Pi'_{\gamma \text{ ren}}(q^2/m^2) = -\frac{\alpha}{\pi} \frac{q^2}{m^2} \int_0^1 dt \frac{\rho_2(t)}{\frac{q^2}{m^2} - 4/(1-t^2)}, \tag{3.155}$$

with<sup>32</sup>

$$\rho_2(t) = \frac{t^2 (1 - t^2/3)}{1 - t^2}, \tag{3.156}$$

and we may write

$$a_\mu^{(X)} = \left(\frac{\alpha}{\pi}\right)^2 \int_0^1 dx (1-x) \int_0^1 dt \frac{\rho_2(t)}{W_t(x)}, \tag{3.157}$$

where

$$1/W_t(x) = \frac{q^2}{m^2} \frac{1}{\frac{q^2}{m^2} - \frac{4}{1-t^2}} \Bigg|_{\frac{q^2}{m^2} = -\frac{x^2}{1-x} \frac{m_\mu^2}{m^2}}$$

and hence

$$W_t(x) = 1 + \frac{4m^2}{(1-t^2)m_\mu^2} \frac{1-x}{x^2}. \tag{3.158}$$

---

<sup>32</sup>We adopt the notation of Kinoshita [186] and mention that the densities  $\rho(t)$  used here are not to be confused with the  $\rho(s)$  used just before, although they are corresponding to each other.

If  $n$  equal loops are inserted we have

$$a_\mu^{(X)} = \frac{\alpha}{\pi} \int_0^1 dx (1-x) \left( \frac{\alpha}{\pi} \int_0^1 dt \frac{\rho(t)}{W_t(x)} \right)^n \quad (3.159)$$

according to the factorization theorem demonstrated before. This formula is suitable for calculating the contribution to the lepton anomalous magnetic moment once the spectral function  $\rho(t)$  is known. For the one-loop 1PI self-energy we have  $\rho_2(t)$  given by (3.156) and the corresponding density for the two-loop case reads [175, 176, 188]

$$\begin{aligned} \rho_4(t) = & \frac{2t}{3(1-t^2)} \left\{ \frac{(3-t^2)(1+t^2)}{2} \left( \text{Li}_2(1) + \ln \frac{1+t}{2} \ln \frac{1+t}{1-t} \right) \right. \\ & + 2 \left( \text{Li}_2 \left( \frac{1-t}{1+t} \right) + \text{Li}_2 \left( \frac{1+t}{2} \right) - \text{Li}_2 \left( \frac{1-t}{2} \right) \right) - 4 \text{Li}_2(t) + \text{Li}_2(t^2) \\ & + \left( \frac{11}{16}(3-t^2)(1+t^2) + \frac{1}{4}t^4 - \frac{3}{2}t(3-t^2) \right) \ln \frac{1+t}{1-t} \\ & \left. + t(3-t^2) \left( 3 \ln \frac{1+t}{2} - 2 \ln t \right) + \frac{3}{8}t(5-3t^2) \right\}. \end{aligned} \quad (3.160)$$

The corresponding result for the three-loop photon self-energy has been calculated in [189]. For four-loops an approximate result is available [190]. Generally, the contribution to  $a_\mu$  which follow from the lowest order lepton ( $\ell$ ) vertex diagram by modifying the photon propagator with  $l$  electron loops of order  $2i$ ,  $m$  muon loops of order  $2j$  and  $n$  tau loops of order  $2k$  is given by

$$\begin{aligned} a_\ell = & \left( \frac{\alpha}{\pi} \right)^{(1+il+jm+kn)} \int_0^1 dx (1-x) \left( \int_0^1 dt_1 \frac{\rho_{2i}(t_1)}{1 + \frac{4}{1-t_1^2} \frac{1-x}{x^2} \left( \frac{m_e}{m_\ell} \right)^2} \right)^l \\ & \cdot \left( \int_0^1 dt_2 \frac{\rho_{2j}(t_2)}{1 + \frac{4}{1-t_2^2} \frac{1-x}{x^2} \left( \frac{m_\mu}{m_\ell} \right)^2} \right)^m \cdot \left( \int_0^1 dt_3 \frac{\rho_{2k}(t_3)}{1 + \frac{4}{1-t_3^2} \frac{1-x}{x^2} \left( \frac{m_\tau}{m_\ell} \right)^2} \right)^n. \end{aligned} \quad (3.161)$$

The same kind of approach works for the calculation of diagrams with VP insertions not only for the lowest order vertex. For any group of diagrams we may calculate in place of the true QED contribution the one obtained in massive QED with a photon of mass  $\sqrt{s}$ , and then convolute the result with the desired density of the photon VP analogous to (3.150) where (3.149) gets replaced by a different more complicated kernel function (see e.g. [103, 191] and below). It also should be noted that the representation presented here only involve integration over finite intervals ( $[0,1]$ ) and

hence are particularly suited for numerical integration of higher order contributions when analytic results are not available.

The formalism developed here also is the key tool to evaluate the *hadronic contributions*, for which perturbation theory fails because of the strong interactions. In this case we represent  $\text{Im } \Pi'_\gamma{}^{\text{had}}(s)$  via (3.139) in terms of

$$\sigma_{\text{had}}(s) = \sigma(e^+e^- \rightarrow \text{hadrons})$$

where

$$\sigma_{\text{had}}(s) = \frac{4\pi^2 |\alpha(s)|^2}{\alpha s} \frac{1}{\pi} \text{Im } \Pi'_\gamma{}^{\text{had}}(s) \quad (3.162)$$

or in terms of the cross section ratio  $R(s)$  defined by (3.139) where both  $\sigma_{\text{had}}(s)$  or equivalently  $R_{\text{had}}(s)$  will be taken from experiment, since they are not yet calculable reliably from first principles at present.

Starting point is the basic integral representation (from (3.150) using (3.139))

$$a_\mu^{\text{had}} = \frac{\alpha}{\pi} \int_0^\infty \frac{ds}{s} \int_0^1 dx \frac{x^2(1-x)}{x^2 + (1-x)s/m_\mu^2} \frac{\alpha}{3\pi} R(s) . \quad (3.163)$$

If we first integrate over  $x$  we find the well known standard representation

$$a_\mu^{\text{had}} = \frac{\alpha}{3\pi} \int_0^\infty \frac{ds}{s} K_\mu^{(2)}(s) R(s) \quad (3.164)$$

as an integral along the cut of the vacuum polarization amplitude in the time-like region, while an interchange of the order of integrations yields the analog of (3.151): an integral over the hadronic shift of the fine structure constant (3.121) in the space-like domain [192]:

$$a_\mu^{\text{had}} = \frac{\alpha}{\pi} \int_0^1 dx (1-x) \Delta\alpha_{\text{had}}^{(5)}(-Q^2(x)) \quad (3.165)$$

where  $Q^2(x) \equiv \frac{x^2}{1-x} m_\mu^2$  is the space-like square momentum-transfer or

$$x = \frac{Q^2}{2m_\mu^2} \left( \sqrt{1 + \frac{4m_\mu^2}{Q^2}} - 1 \right) .$$

In Fig. 3.15 we display the integrand of the representation (3.165) Alternatively, by writing  $(1-x) = -\frac{1}{2} \frac{d}{dx} (1-x)^2$  and performing a partial integration in (3.165) one

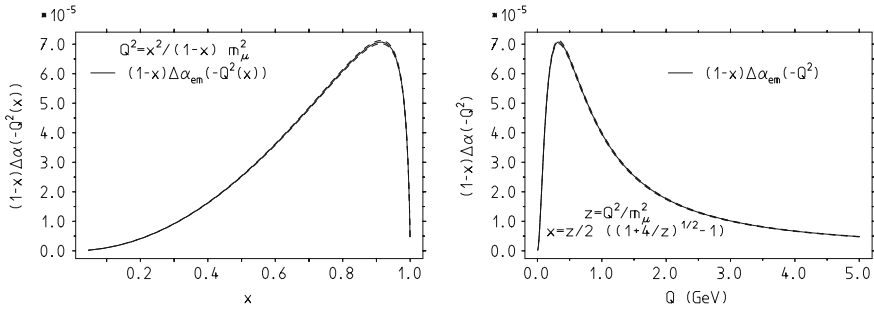


**Fig. 3.15** The integrand of the vacuum polarization representation (3.165) as a function of  $x$  and as a function of the energy scale  $Q$ . As we see the integrand is strongly peaked as a function of  $Q$  at about 330 MeV.  $\Pi(Q^2)$  data come from [197]. The *dashed lines* mark the error band from the experimental data

finds

$$a_\mu^{\text{had}} = \frac{\alpha^2}{6\pi^2} m_\mu^2 \int_0^1 dx x (2-x) (D(Q^2(x))/Q^2(x)) \tag{3.166}$$

where  $D(Q^2)$  is the *Adler–function* [193] defined as a derivative of the shift of the fine structure constant

$$D(-s) = -(12\pi^2) s \frac{d\Pi'_\gamma(s)}{ds} = \frac{3\pi}{\alpha} s \frac{d}{ds} \Delta\alpha_{\text{had}}(s) . \tag{3.167}$$

The Adler–function is represented by

$$D(Q^2) = Q^2 \left( \int_{4m_\pi^2}^\infty \frac{R(s)}{(s+Q^2)^2} ds \right) \tag{3.168}$$

in terms of  $R(s)$ , i.e., in the case of hadrons it can be evaluated in terms of experimental  $e^+e^-$ -data. The Adler–function is discussed in [194] and in Fig. 5.18 a comparison between theory and experiment is shown. The Adler–function is an excellent monitor for checking where pQCD works in the Euclidean region (see also [71]), and, in principle, it allows one to calculate  $a_\mu^{\text{had}}$  relying more on pQCD and less on  $e^+e^-$ -data, in a well controllable manner. The advantage of this method at present is limited by the inaccuracies of the quark masses, in particular of the charm mass [195, 196]. The integrand of the representation (3.166) is displayed in Fig. 3.16.

It is interesting to note that the representation (3.165) as well as (3.166) requires the hadronic vacuum polarization function in the spacelike region, which is the appropriate representation for ab initio calculations in the non-perturbative lattice



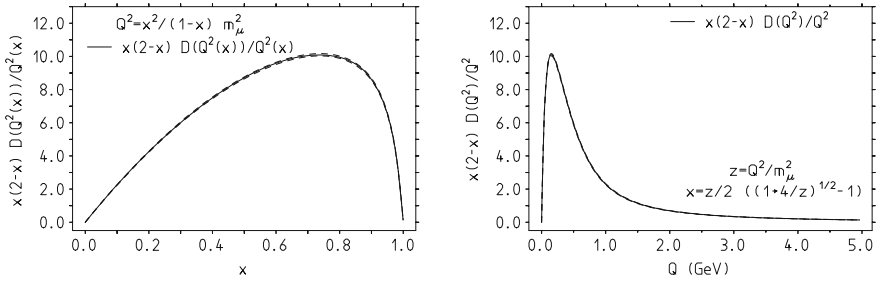


**Fig. 3.16** The integrand of the Adler function representation (3.166) as a function of  $x$  and as a function of the energy scale  $Q$ . The right-hand panel shows that the integrand is sharply peaked as a function of  $Q$  at a rather low scale ( $\sim 150$  MeV). Adler function data come from [198]. The dashed lines mark the error band from the experimental data

QCD approach.<sup>33</sup> The lattice QCD approach and results will be discussed in Sect. 5.3 of Chap. 5.

The Adler-function  $D(Q^2)$  is bounded asymptotically by perturbative QCD:  $D(Q^2) \rightarrow N_c \sum_f Q_f^2$ , with  $Q_f$  the quark charges and  $N_c = 3$  the color factor, up to perturbative corrections, which asymptotically vanish because of asymptotic freedom which implies  $\alpha_s(Q^2) \rightarrow 0$  as  $Q^2 \rightarrow \infty$  (see [194]). Obviously, then  $D(Q^2)/Q^2$  is a positive monotonically decreasing function<sup>34</sup> bounded by

$$\frac{D(Q^2)}{Q^2} = \int_{4m_\pi^2}^{\infty} \frac{R(s)}{(s + Q^2)^2} ds < \bar{P}_1 \equiv \int_{4m_\pi^2}^{\infty} \frac{R(s)}{s^2} ds = \left. \frac{D(Q^2)}{Q^2} \right|_{Q^2=0}, \quad (3.169)$$

the slope of the vacuum polarization function at zero momentum square. Obviously the slope  $D(Q^2)/Q^2$  is finite for  $Q^2 \rightarrow 0$ , which shows that the integrand of the representation (3.166) is well behaved as  $x \rightarrow 0$ .

<sup>33</sup>A new approach to evaluate the leading hadronic corrections to the muon  $g-2$  attempts to evaluate  $\Delta\alpha_{\text{had}}(t)$  directly in the spacelike region from Bhabha scattering data [199] or from the simpler process of  $\mu^-e^- \rightarrow \mu^-e^-$  scattering (a high energy muon beam on a low  $Z$  nuclear target) [200]. Direct experimental  $\Delta\alpha_{\text{had}}(t)$  data would also provide a direct comparison with corresponding LQCD results.

<sup>34</sup>Note that while

$$\left( D(Q^2)/Q^2 \right)' = -2 \left( \int_{4m_\pi^2}^{\infty} \frac{R(s)}{(s + Q^2)^3} ds \right) < 0,$$

the Adler function itself is not monotonic as

$$\left( D(Q^2)_{\text{cut}} \right)' = \left( \int_{4m_\pi^2}^{s_{\text{cut}}} \frac{(s - Q^2) R(s)}{(s + Q^2)^3} ds \right),$$

which always has a zero if  $s_{\text{cut}}$  is finite, and for  $s_{\text{cut}} = \infty$  it has zero because  $R(s)$  is increasing with  $s$ . The “experimental” Adler function has a maximum in the 30 GeV region.

Note that alternatively, using (3.167) we may write

$$\bar{P}_1 = -\frac{3\pi}{\alpha} \frac{d}{ds} \Delta\alpha_{\text{had}}(s)|_{s=-Q^2, Q^2 \rightarrow 0} . \quad (3.170)$$

Therefore, (3.168) together with (3.166) yields a bound (see also [113])

$$a_\mu^{\text{had}} < \frac{\alpha^2}{6\pi^2} m_\mu^2 \frac{2}{3} \bar{P}_1 . \quad (3.171)$$

The integral over a compilation of  $R(s)$ -data, discussed in detail later in Chap. 5, yields  $\bar{P}_1 = 11.83(8) \text{ GeV}^{-2}$  and hence

$$a_\mu^{\text{had}} < 791(5) \times 10^{-10} . \quad (3.172)$$

As we will see an evaluation of (3.164) yields a value substantially lower:  $a_\mu^{\text{had}} \simeq 688.1 \pm 4.1 \times 10^{-10}$ .

Actually, we may write (3.164) in the form

$$a_\mu^{\text{had}} = \left( \frac{\alpha m_\mu}{3\pi} \right)^2 \int_0^\infty \frac{ds}{s^2} \hat{K}(s) R(s) \quad (3.173)$$

where

$$\hat{K}(s) = \frac{3s}{m_\mu^2} K_\mu^{(2)}(s) , \quad (3.174)$$

in which  $\hat{K}(s)$  is a bounded monotonically increasing function, with  $\hat{K}(4m_\pi^2) \simeq 0.63$  increasing to 1 at  $s \rightarrow \infty$ . Setting  $\hat{K}(s) = 1$  we obtain the bound presented above. A lower bound then is obtained by setting  $\hat{K}(s) = \hat{K}(4m_\pi^2) \approx 0.63$ , which implies  $a_\mu^{\text{had}} > 498(3) \times 10^{-10}$  again a very rough bound only, but a true bound.

The bound (3.171) can be improved by a moment expansion of the kernel as advocated in Ref. [201] and analyzed in detail in [202].

The best checks is to compare lattice results in terms of the Adler function as it enters in the representation (3.166) as advocated in [195] and actually performed in [203, 204] recently. An up-to-date evaluation of the “experimental” Adler function is available via the link [198].

### 3.9 $\zeta$ -Values, Polylogarithms and Related Special Functions

For later reference we list some transcendental constants and definitions of special functions which are encountered in higher order Feynman graph calculations. Typi-

cally analytic results for the mass independent universal lepton  $g - 2$  contributions are of the form of sums of terms exhibiting rational numbers as coefficients of transcendental objects. The most frequent such object are the Riemann *zeta function*

$$\zeta(n) = \sum_{k=1}^{\infty} \frac{1}{k^n} \tag{3.175}$$

and the *polylogarithmic integrals*

$$\text{Li}_n(x) = \frac{(-1)^{n-1}}{(n-2)!} \int_0^1 \frac{\ln^{n-2}(t) \ln(1-xt)}{t} dt = \sum_{k=1}^{\infty} \frac{x^k}{k^n}, \tag{3.176}$$

where the dilogarithm  $\text{Li}_2(x)$  is often referred to as the Spence function which we encountered in Sect. 2.6.3 (2.208). The series representation holds for  $|x| \leq 1$ . The dilogarithm is an analytic function with the same cut as the logarithm. Useful relations are

$$\begin{aligned} \text{Sp}(x) &= -\text{Sp}(1-x) + \frac{\pi^2}{6} - \ln x \ln(1-x), \\ \text{Sp}(x) &= -\text{Sp}\left(\frac{1}{x}\right) - \frac{\pi^2}{6} - \frac{1}{2} \ln^2(-x), \\ \text{Sp}(x) &= -\text{Sp}(-x) + \frac{1}{2} \text{Sp}(x^2). \end{aligned} \tag{3.177}$$

Special values are:

$$\text{Sp}(0) = 0, \quad \text{Sp}(1) = \frac{\pi^2}{6}, \quad \text{Sp}(-1) = -\frac{\pi^2}{12}, \quad \text{Sp}\left(\frac{1}{2}\right) = \frac{\pi^2}{12} - \frac{1}{2}(\ln 2)^2. \tag{3.178}$$

Special  $\zeta(n)$  values we will need are

$$\zeta(2) = \frac{\pi^2}{6}, \quad \zeta(3) = 1.202\ 056\ 903\dots, \quad \zeta(4) = \frac{\pi^4}{90}, \quad \zeta(5) = 1.036\ 927\ 755\dots \tag{3.179}$$

Also the constants

$$\begin{aligned} \text{Li}_n(1) &= \zeta(n), \quad \text{Li}_n(-1) = -[1 - 2^{1-n}] \zeta(n), \\ a_4 &\equiv \text{Li}_4\left(\frac{1}{2}\right) = \sum_{n=1}^{\infty} \frac{1}{(2^n n^4)} = 0.517\ 479\ 061\ 674\dots, \end{aligned} \tag{3.180}$$

related to polylogarithms, will be needed for the evaluation of analytical results. A generalization are the *Nielsen integrals*

$$S_{n,p}(x) = \frac{(-1)^{n+p-1}}{(n-1)!p!} \int_0^1 \frac{\ln^{n-1}(t) \ln^p(1-xt)}{t} dt, \tag{3.181}$$

which have representations as sums of the type

$$S_{1,2}(x) = \sum_2^\infty \frac{x^k}{k^2} S_1(k-1); \quad S_{2,2}(x) = \sum_2^\infty \frac{x^k}{k^3} S_1(k-1),$$

where

$$S_1(k) = \sum_1^k \frac{1}{l}$$

is a *harmonic sum*. And higher sums are obtained by the recurrences

$$\frac{d}{dx} S_{n,p}(x) = \frac{1}{x} S_{n-1,p}(x); \quad \int_0^x \frac{S_{n,p}(t)}{t} dt = S_{n+1,p}(x).$$

The general *harmonic series* are defined by [205]

$$S_m(n) = \sum_{i=1}^n \frac{1}{i^m}; \quad S_{-m}(n) = \sum_{i=1}^n \frac{(-1)^i}{i^m}, \tag{3.182}$$

in which  $m > 0$ . Higher harmonic series are defined by the recurrences

$$S_{m,j_1,\dots,j_p}(n) = \sum_{i=1}^n \frac{1}{i^m} S_{j_1,\dots,j_p}(i); \quad S_{-m,j_1,\dots,j_p}(n) = \sum_{i=1}^n \frac{(-1)^i}{i^m} S_{j_1,\dots,j_p}(i), \tag{3.183}$$

where again  $m > 0$ . The  $m$  and the  $j_i$  are referred to as the indices of the harmonic series. Hence, for example

$$S_{1,-5,3}(n) = \sum_{i=1}^n \frac{1}{i} \sum_{j=1}^i \frac{(-1)^j}{j^5} \sum_{k=1}^j \frac{1}{k^3}. \tag{3.184}$$

Basic transcendental constants of increasing transcendental weight are (examples we will find in Chap.4)

$$\left\{ [S_1(\infty), \ln(2)]; \zeta_2; \zeta_3; \text{Li}_4(1/2); (\zeta_5, \text{Li}_5(1/2)); [\text{Li}_6(1/2), S_{-5,-1}(\infty)]; \right. \\ \left. [\zeta_7, \text{Li}_7(1/2), S_{-5,1,1}(\infty), S_{5,-1,-1}(\infty)]; \dots \right\} \tag{3.185}$$

where  $S_{...} = S_{...}(\infty)$ . The numerical values have been calculated in [205]:

$$\begin{aligned}
 \text{Li}_4(1/2) &= 0.51747906167389938633 \\
 \text{Li}_5(1/2) &= 0.50840057924226870746 \\
 \text{Li}_6(1/2) &= 0.50409539780398855069 \\
 \text{Li}_7(1/2) &= 0.50201456332470849457 \\
 S_{-5,-1}(\infty) &= 0.98744142640329971377 \\
 -S_{-5,1,1}(\infty) &= 0.95296007575629860341 \\
 S_{5,-1,-1}(\infty) &= 1.02912126296432453422 .
 \end{aligned} \tag{3.186}$$

The harmonic polylogarithms (HPL)  $H(a_1, \dots, a_k; x)$  are functions of one variable  $x$  labeled by a vector  $a = (a_1, \dots, a_k)$ . The dimension  $k$  of the vector  $a$  is called the weight of the HPL [206]. Given the functions

$$f_1(x) = \frac{1}{1-x} ; \quad f_0(x) = \frac{1}{x} ; \quad f_{-1}(x) = \frac{1}{1+x} , \tag{3.187}$$

the HPLs are defined recursively through integration of these functions. For *weight one* we have

$$\begin{aligned}
 H(1; x) &= \int_0^x f_1(t) dt = \int_0^x \frac{1}{1-t} dt = -\log(1-x) \\
 H(0; x) &= \log(x) \\
 H(-1; x) &= \int_0^x f_{-1}(t) dt = \int_0^x \frac{1}{1+t} dt = \log(1+x),
 \end{aligned} \tag{3.188}$$

and for higher weights

$$H({}^n 0; x) = \frac{1}{n!} \log^n x ; \quad H(a, a_{1,\dots,k}; x) = \int_0^x f_a(t) H(a_{1,\dots,k}; t) dt , \tag{3.189}$$

where we used the notations  ${}^n i = \underbrace{i, \dots, i}_n$  and  $a_{1,\dots,k} = a_1, \dots, a_k$ .

Examples are,

$$H(0, 0, 1, 1; x) = S_{2,2}(x) ; \quad H(-1, 0, 0, 1; x) = \int_0^x \frac{dz}{1+z} \text{Li}_3(z) .$$

The formula for the derivative of the HPLs follows directly from their definition

$$\frac{d}{dx} H(a, a_{1,\dots,k}; x) = f_a(x) H(a_{1,\dots,k}; x). \quad (3.190)$$

An *elliptic integral* is defined as any function  $f$  which can be expressed in the form [207]

$$f(x) = \int_c^x R\left(t, \sqrt{P(t)}\right) dt$$

where  $R$  is a rational function of its two arguments,  $P$  is a polynomial of degree 3 or 4 with no repeated roots, and  $c$  is a constant. In general, integrals in this form cannot be expressed in terms of elementary functions. Exceptions to this general rule are when  $P$  has repeated roots, or when  $R(x, y)$  contains no odd powers of  $y$ . However, with the appropriate reduction formula, every elliptic integral can be brought into a form that involves integrals over rational functions and the three canonical forms, the elliptic integrals of the first, second and third kind. The incomplete *elliptic integral of the first kind*  $F$  is defined as

$$F(\varphi; m) = \int_0^\varphi \frac{d\theta}{\sqrt{1-m\sin^2\theta}} = \int_0^{x=\sin\varphi} \frac{dt}{\sqrt{(1-t^2)(1-mt^2)}}.$$


The incomplete *elliptic integral of the second kind*  $E$  may be defined as

$$E(\varphi; m) = \int_0^\varphi d\theta \sqrt{1-m\sin^2\theta} = \int_0^{x=\sin\varphi} \frac{\sqrt{1-mt^2}}{\sqrt{1-t^2}} dt.$$

The incomplete *elliptic integral of the third kind*  $\Pi$  is defined by

$$\Pi(n; \varphi | m) = \int_0^\varphi \frac{1}{1-n\sin^2\theta} \frac{d\theta}{\sqrt{1-m\sin^2\theta}} = \int_0^{x=\sin\varphi} \frac{1}{1-nt^2} \frac{dt}{\sqrt{(1-t^2)(1-mt^2)}},$$

where  $m = \sin^2 \alpha$  is a parameter. For  $\varphi = \pi/2$  and  $x = 1$  we obtain the complete elliptic integrals.

The simplest diagram leading to an elliptic integral is the scalar massive triple line graph (sunrise diagram) , which plays a role in the self-energy of the  $\omega$  vector meson which decays predominantly via  $\omega \rightarrow \pi^+\pi^-\pi^0$  (see also [208]). In the context of dimensional regularization and  $\epsilon$ -expansion various types of generalized and Appell hypergeometric functions show up [209–213]. For further reading see e.g. [214–217] and references therein.

## References

1. J.D. Bjorken, S.D. Drell, *Relativistic Quantum Mechanics*, 1st edn. (McGraw-Hill, New York, 1964), 300 p; *Relativistic Quantum Fields*, 1st edn. (McGraw-Hill, New York, 1965), p. 396
2. L.H. Thomas, *Philos. Mag.* **3**, 1 (1927); V. Bargmann, L. Michel, V.A. Telegdi. *Phys. Rev. Lett.* **2**, 435 (1959)
3. P.A.M. Dirac, *Proc. R. Soc. A* **117**, 610 (1928); **A 118**, 351 (1928)
4. P.J. Mohr, D.B. Newell, B.N. Taylor, *Rev. Mod. Phys.* **88**, 035009 (2016)
5. B. Odom, D. Hanneke, B. D’Urso, G. Gabrielse, *Phys. Rev. Lett.* **97**, 030801 (2006)
6. D. Hanneke, S. Fogwell, G. Gabrielse, [arXiv:0801.1134](https://arxiv.org/abs/0801.1134) [physics.atom-ph]
7. P.J. Mohr, B.N. Taylor, D.B. Newell, *Rev. Mod. Phys.* **84**, 1527 (2012)
8. G. Gabrielse, D. Hanneke, T. Kinoshita, M. Nio, B. Odom, *Phys. Rev. Lett.* **97**, 030802 (2006) [Erratum-ibid. **99**, 039902 (2007)]
9. T. Aoyama, M. Hayakawa, T. Kinoshita, M. Nio, *Phys. Rev. Lett.* **99**, 110406 (2007)
10. T. Aoyama, M. Hayakawa, T. Kinoshita, M. Nio, *Phys. Rev. Lett.* **109**, 111807 (2012)
11. S. Laporta, [arXiv:1704.06996](https://arxiv.org/abs/1704.06996) [hep-ph]
12. K.A. Olive et al. [Particle Data Group], *Chin. Phys. C* **38**, 090001 (2014); C. Patrignani et al., *Part. Data Group Chin. Phys. C* **40**, 100001 (2016)
13. S. Eidelman et al. [Particle Data Group], *Phys. Lett. B* **592**, 1 (2004)
14. P.J. Mohr, B.N. Taylor, *Rev. Mod. Phys.* **72**, 351 (2000); **77**, 1 (2005)
15. F. Gianotti (the ATLAS Collab.), CERN Seminar, July 4th, 2012; J. Incandela (the CMS Collab.), CERN Seminar, July 4th, 2012
16. G. Aad et al. [ATLAS Collab.], *Phys. Lett. B* **716**, 1 (2012). *Science* **338**, 1576 (2012)
17. S. Chatrchyan et al. [CMS Collab.], *Phys. Lett. B* **716**, 30 (2012) *Science* **338**, 1569 (2012);
18. F. Jegerlehner, M.Y. Kalmykov, B.A. Kniehl, *Phys. Lett. B* **722**, 123 (2013)
19. B.A. Kniehl, A.F. Pikelner, O.L. Veretin, *Nucl. Phys. B* **896**, 19 (2015)
20. F. Jegerlehner, A. Nyffeler, *Phys. Rep.* **477**, 1 (2009)
21. J.S. Schwinger, *Phys. Rev.* **73**, 416 (1948)
22. D.J. Broadhurst, D. Kreimer, *J. Symb. Comput.* **27**, 581 (1999); *Int. J. Mod. Phys. C* **6**, 519 (1995); *Phys. Lett. B* **393**, 403 (1997); D.J. Broadhurst, J.A. Gracey, D. Kreimer, *Z. Phys. C* **75**, 559 (1997)
23. A. Devoto, D.W. Duke, *Riv. Nuovo Cimento* **7N6**, 1 (1984)
24. R. Karplus, N.M. Kroll, *Phys. Rep. C* **77**, 536 (1950)
25. A. Petermann, *Helv. Phys. Acta* **30**, 407 (1957); *Nucl. Phys.* **5**, 677 (1958)
26. C.M. Sommerfield, *Phys. Rev.* **107**, 328 (1957); *Ann. Phys. (N.Y.)* **5**, 26 (1958)
27. M.V. Terentev, *Sov. Phys. JETP* **16**, 444 (1963); [*Zh. Eksp. Teor. Fiz.* **43**, 619 (1962)]
28. S. Laporta, E. Remiddi, *Phys. Lett. B* **379**, 283 (1996)
29. T. Kinoshita, *Phys. Rev. Lett.* **75**, 4728 (1995)
30. T. Kinoshita, W.J. Marciano, in *Quantum Electrodynamics*, ed. by T. Kinoshita (World Scientific, Singapore, 1990), pp. 419–478
31. T. Kinoshita, M. Nio, *Phys. Rev. Lett.* **90**, 021803 (2003); *Phys. Rev. D* **70**, 113001 (2003)
32. T. Kinoshita, M. Nio, *Phys. Rev. D* **73**, 013003 (2006)
33. T. Aoyama, M. Hayakawa, T. Kinoshita, M. Nio, *Phys. Rev. D* **91**, 033006 (2015)
34. T. Kinoshita, *Int. J. Mod. Phys. A* **29**, 1430003 (2014)
35. M. Hayakawa, *Springer Tracts Mod. Phys.* **256**, 41 (2014)
36. H. Suura, E. Wichmann, *Phys. Rev.* **105**, 1930 (1957); A. Petermann, *Phys. Rev.* **105**, 1931 (1957)
37. H.H. Elend, *Phys. Lett.* **20**, 682 (1966); Erratum-ibid, **21**, 720 (1966)
38. B.E. Lautrup, E. de Rafael, *Nucl. Phys. B* **70**, 317 (1974)
39. P.A. Baikov, K.G. Chetyrkin, J.H. Kühn, C. Sturm, *Nucl. Phys. B* **867**, 182 (2013)
40. S. Laporta, *Nuovo Cimento A* **106**, 675 (1993)
41. A. Czarnecki, M. Skrzypek, *Phys. Lett. B* **449**, 354 (1999)
42. S. Friot, D. Greynat, E. De Rafael, *Phys. Lett. B* **628**, 73 (2005)

43. S. Laporta, E. Remiddi, Phys. Lett. B **301**, 440 (1993)
44. J.H. Kühn, A.I. Onishchenko, A.A. Pivovarov, O.L. Veretin, Phys. Rev. D **68**, 033018 (2003)
45. J. Aldins, T. Kinoshita, S.J. Brodsky, A.J. Dufner, Phys. Rev. Lett. **23**, 441 (1969); Phys. Rev. D **1**, 2378 (1970)
46. J. Bailey et al., Phys. Lett. B **28**, 287 (1968)
47. A.S. Elkhovskiy, Sov. J. Nucl. Phys. **49**, 656 (1989); [Yad. Fiz. **49**, 1059 (1989)]
48. M. Passera, J. Phys. G **31**, R75 (2005); Phys. Rev. D **75**, 013002 (2007)
49. M. Caffo, S. Turrini, E. Remiddi, Phys. Rev. D **30**, 483 (1984); E. Remiddi, S.P. Sorella, Lett. Nuovo Cim. **44**, 231 (1985); D.J. Broadhurst, A.L. Kataev, O.V. Tarasov, Phys. Lett. B **298**, 445 (1993); S. Laporta, Phys. Lett. B **312**, 495 (1993); P.A. Baikov, D.J. Broadhurst, [arXiv:hep-ph/9504398](https://arxiv.org/abs/hep-ph/9504398)
50. A.L. Kataev, Phys. Rev. D **86**, 013010 (2012)
51. T. Aoyama, M. Hayakawa, T. Kinoshita, M. Nio, Phys. Rev. Lett. **109**, 111808 (2012)
52. S.G. Karshenboim, Phys. At. Nucl. **56**, 857 (1993); [Yad. Fiz. **56N6**, 252 (1993)]
53. T. Kinoshita, M. Nio, Phys. Rev. D **73**, 053007 (2006)
54. A.L. Kataev, Nucl. Phys. Proc. Suppl. **155**, 369 (2006); [arXiv:hep-ph/0602098](https://arxiv.org/abs/hep-ph/0602098); Phys. Rev. D **74**, 073011 (2006)
55. P.A. Baikov, K.G. Chetyrkin, C. Sturm, Nucl. Phys. Proc. Suppl. **183**, 8 (2008)
56. R. Lee, P. Marquard, A.V. Smirnov, V.A. Smirnov, M. Steinhauser, JHEP **1303**, 162 (2013)
57. A. Kurz, T. Liu, P. Marquard, A.V. Smirnov, V.A. Smirnov, M. Steinhauser, Phys. Rev. D **92**, 073019 (2015)
58. A. Kurz, T. Liu, P. Marquard, A. Smirnov, V. Smirnov, M. Steinhauser, Phys. Rev. D **93**, 053017 (2016)
59. H. Fritzsch, M. Gell-Mann, H. Leutwyler, Phys. Lett. **47B**, 365 (1973)
60. H.D. Politzer, Phys. Rev. Lett. **30**, 1346 (1973); D. Gross, F. Wilczek, Phys. Rev. Lett. **30**, 1343 (1973)
61. S.G. Gorishnii, A.L. Kataev, S.A. Larin, Phys. Lett. B **259**, 144 (1991); L.R. Surguladze, M.A. Samuel, Phys. Rev. Lett. **66**, 560 (1991) [Erratum-ibid. **66**, 2416 (1991)]; K.G. Chetyrkin, Phys. Lett. B **391**, 402 (1997)
62. K.G. Chetyrkin, J.H. Kühn, Phys. Lett. B **342**, 356 (1995); K.G. Chetyrkin, R.V. Harlander, J.H. Kühn, Nucl. Phys. B **586**, 56 (2000) [Erratum-ibid. B **634**, 413 (2002)]
63. R.V. Harlander, M. Steinhauser, Comput. Phys. Commun. **153**, 244 (2003)
64. S. Eidelman, F. Jegerlehner, Z. Phys. C **67**, 585 (1995)
65. A.E. Blinov et al. [MD-1 Collab.], Z. Phys. C **70**, 31 (1996)
66. J.Z. Bai et al. [BES Collab.], Phys. Rev. Lett. **84**, 594 (2000); Phys. Rev. Lett. **88**, 101802 (2002)
67. R.R. Akhmetshin et al. [CMD-2 Collab.], Phys. Lett. B **578**, 285 (2004); Phys. Lett. B **527**, 161 (2002)
68. A. Aloisio et al. [KLOE Collab.], Phys. Lett. B **606**, 12 (2005)
69. M.N. Achasov et al. [SND Collab.], J. Exp. Theor. Phys. **103**, 380 (2006) [Zh. Eksp. Teor. Fiz. **130**, 437 (2006)]
70. V. M. Aulchenko et al. [CMD-2], JETP Lett. **82** (2005) 743 [Pisma Zh. Eksp. Teor. Fiz. **82** (2005) 841]; R. R. Akhmetshin et al., JETP Lett. **84** (2006) 413 [Pisma Zh. Eksp. Teor. Fiz. **84** (2006) 491]; Phys. Lett. B **648** (2007) 28
71. F. Jegerlehner, Nucl. Phys. Proc. Suppl. **162**, 22 (2006), [arXiv:hep-ph/0608329](https://arxiv.org/abs/hep-ph/0608329)
72. F. Jegerlehner, R. Szafron, Eur. Phys. J. C **71**, 1632 (2011)
73. F. Jegerlehner, Acta Phys. Pol. B **44**, 2257 (2013)
74. F. Jegerlehner, EPJ Web Conf. **118**, 01016 (2016). [arXiv:1705.00263](https://arxiv.org/abs/1705.00263) [hep-ph]
75. B. Ananthanarayan, I. Caprini, D. Das, I.S. Imsong, Phys. Rev. D **93**, 116007 (2016)
76. H. Leutwyler, Electromagnetic form factor of the pion, in *Continuous Advances in QCD 2002: Proceedings* ed. by K.A. Olive, M.A. Shifman, M.B. Voloshin (World Scientific, Singapore, 2002), 646p, [arXiv:hep-ph/0212324](https://arxiv.org/abs/hep-ph/0212324)
77. G. Colangelo, Nucl. Phys. Proc. Suppl. **131**, 185 (2004); *ibid.* **162**, 256 (2006)



78. H. Leutwyler, Electromagnetic form factor of the pion, in *Continuous Advances in QCD 2002: Proceedings*, ed. by K.A. Olive, M.A. Shifman, M.B. Voloshin (World Scientific, Singapore, 2002), 646p, [arXiv:hep-ph/0212324](https://arxiv.org/abs/hep-ph/0212324); G. Colangelo, Nucl. Phys. Proc. Suppl. **131**, 185 (2004); *ibid.* **162**, 256 (2006)
79. R.R. Akhmetshin et al. [CMD-2 Collab.], Phys. Lett. B **578**, 285 (2004)
80. A. Aloisio et al. [KLOE Collab.], Phys. Lett. B **606**, 12 (2005); F. Ambrosino et al. [KLOE Collab.], Phys. Lett. B **670**, 285 (2009)
81. F. Ambrosino et al. [KLOE Collab.], Phys. Lett. B **700**, 102 (2011)
82. D. Babusci et al. [KLOE Collab.], Phys. Lett. B **720**, 336 (2013)
83. B. Aubert et al. [BABAR Collab.], Phys. Rev. Lett. **103**, 231801 (2009); J.P. Lees et al., Phys. Rev. D **86**, 032013 (2012)
84. M. Ablikim et al. [BESIII Collab.], Phys. Lett. B **753**, 629 (2016)
85. K. Hagiwara, A.D. Martin, D. Nomura, T. Teubner, Phys. Lett. B **649**, 173 (2007)
86. M. Davier, S. Eidelman, A. Höcker, Z. Zhang, Eur. Phys. J. C **27**, 497 (2003); *ibid.* **31**, 503 (2003)
87. S. Eidelman, *Proceedings of the XXXIII International Conference on High Energy Physics, July 27 – August 2, 2006, Moscow (Russia)*, World Scientific, to appear; M. Davier, Nucl. Phys. Proc. Suppl. **169**, 288 (2007)
88. M. Davier et al., Eur. Phys. J. C **66**, 127 (2010)
89. M. Davier, A. Höcker, B. Malaescu, Z. Zhang, Eur. Phys. J. C **71**, 1515 (2011)[Erratum-*ibid.* C **72**, 1874 (2012)]
90. R. Akhmetshin et al. [CMD-3 Collab.], Phys. Lett. B **723**, 82 (2013)
91. M. Achasov et al. [SND Collab.], Phys. Rev. D **88**, 054013 (2013)
92. J. Lees et al. [BABAR Collab.], Phys. Rev. D **87**, 092005 (2013)
93. J. Lees et al. [BABAR Collab.], Phys. Rev. D **88**, 032013 (2013)
94. J. Lees et al. [BABAR Collab.], Phys. Rev. D **89**, 092002 (2014)
95. R. Alemany, M. Davier, A. Höcker, Eur. Phys. J. C **2**, 123 (1998)
96. R. Barate et al. [ALEPH Collab.], Z. Phys. C **76**, 15 (1997); Eur. Phys. J. C **4** (1998) 409; S. Schael et al. [ALEPH Collab.], Phys. Rep. **421**, 191 (2005)
97. M. Davier et al., Eur. Phys. J. C **74**, 2803 (2014)
98. K. Ackersstaff et al. [OPAL Collab.], Eur. Phys. J. C **7**, 571 (1999)
99. S. Anderson et al. [CLEO Collab.], Phys. Rev. D **61**, 112002 (2000)
100. M. Fujikawa et al. [Belle Collab.], Phys. Rev. D **78**, 072006 (2008)
101. S. Ghozzi, F. Jegerlehner, Phys. Lett. B **583**, 222 (2004)
102. M. Benayoun, P. David, L. DelBuono, F. Jegerlehner, Eur. Phys. J. C **72**, 1848 (2012)
103. R. Barbieri, E. Remiddi, Phys. Lett. B **49**, 468 (1974); Nucl. Phys. B **90**, 233 (1975)
104. B. Krause, Phys. Lett. B **390**, 392 (1997)
105. J. Calmet, S. Narison, M. Perrottet, E. de Rafael, Phys. Lett. B **61**, 283 (1976)
106. T. Kinoshita, B. Nizic, Y. Okamoto, Phys. Rev. Lett. **52**, 717 (1984); Phys. Rev. D **31**, 2108 (1985)
107. K. Hagiwara, A.D. Martin, D. Nomura, T. Teubner, Phys. Lett. B **557**, 69 (2003); Phys. Rev. D **69**, 093003 (2004)
108. A. Kurz, T. Liu, P. Marquard, M. Steinhauser, Phys. Lett. B **734**, 144 (2014)
109. A. Kurz, T. Liu, P. Marquard, A.V. Smirnov, V.A. Smirnov, M. Steinhauser, EPJ Web Conf. **118**, 01033 (2016)
110. H. Kolanoski, P. Zerwas, Two-photon physics, in *High Energy Electron-Positron Physics*, ed. by A. Ali, P. Söding (World Scientific, Singapore, 1988), pp. 695–784; D. Williams et al. [Crystal Ball Collab.], SLAC-PUB-4580, 1988, unpublished
111. G. Ecker, J. Gasser, A. Pich, E. de Rafael, Nucl. Phys. B **321**, 311 (1989); G. Ecker, J. Gasser, H. Leutwyler, A. Pich, E. de Rafael, Phys. Lett. B **223**, 425 (1989)
112. J. Bijnens, E. Pallante, J. Prades, Phys. Rev. Lett. **75**, 1447 (1995) [Erratum-*ibid.* **75**, 3781 (1995)]; Nucl. Phys. B **474**, 379 (1996); [Erratum-*ibid.* **626**, 410 (2002)]
113. E. de Rafael, Phys. Lett. B **322**, 239 (1994); J.S. Bell, E. de Rafael, Nucl. Phys. B **11**, 611 (1969)

114. M. Hayakawa, T. Kinoshita, A.I. Sanda, Phys. Rev. Lett. **75**, 790 (1995); Phys. Rev. D **54**, 3137 (1996)
115. M. Hayakawa, T. Kinoshita, Phys. Rev. D **57**, 465 (1998) [Erratum-ibid. D **66**, 019902 (2002)]
116. M. Knecht, A. Nyffeler, M. Perrottet, E. De Rafael, Phys. Rev. Lett. **88**, 071802 (2002)
117. G. 't Hooft, Nucl. Phys. B **72**, 461 (1974); *ibid.* **75**, 461 (1974)
118. A.V. Manohar, Hadrons in the  $1/N$  Expansion, in *At the frontier of Particle Physics*, vol. 1, ed. by M. Shifman (World Scientific, Singapore, 2001), pp. 507–568
119. S. Peris, M. Perrottet, E. de Rafael, JHEP **9805**, 011 (1998); M. Knecht, S. Peris, M. Perrottet, E. de Rafael, Phys. Rev. Lett. **83**, 5230 (1999); M. Knecht, A. Nyffeler. Eur. Phys. J. C **21**, 659 (2001)
120. M. Knecht, A. Nyffeler, Phys. Rev. D **65**, 073034 (2002)
121. I. Blokland, A. Czarnecki, K. Melnikov, Phys. Rev. Lett. **88**, 071803 (2002)
122. M. Ramsey-Musolf, M.B. Wise, Phys. Rev. Lett. **89**, 041601 (2002)
123. K. Melnikov, A. Vainshtein, Phys. Rev. D **70**, 113006 (2004)
124. A. Nyffeler, Nucl. Phys. B (Proc. Suppl.) **131**, 162 (2004)
125. J. Prades, E. de Rafael, A. Vainshtein, Adv. Ser. Direct. High Energy Phys. **20**, 303 (2009); ed. by B.L. Roberts, W. Marciano, [arXiv:0901.0306](https://arxiv.org/abs/0901.0306) [hep-ph]
126. R. Jackiw, S. Weinberg, Phys. Rev. D **5**, 2396 (1972); I. Bars, M. Yoshimura, Phys. Rev. D **6**, 374 (1972); G. Altarelli, N. Cabibbo, L. Maiani, Phys. Lett. B **40**, 415 (1972); W.A. Bardeen, R. Gastmans, B. Lautrup, Nucl. Phys. B **46**, 319 (1972); K. Fujikawa, B.W. Lee, A.I. Sanda, Phys. Rev. D **6**, 2923 (1972)
127. E.A. Kuraev, T.V. Kukhto, A. Schiller, Sov. J. Nucl. Phys. **51**, 1031 (1990) [Yad. Fiz. **51**, 1631 (1990)]; T.V. Kukhto, E.A. Kuraev, A. Schiller, Z.K. Silagadze, Nucl. Phys. B **371**, 567 (1992)
128. S.L. Adler, Phys. Rev. **177**, 2426 (1969); J.S. Bell, R. Jackiw, Nuovo Cimento **60A**, 47 (1969); W.A. Bardeen, Phys. Rev. **184**, 1848 (1969); C. Bouchiat, J. Iliopoulos, P. Meyer, Phys. Lett. **38B**, 519 (1972); D. Gross, R. Jackiw, Phys. Rev. D **6**, 477 (1972); C.P. Korthals Altes, M. Perrottet, Phys. Lett. **39B**, 546 (1972)
129. S. Peris, M. Perrottet, E. de Rafael, Phys. Lett. B **355**, 523 (1995)
130. A. Czarnecki, B. Krause, W. Marciano, Phys. Rev. D **52**, R2619 (1995)
131. G. Degrassi, G.F. Giudice, Phys. Rev. **58D**, 053007 (1998)
132. M. Knecht, S. Peris, M. Perrottet, E. de Rafael, JHEP **0211**, 003 (2002)
133. A. Czarnecki, W.J. Marciano, A. Vainshtein, Phys. Rev. D **67**, 073006 (2003) [Erratum-ibid. D **73**, 119901 (2006)]
134. E. D'Hoker, Phys. Rev. Lett. **69**, 1316 (1992)
135. A. Czarnecki, B. Krause, W.J. Marciano, Phys. Rev. Lett. **76**, 3267 (1996)
136. S. Heinemeyer, D. Stöckinger, G. Weiglein, Nucl. Phys. B **699**, 103 (2004)
137. T. Gribouk, A. Czarnecki, Phys. Rev. D **72**, 053016 (2005)
138. R.S. Van Dyck, P.B. Schwinberg, H.G. Dehmelt, Phys. Rev. Lett. **59**, 26 (1987)
139. D. Hanneke, S.F. Hoogerheide, G. Gabrielse, Phys. Rev. A **83**, 052122 (2011)
140. P. Cladé et al., Phys. Rev. Lett. **96**, 033001 (2006)
141. V. Gerginov et al., Phys. Rev. A **73**, 032504 (2006)
142. R. Bouchendir, P. Clade, S. Guellati-Khelifa, F. Nez, F. Biraben, Phys. Rev. Lett. **106**, 080801 (2011)
143. C. Schwob et al., Phys. Rev. Lett. **82**, 4960 (1999)
144. M.P. Bradley et al., Phys. Rev. Lett. **83**, 4510 (1999)
145. T. Beier et al., Phys. Rev. Lett. **88**, 011603 (2002)
146. D.L. Farnham, R.S. Van Dyck, P.B. Schwinberg, Phys. Rev. Lett. **75**, 3598 (1995)
147. S. Sturm, F. Köhler, J. Zatorski, A. Wagner, Z. Harman, G. Werth, W. Quint, C.H. Keitel et al., Nature **506**(7489), 467 (2014)
148. T. Udem et al., Phys. Rev. Lett. **82**, 3568 (1999)
149. A. Wicht et al., in *Proceedings of the 6th Symposium on Frequency Standards and Metrology* (World Scientific, Singapore, 2002), pp. 193–212; Phys. Scr. **T102** (2002) 82
150. G.F. Giudice, P. Paradisi, M. Passera, JHEP **1211**, 113 (2012)

151. F. Terranova, G.M. Tino, Phys. Rev. A **89**, 052118 (2014)
152. G. Mishima, [arXiv:1311.7109](https://arxiv.org/abs/1311.7109) [hep-ph]
153. M. Fael, M. Passera, Phys. Rev. D **90**, 056004 (2014)
154. K. Melnikov, A. Vainshtein, M. Voloshin, Phys. Rev. D **90**, 017301 (2014)
155. M.I. Eides, Phys. Rev. D **90**, 057301 (2014)
156. M. Hayakawa, [arXiv:1403.0416](https://arxiv.org/abs/1403.0416) [hep-ph]
157. M.A. Braun, Zh. Eksp. Teor. Fiz. **54**, 1220 (1968) [Sov. Phys. JETP. **27**, 652 (1968)]
158. R. Barbieri, P. Christillin, E. Remiddi, Phys. Rev. A **8**, 2266 (1973)
159. G.W. Bennett et al. [Muon (g-2) Collab.], Phys. Rev. Lett. **92**, 161802 (2004)
160. J. Grange et al. [Muon g-2 Collab.], [arXiv:1501.06858](https://arxiv.org/abs/1501.06858) [physics.ins-det]
161. F. Jegerlehner, J. Fleischer, Phys. Lett. B **151**, 65 (1985); Acta Phys. Pol. B **17**, 709 (1986)
162. Ya B. Zeldovich, Sov. Phys. JETP **6**, 1184 (1958)
163. Ya B. Zeldovich, A.M. Perelomov, Sov. Phys. JETP **12**, 777 (1961)
164. R.E. Marshak, Riazuddin, C.P. Ryan, *Theory of Weak Interactions in Particle Physics* (Wiley-Interscience, New York, 1969), p. 776
165. H. Czyż, K. Kołodziej, M. Zralek, P. Khristova, Can. J. Phys. **66**, 132 (1988); H. Czyż, M. Zralek. Can. J. Phys. **66**, 384 (1988)
166. A. Gongora, R.G. Stuart, Z. Phys. C **55**, 101 (1992)
167. L.D. Landau, Nucl. Phys. **3**, 127 (1957); Sov. Phys. JETP **5**, 336 (1957) [Zh. Eksp. Teor. Fiz. **32**, 405 (1957)]
168. Ya.B. Zeldovich, Sov. Phys. JETP **12**, 1030 (1960) [Zh. Eksp. Teor. Fiz. **39**, 1483 (1960)]
169. F. Hoogeveen, Nucl. Phys. B **341**, 322 (1990)
170. C. Jarlskog, Phys. Rev. Lett. **55**, 1039 (1985)
171. B.C. Regan, E.D. Commins, C.J. Schmidt, D. DeMille, Phys. Rev. Lett. **88**, 071805 (2002)
172. J. Bailey et al., Nucl. Phys. B **150**, 1 (1979)
173. F.J.M. Farley et al., Phys. Rev. Lett. **93**, 052001 (2004); M. Aoki et al. [J-PARC Letter of Intent], *Search for a Permanent Muon Electric Dipole Moment at the  $\times 10^{-24}$  e·cm Level*, <http://www-ps.kek.jp/jhf-np/LOIlist/pdf/L22.pdf>
174. W. Bernreuther, M. Suzuki, Rev. Mod. Phys. **63**, 313 (1991) [Erratum-ibid. **64**, 633 (1992)]
175. G. Källén, A. Sabry, K. Dan, Vidensk. Selsk. Mat.-Fys. Medd. **29**, 17 (1955)
176. R. Barbieri, E. Remiddi, Nuovo Cimento A **13**, 99 (1973)
177. D.J. Broadhurst, Phys. Lett. **101**, 423 (1981); S. Generalis, Open University preprint OUT-4102-13; T.H. Chang, K.J.F. Gaemers, W.L. van Neerven, Nucl. Phys. B **202**, 407 (1982); L.J. Reinders, H.R. Rubinstein, S. Yazaki, Phys. Rep. **127**, 1 (1985); B.A. Kniehl, Nucl. Phys. B **347**, 86 (1990)
178. M. Steinhauser, Phys. Lett. B **429**, 158 (1998)
179. M. Acciari et al. [L3 Collab.], Phys. Lett. B **476**, 40 (2000); G. Abbiendi et al. [OPAL Collab.], Eur. Phys. J. C **45**, 1 (2006)
180. L. Trentadue, Nucl. Phys. Proc. Suppl. **162**, 73 (2006)
181. G. Källén, Helv. Phys. Acta **25**, 417 (1952); H. Lehmann, Nuovo Cimento **11**, 342 (1954)
182. L.D. Landau, Nucl. Phys. **13**, 181 (1959); S. Mandelstam, Phys. Rev. **112**, 1344 (1958); **115**, 1741 (1959); R.E. Cutkosky, J. Math. Phys. **1**, 429 (1960)
183. M.J.G. Veltman, Physica **29**, 186 (1963)
184. V.B. Berestetskii, O.N. Krokhnin, A.K. Khelbnikov, Sov. Phys. JETP **3**, 761 (1956) [Zh. Eksp. Teor. Fiz. **30**, 788 (1956)]
185. S.J. Brodsky, E. De Rafael, Phys. Rev. **168**, 1620 (1968)
186. T. Kinoshita, Nuovo Cimento B **51**, 140 (1967); T. Kinoshita, W.B. Lindquist, Phys. Rev. D **27**, 867 (1983)
187. B. Lautrup, Phys. Lett. B **69**, 109 (1977)
188. T. Kinoshita, W.B. Lindquist, Phys. Rev. D **27**, 877 (1983)
189. A.H. Hoang, J.H. Kühn, T. Teubner, Nucl. Phys. B **452**, 173 (1995)
190. D.J. Broadhurst, A.L. Kataev, O.V. Tarasov, Phys. Lett. B **298**, 445 (1993); P.A. Baikov, D.J. Broadhurst, in *Proceedings of the 4th International Workshop on Software Engineering and Artificial Intelligence for High Energy and Nuclear Physics (AIHENP95), Pisa, Italy (1995)*, p. 167, [arXiv:hep-ph/9504398](https://arxiv.org/abs/hep-ph/9504398)

191. M. Caffo, E. Remiddi, S. Turrini, Nucl. Phys. B **141**, 302 (1978); J.A. Mignaco, E. Remiddi (1969) (unpublished)
192. B.E. Lautrup, A. Peterman, E. de Rafael, Phys. Rep. **3C**, 193 (1972)
193. S.L. Adler, Phys. Rev. D **10**, 3714 (1974); A. De Rujula, H. Georgi, Phys. Rev. D **13**, 1296 (1976)
194. S. Eidelman, F. Jegerlehner, A.L. Kataev, O. Veretin, Phys. Lett. B **454**, 369 (1999)
195. F. Jegerlehner, J. Phys. G **29**, 101 (2003)
196. F. Jegerlehner, in *Radiative Corrections*, ed. by J. Solà (World Scientific, Singapore, 1999), pp. 75–89
197. <http://www-com.physik.hu-berlin.de/~fjeger/alphaQED.tar.gz>, <http://www-com.physik.hu-berlin.de/~fjeger/alphaQED.pdf>
198. <http://www-com.physik.hu-berlin.de/~fjeger/pQCDAdler.tar.gz>, <http://www-com.physik.hu-berlin.de/~fjeger/pQCDAdler.pdf>
199. C.M. Carloni Calame, M. Passera, L. Trentadue, G. Venanzoni, Phys. Lett. B **746**, 325 (2015)
200. G. Abbiendi et al., Eur. Phys. J. C **77**, 139 (2017)
201. E. de Rafael, Phys. Lett. B **736**, 522 (2014)
202. M. Benayoun, P. David, L. DelBuono, F. Jegerlehner, [arXiv:1605.04474](https://arxiv.org/abs/1605.04474) [hep-ph]
203. M. Della Morte, A. Francis, G. Herdofoza, H. Horch, B. Jäger, A. Jüttner, H. Meyer, H. Wittig, PoS LATTICE **2014**, 162 (2014)
204. A. Francis, G. Herdofoza, H. Horch, B. Jäger, H.B. Meyer, H. Wittig, PoS LATTICE **2014**, 163 (2014)
205. J.A.M. Vermaseren, Int. J. Mod. Phys. A **14**, 2037 (1999)
206. E. Remiddi, J.A.M. Vermaseren, Int. J. Mod. Phys. A **15**, 725 (2000)
207. M. Abramowitz, I. Stegun, *Handbook of Mathematical Functions* (Dover, New York, 1965) (Chap. 17 and formulas 17.2.7/17.2.9/17.2.15 there)
208. O.V. Tarasov, Phys. Lett. B **638**, 195 (2006)
209. A.I. Davydychev, Phys. Rev. D **61**, 087701 (2000)
210. J. Fleischer, F. Jegerlehner, O.V. Tarasov, Nucl. Phys. B **672**, 303 (2003)
211. M.Y. Kalmykov, JHEP **0604**, 056 (2006)
212. A. Erdélyi et al., *Higher Transcendental Functions*, vol. 1 (McGraw-Hill, New York, 1953)
213. P. Appell, J. Kampé de Fériet, *Fonctions Hypergeometriques et Hyperspheriques. Polynome d'Hermite* (Gauthier-Villars, Paris, 1926)
214. O.V. Tarasov, Phys. Lett. B **670**, 67 (2008)
215. O.V. Tarasov, [arXiv:1512.09024](https://arxiv.org/abs/1512.09024) [hep-ph]
216. A.I. Davydychev, M.Y. Kalmykov, Nucl. Phys. B **605**, 266 (2001)
217. S. Moch, P. Uwer, S. Weinzierl, J. Math. Phys. **43**, 3363 (2002)
218. S. Bethke, Phys. Rep. **403–404**, 203 (2004)
219. S. Narison, Phys. Lett. B **568**, 231 (2003)
220. V.V. Ezhela, S.B. Lugovsky, O.V. Zenin, [arXiv:hep-ph/0312114](https://arxiv.org/abs/hep-ph/0312114)
221. J.F. de Troconiz, F.J. Yndurain, Phys. Rev. D **71**, 073008 (2005)
222. K. Hagiwara, R. Liao, A.D. Martin, D. Nomura, T. Teubner, J. Phys. G G **38**, 085003 (2011)
223. M. Benayoun, P. David, L. DelBuono, F. Jegerlehner, Eur. Phys. J. C **73**, 2453 (2013)
224. M. Benayoun, P. David, L. DelBuono, F. Jegerlehner, Eur. Phys. J. C **75**, 613 (2015)
225. M. Davier, [arXiv:1612.02743](https://arxiv.org/abs/1612.02743) [hep-ph]